i

SCIENTIFIC CONTRIBUTIONS
OIL & GAS

SCIENTIFIC CONTRIBUTIONS
OIL & GAS

Volume 44, Number 2, August 2021

CONTENTS

PREFACE

Dear Readers,

In this edition, we discuss in situ stress is importance in the petroleum industry because it will significantly enhance our understanding of present-day deformation in a sedimentary basin. The Northeast Java Basin is an example of a tectonically active basin in Indonesia. However, the in situ stress in this basin is still little known, This study attempts to analyze the regional in situ stress magnitude and orientation, and stress regime in the onshore part of the Northeast Java Basin based on twelve wells data, consist of density log, direct/indirect pressure test, and leak-off test (LOT) data.

Other topic in this edition elaborates the carbon capture utilization and storage (CCUS) referred in this paper is limited to the use of CO_2 to the enhanced oil recovery (CO_2-EOR). The CCUS CO_2-EOR technology can magnify oil production substantially while a consistent amount of the CO_2 injected remains sequestrated in the reservoir, which is beneficial for reducing the greenhouse gas emission.

Briefly, the most of today's global oil production comes from mature fields. Oil companies and governments are both concerned about increasing oil recovery from aging resources. To maintain oil production, the mature field must apply the Enhanced Oil Recovery method.

Next, shale is one of the rocks that often causes drilling problems because shale tends to swell or swell when in contact with mud filtrate, mainly Water-base Mud (WBM). This study aims to determine how the performance of Oil-base Mud (OBM) based on Crude Coconut Oil (CCO) in overcoming the swelling problem.

The other topic discuss hydraulic fracturing has been established as one of production enhancement methods in the petroleum industry. This method is proven to increase productivity and reserves in low permeability reservoirs, while in medium permeability, it accelerates production without affecting well reserves.

This edition will identify Enhanced oil recovery (EOR) has become one of the most favorable method in maximizing the production of mature fields with various applications and researches has been done on each type, including microbial EOR (MEOR). The field is a mature oil field located in South Sumatra that has been actively producing for more than 80 years and currently implementing MEOR using huff and puff injection.

Last but not least, as a source of energy, industrial raw materials, and foreign exchange for exports, the oil and gas sub-sector has a strategic role in national development. In the period 2020-2024, the management and utilization of oil and gas resources will face several challenges.

The Editorial Board and the Publisher Council would like to thank reviewers, editors, and authors who have contributed results of their research to the 2nd edition of Scientific Contribution Oil and Gas.

Jakarta, August 2021
Best regards,

Editorial Board

ABSTRACTS

The descriptions given are free terms. This abstract sheet may be reproduced without permission or charge

Agus M. Ramdhan, Applied Geology Research Group, Faculty of Earth Sciences and Technology, Bandung Institute of Technology, Jl. Ganesa No. 10, Bandung, Indonesia; Email: agusmr@gl.itb.ac.id

In Situ Stress and Stress Regime in the Offshore Part of the Northeast Java Basin

ABSTRACT

In situ stress is important in the petroleum industry because it will significantly enhance our understanding of present-day deformation in a sedimentary basin. The Northeast Java Basin is an example of a tectonically active basin in Indonesia. However, the in situ stress in this basin is still little known. This study attempts to analyze the regional in situ stress (i.e., vertical stress, minimum and maximum horizontal stresses) magnitude and orientation, and stress regime in the onshore part of the Northeast Java Basin based on twelve wells data, consist of density log, direct/indirect pressure test, and leak-off test (LOT) data. The magnitude of vertical (S_v) and minimum horizontal (S_{hmin}) stresses were determined using density log and LOT data, respectively. Meanwhile, the orientation of maximum horizontal stress (S_{hmax}) was determined using image log data, while its magnitude was determined based on pore pressure, mudweight, and the vertical and minimum horizontal stresses. The stress regime was simply analyzed based on the magnitude of in situ stress using Anderson's faulting theory. The results show that the vertical stress (S_v) in wells that experienced less erosion can be determined using the following equation: $S_v = 0.7622z^{1.0201}$ where is in psi, and z is in ft. However, wells that experienced severe erosion have vertical stress gradients higher than one psi/ft ($S_v = 1.0599z^{0.9982}$). The minimum horizontal stress (S_{hmin}) in the hydrostatic zone can be estimated as $S_{hmin} = 1.0599z^{0.963}$, while in the overpressured zone, $S_{hmin} = 0.7446z^{1.0228}$. The maximum horizontal stress (S_{hmax}) in the shallow and deep hydrostatic zones can be estimated using equations: $S_{hmax} = 2.4193z^{.9432}$ and $S_{hmax} = 2.4902z^{0.9396}$, respectively. While in the overpressured zone, $S_{hmax} = 67.743z^{0.5362}$. The orientation of S_{hmax} is ~NE-SW, with a strike-slip faulting stress regime.

(Author)

Usman, Dadan DSM Saputra, and Nurus Firdaus, "LEMIGAS" R & D Centre for Oil and Gas Technology, Jl. Ciledug Raya, Kav. 109, Cipulir, Kebayoran Lama, P.O. Box 1089/JKT, Jakarta Selatan 12230 INDONESIA, Tromol Pos: 6022/KBYB-Jakarta 12120, Telephone: 62-21-7394422, Faxsimile: 62-21-7246150, Email:usman@esdm.go.id

Source Sink Matching for Field Scale CCUS CO_2-EOR Application in Indonesia

ABSTRACT

The carbon capture utilization and storage (CCUS) referred in this paper is limited to the use of CO_2 to the enhanced oil recovery (CO_2-EOR). The CCUS CO_2-EOR technology can magnify oil production substantially while a consistent amount of the CO_2 injected remains sequestrated in the reservoir, which is beneficial for reducing the greenhouse gas emission. Therefore, this technology is a potentially attractive win-win solution for Indonesia to meet the goal of improved energy supply and security, while also reducing CO_2 emissions over the long term. The success of CCUS depends on the proper sources-sinks matching. This paper presents a systematic approach to pairing the CO_2 captured from industrial activities with suitable oil fields for CO_2-EOR. Inventories of CO_2 sources and oil reservoirs were done through survey and data questionnaires. The process of sources-sinks matching was preceded by identifying the CO_2 sources within the radius of 100 and 200 km from each oil field and

clustering the fields within the same radius from each CO_2 source. Each cluster is mapped on the GIS platform included existing and planning right of way for trunk pipelines. Pairing of source-sink are ranked to identify high priority development. Results of this study should be interest to project developers, policymakers, government agencies, academicians, civil society and environmental non-governmental organization in order to enable them to assess the role of CCUS CO_2-EOR as a major carbon management strategy.

(Author)

Steven Chandra, Prasandi A. Aziz, Muhammad R. Naufal and Wijoyo N. Daton, Petroleum Engineering Study Program, Institut Teknologi Bandung, Jl. Ganesha No. 10, Lb. Siliwangi, Bandung, Jawa Barat 40132, Email: suliantara@esdm.go.id

Well Integrity Study for WAG Application in Mature Field X, South Sumatra Area for the Fulfillment as CO_2 Sequestration Sink

ABSTRACT

The most of today's global oil production comes from mature fields. Oil companies and governments are both concerned about increasing oil recovery from aging resources. To maintain oil production, the mature field must apply the Enhanced Oil Recovery method. CO_2 water-alternating-gas (WAG) injection is an enhanced oil recovery method designed to improve sweep efficiency during CO_2 injection with the injected water to control the mobility of CO_2. This study will discuss possible corrosion during CO_2 and water injection and the casing load calculation along with the production tubing during the injection phase. The following study also performed a suitable material selection for the best performance injection. This research was conducted by evaluating casing integrity for simulate CO_2 water-alternating-gas (WAG) to be applied in the X-well in the Y-field, South Sumatra, Indonesia. Corrosion prediction were performed using Electronic Corrosion Engineer (ECE®) corrosion model and for the strength of tubing which included burst, collapse, and tension of production casing was assessed using Microsoft Excel. This study concluded that for the casing load calculation results in 600 psi of burst pressure, collapse pressure of 2,555.64 psi, and tension of 190,528 lbf. All of these results are still following the K-55 production casing rating. While injecting CO_2, the maximum corrosion rate occurs. It has a maximum corrosion rate of 2.02 mm/year and a minimum corrosion rate of 0.36 mm/year. With this value, it is above NORSOK Standard M-001 which is 2 mm/year and needs to be evaluated to prevent the rate to remain stable and not decrease in the following years. To prevent the effect of maximum corrosion rate, the casing material must use a SM13CR (Martensitic Stainless Steel) which is not sour service material.

(Author)

KRT Nur Suhascaryo[1], Endah Wahyurini[2], and Yuan Cahyo Guntoro[1], [1]Department of Petroleum Engineering, Faculty of Mineral Technology, Universitas Pembangunan Nasional "Veteran" Yogyakarta; Jl. SWK 104 Condongcatur, Sleman, Yogyakarta, Indonesia 55281, [2]Department of Agrotechnology, Faculty of Agriculture, Universitas Pembangunan Nasional "Veteran" Yogyakarta, Jl. SWK 104 Condongcatur, Sleman, Yogyakarta, Indonesia 55281, Email: nur.suhascaryo@unpyk.ac.id, endaywahyurini@yahoo.com

Utilization of Crude Oil (CCO) as an Alternative Oil Base Mud (OBM) Drilling Operation by "VICOIL" Standard Drilling Simulation Rig in MGTM Well UPN "Veteran" Yogyakarta Education Park Mineral Geotechnology Museum Field

ABSTRACT

Shale is one of the rocks that often causes drilling problems because shale tends to swell or swell when in contact with mud filtrate, mainly Water-base Mud (WBM). This study aims to determine how the performance of Oil-base Mud (OBM) based on Crude Coconut Oil (CCO) in overcoming

the swelling problem. The methodology used consists of drilling simulation and cutting analysis in the X-Ray Diffraction (XRD) laboratory. The series of activities in the study began with the preparation of rock layers, followed by testing the penetration rate using Water-base Mud as a comparison. After cutting analysis was carried out in the XRD laboratory of UPN "Veteran" Yogyakarta with the Rigaku tool, then replaced the type of drilling fluid Oil-base Mud with basic materials alternative to Crude Coconut Oil (CCO) and followed by a penetration test. Rate of Penetration (ROP) test results from WBM with Rheology 1 at interval A or a depth of 1.96 ft-4.92 ft is 442.8 ft/h, Rheology 2 at interval B or a depth of 4.92-10.5 ft is 118.5 ft/hr on the first day. Swelling occurred and resulted in pipe sticking at depth of 6.5 ft. Based on the Bulk Mineral analysis, clay mineral content is 23.84%. Based on the Clay Oriented, smectite dominates the clay by 29.09%. Based on MBT, shale belongs to class B (illite and mixed-layer montmorillonite illite), where this mineral can expand. Based on a Geonor As test, 5.18% of the cutting can develop when exposed to water. The drilling fluid was replaced with Oil-base Mud based on alternative Crude Coconut Oil (CCO), and obtained ROP Rheology 1 at Interval A of 492 ft/h and Rheology 2 at Interval B of 480 ft/h. The results of the Compressive Strength test interval A on the first, third, and fifth days were 31,699 psi, 42,265 psi, and 52,831 psi. The results of the Compressive Strength test interval B on the first, second, and third days were 31,496 psi, 41,517 psi, and 52,971 psi. Based on clay mineral analysis and magnitude of ROP value, is known that Crude Coconut Oil (CCO) based Oil-base Mud is effective because during the simulation, there are no drilling problems, and the resulting ROP value is greater than the first day Water-base Mud.

(Author)

Keywords: Swelling, Minerals, Crude Coconut Oil, Oil Base Mud, Rate of Penetration

Kamal Hamzah[1,2], Amega Yasutra[2], and Dedy Irawan[2], [1]PT. Medco E&P Indonesia, The Energy Building 36th Floor, SCBD Lot 11A, Jl. Jendral Sudirman, Kav. 52-53, Jakarta 12190, Indonesia; [2]Institut Teknologi Bandung Jl. Ganesha 10, Lb. Siliwangi, Kec. Coblong, Bandung, Jawa Barat 40132 Indonesia, Email: humas@itb.ac.id

Prediction of Hydraulic Fractured Well Performance using Empirical Correlation and Machine Learning

ABSTRACT

Hydraulic fracturing has been established as one of production enhancement methods in the petroleum industry. This method is proven to increase productivity and reserves in low permeability reservoirs, while in medium permeability, it accelerates production without affecting well reserves. However, production result looks scattered and appears to have no direct correlation to individual parameters. It also tend to have a decreasing trend, hence the success ratio needs to be increased. Hydraulic fracturing in the South Sumatra area has been implemented since 2002 and there is plenty of data that can be analyzed to resolve the relationship between actual production with reservoir parameters and fracturing treatment. Empirical correlation approach and machine learning (ML) methods are both used to evaluate this relationship. Concept of Darcy's equation is utilized as basis for the empirical correlation on the actual data. The ML method is then applied to provide better predictions both for production rate and water cut. This method has also been developed to solve data limitations so that the prediction method can be used for all wells. Empirical correlation can gives an R^2 of 0.67, while ML can give a better R^2 that is close to 0.80. Further-more, this prediction method can be used for well candidate selection means.

(Author)

Keywords: Hydraulic Fracturing, Well Performance, Empirical Correlation, Machine Learning.

Ainuddin, and Muhammad Adam Suryadilaga, Universitas Islam Al-Azhar Mataram, Unizar, Jl. Unizar No. 20, Turida, Kec. Sandubaya, Kota Mataram, Nusa Tenggara Barat 83232, Indonesia, E-mail: veteranlast86@gmail.com

Oil and Gas in the Dynamics of Time and Development

ABSTRACT

As a source of energy, industrial raw materials, and foreign exchange for exports, the oil and gas sub-sector has a strategic role in national development. In the period 2020-2024, the management and utilization of oil and gas resources will face several challenges. The purpose of this study is to determine the profile of oil and gas development. The method used and the description in the data is qualitative. The results of this study allow us to statistically understand cluster dynamics. The impact of this research is to map the dynamics of oil and gas as a whole.

(Author)

Keywords: Strategic, dynamics, oil and gas.
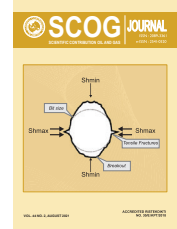
In Situ Stress and Stress Regime in the Offshore Part of the Northeast Java Basin

Agus M. Ramdhan

Applied Geology Research Group, Faculty of Earth Sciences and Technology,
Bandung Institute of Technology, Jl. Ganesa No. 10, Bandung, Indonesia
Corresponding author: agusmr@gl.itb.ac.id

ABSTRACT - In situ stress is important in the petroleum industry because it will significantly enhance our understanding of present-day deformation in a sedimentary basin. The Northeast Java Basin is an example of a tectonically active basin in Indonesia. However, the in situ stress in this basin is still little known. This study attempts to analyze the regional in situ stress (i.e., vertical stress, minimum and maximum horizontal stresses) magnitude and orientation, and stress regime in the onshore part of the Northeast Java Basin based on twelve wells data, consist of density log, direct/indirect pressure test, and leak-off test (LOT) data. The magnitude of vertical (S_v) and minimum horizontal (S_{hmin}) stresses were determined using density log and LOT data, respectively. Meanwhile, the orientation of maximum horizontal stress (S_{hmax}) was determined using image log data, while its magnitude was determined based on pore pressure, mudweight, and the vertical and minimum horizontal stresses. The stress regime was simply analyzed based on the magnitude of in situ stress using Anderson's faulting theory. The results show that the vertical stress (S_v) in wells that experienced less erosion can be determined using the following equation: $S_v = 0.7622z^{1.0201}$ where is in psi, and z is in ft. However, wells that experienced severe erosion have vertical stress gradients higher than one psi/ft ($S_v = 1.0599z^{0.9982}$). The minimum horizontal stress (S_{hmin}) in the hydrostatic zone can be estimated as $S_{hmin} = 1.0599z^{0.963}$, while in the overpressured zone, $S_{hmin} = 0.7446z^{1.0228}$. The maximum horizontal stress (S_{hmax}) in the shallow and deep hydrostatic zones can be estimated using equations: $S_{hmax} = 2.4193z^{0.9432}$ and $S_{hmax} = 2.4902z^{0.9396}$, respectively. While in the overpressured zone, $S_{hmax} = 67.743z^{0.5362}$. The orientation of S_{hmax} is ~NE-SW, with a strike-slip faulting stress regime.

Keywords: Northeast Java Basin, in situ stress, stress regime.

INTRODUCTION

Knowledge of in situ stress is very important in hydrocarbon exploration to the production stage. It will provide a better understanding of present-day deformation. Binh, *et al.* (2007) summarized that in situ stress is the main control of borehole stability, reservoir drainage and flooding, fluid flow in fractured reservoirs, hydraulic fracturing, and fault seal breach.

The onshore part of the Northeast (NE) Java Basin is tectonically located in a very active region (Figure 1). However, there is still little known about the in situ stress in this basin. The in situ stress consists of three components, i.e., vertical stress, minimum horizontal stress, and maximum horizontal stress. This study aims to analyze the stress regime and the magnitude of these stresses in the onshore part of the Northeast Java Basin on a regional basis using data from twelve wells (Figure 2).

DATA AND METHODS

A. Geological Setting

1. Tectonic and Stratigraphy

The Northeast Java Basin is a back-arc basin, particularly during Neogene (Koesoemadinata, 2020). Physiographically, the basin can be divided into several zones (Figure 2).

The study area includes Rembang Zone, Randublatung Zone, and Dander High. The deepest part of this basin is the Kendeng zone, a folded thrust zone is indicated by a negative Bouguer gravity anomaly (Figure 2).

The stratigraphy of the Northeast Java Basin is shown in Figure 3. The oldest Cenozoic formation in this basin is the Ngimbang Formation, a syn-rift Middle Eocene–Early Oligocene deposit consists of lacustrine–deltaic sandstones and mudrocks in the lower part and deep marine mudrocks with turbidite sandstone intercalations in the upper part. It is one of the main reservoirs in the Northeast Java Basin. Meanwhile, the youngest sedimentary sequence is the Lidah Formation, which consists of clay deposited in an enclosed marine environment.

The tectonic phases of this basin can be divided into the following phases (Koesoemadinata, 2020):

- Pre-rift
- Extensional rifting with syn-rift deposition in Early Eocene to Early Oligocene
- Sag phase with post-rift stable shelf deposition in Late Oligocene to Early Miocene
- Compressional phase in Middle Miocene to present-day

During the compressional phase, the onshore Northeast Java and Madura zone was down-warped and integrated into the East Java back-arc basin as compressional forces took place (Koesoemadinata, 2020).

B. Data Availability

The main data used in this study consists of density log, direct/indirect pressure test, and leak-off test (LOT) from twelve wells, as can be seen in Table 1. Direct pressure test data was obtained from Repeat
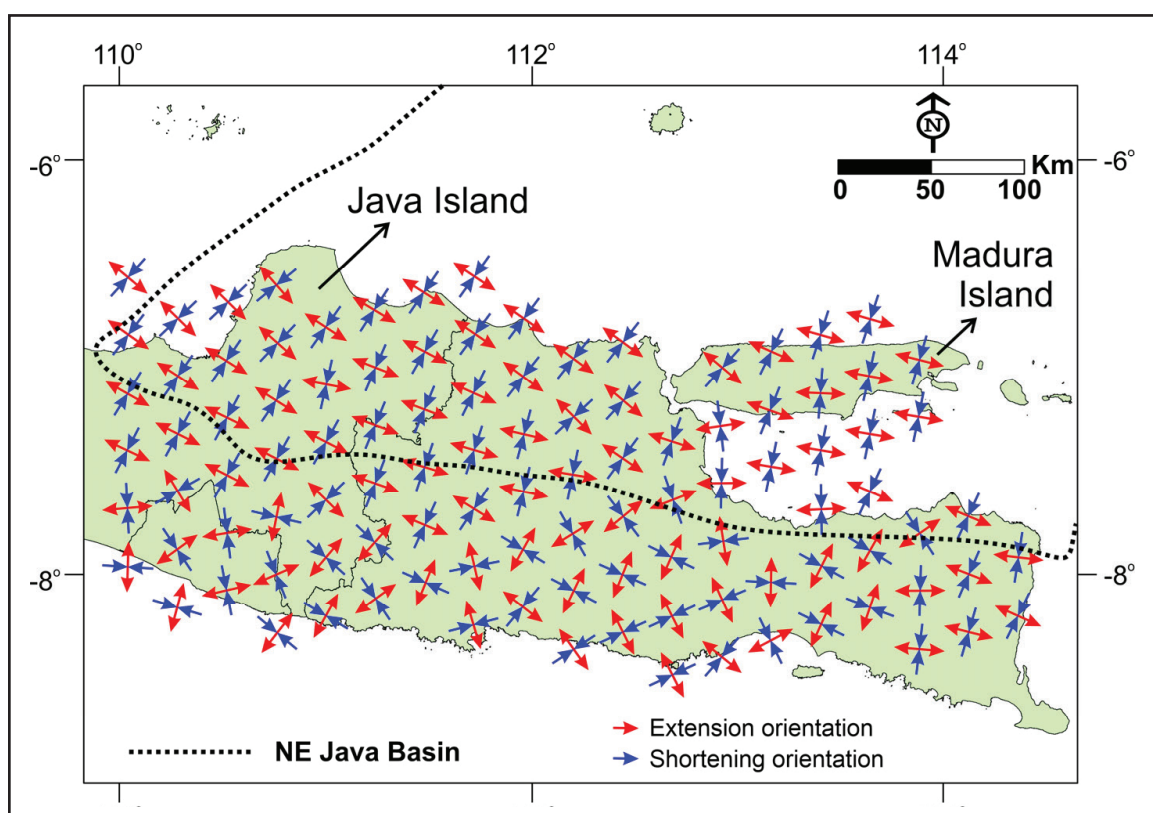
Figure 1
Map showing the orientation of extension and shortening of GPS strain
(modified from Gunawan and Widiyantoro, 2019) indicating active tectonic
in the onshore part of Northeast (NE) Java Basin (the basin boundary is from Koesoemadinata, 2020).
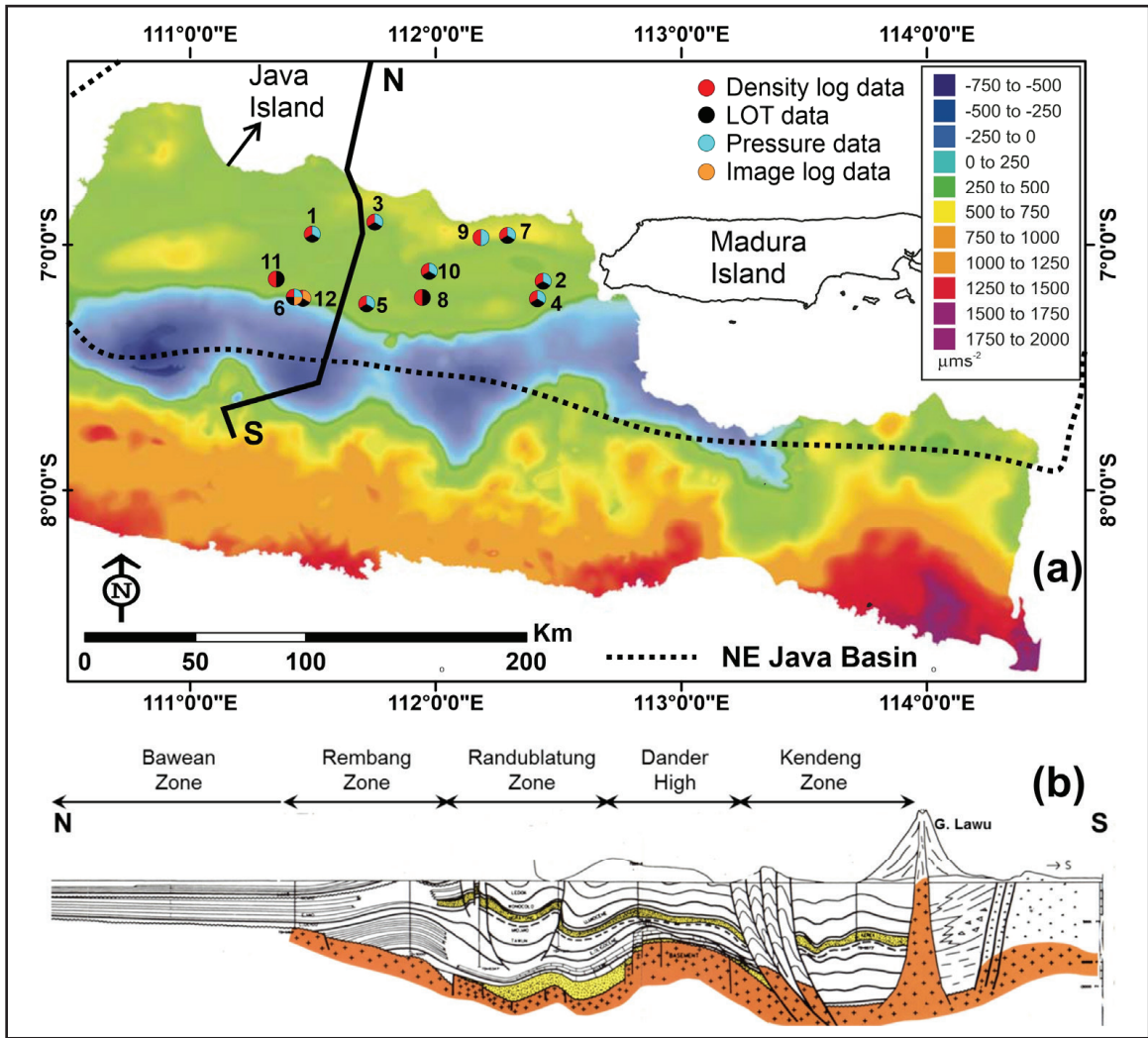
Figure 2
(a) Map showing Bouguer gravity anomaly (modified from Smyth *et al.*, 2008),
the twelve wells location, the available data, and the NE Java Basin boundary (Koesoemadinata, 2020).
(b) The cross-section showing the physiography of the NE Java Basin (Pertamina BPPKA, 1996).

Formation Tester (RFT), Modular Formation Tester (MDT), Reservoir Description Tool (RDT), and Drill Stem Test (DST). Meanwhile, the indirect pressure data were obtained based on mudweight used during the drilling and the drilling event (i.e., kick). Though most of the data are available, the number of the data for each well is limited. Therefore, a common regression analysis (power regression) was also carried out in this study.

C. Vertical Stress

Vertical stress at a given depth is simply stress due to its overlying sediment. Vertical stress in the onshore area is calculated by integrating density log as a function of depth by using this equation:

$$S_v = \int_0^z \rho_b(z)gdz \qquad (1)$$

Where S_v is vertical stress, ρ_b is bulk density of sediments, g is gravitational acceleration, and z is depth.

The data source for obtaining vertical stress is the density log. Unfortunately, this log is not always available over the entire well interval, and its quality is very much affected by hole rugosity, as found in the study area. Most of the density logs of wells on the onshore part of the Northeast Java Basin are either not complete up to the surface or in poor condition due to the presence of hole enlargement caused by washout and caving, especially in the upper section where the lithology is dominated by unconsolidated material, and also in the limestone section. Caliper log was used to select the good density log. If the caliper log indicates the presence of hole enlargement, then the density log data were eliminated from further
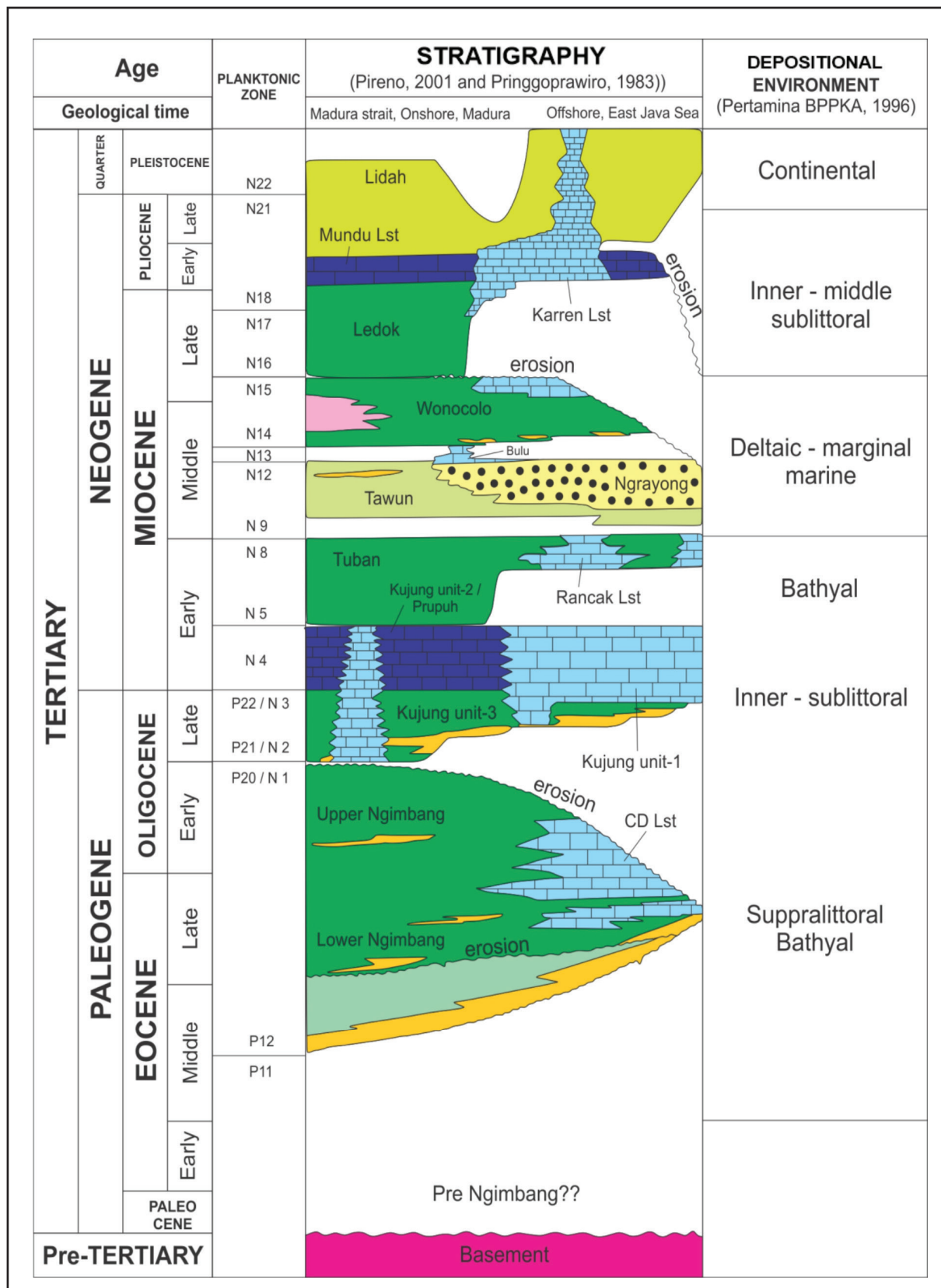
Figure 3
The stratigraphic column of the NE Java Basin
(modified after Mudjiono & Pireno (2001), Pringgoprawiro (1983), and Pertamina BPPKA (1996)).

Table 1
The summary of available data in this study.

Well	Density Log	Pressure Test	LOT
1	available	DST	available
2	available	RFT	available
3	available	Kick	available
4	available	RFT	available
5	available	RDT	available
6	available	MDT	available
7	available	DST	available
8	available	not available	available
9	available	DST	not available
10	available	RFT	available
11	available	not available	available
12	available	not available	available

analysis. The good density log data are interpolate to fill the missing or eliminated density data interval. Moreover, the density log was also manually filtered to remove the bad data reading indicated by the presence of spikes.

The most common assumption is that the average density of sediments is about 2.3 g/cm^3 down to the depth of 4-5 km. This density value gives an increase of vertical stress of 22.5 MPa/km or one psi/ft. This assumption can lead to some erroneous analyses requiring vertical stress as an input, such as pore pressure prediction and defining stress regime.

The more realistic equation relating vertical stress and depth is the power equation instead of the linear equation. This is because the density in the shallow section is relatively low, and then it is increasing through depth. It may reach a constant value at depth when the porosity approaches nearly zero.

By using this relation, the increase in vertical stress (S_v) through depth (z) follows this equation:

$$S_v = az^b \qquad (2)$$

Where a and b are empirical constants obtained by fitted vertical stress with depth.

D. Minimum Horizontal Stress

The minimum horizontal stress can be determined using leak-off test (LOT) data. A summary of several pressure data obtained from LOT as shown in Figure 4 (White, *et al.*, 2002). Basically, the LOT test is performed by pumping the drilling mud into a well. In Figure 4, it can be seen that at the beginning of the test, the pressure inside the borehole will increase linearly as the mud volume is increasing. At Point B, there is a departure from the linearity, indicating that the elasticity of the rock has reached, and it is assigned as LOP (leak-off pressure). At the departure point, the pressure decreases a little bit compared if the linearity does not break up, indicating that the hydraulic fractures start to develop. At Point C, the formation breakdown (FBP) is reached, and in this stage, the fractures will propagate, and until a certain time, the pressure in the wellbore will be relatively constant because the mud will escape into the fractures. After this stage, the pump is turned off, and the pressure will drop. The point where the pressure starts to drop (Point D) is referred to as the instantaneous shut-in pressure (ISIP). The pressure inside the wellbore continues to decrease, and the fractures will close again. The fracture closure pressure (FCP) is determined by the 'double tangent' method, i.e., the cross-point between the ISIP line and the stabilized pressure line (point E). White, *et al.* (2002) stated that ISIP and FCP are the better estimates of the minimum horizontal stress than the LOP because the LOP is affected by stress perturbation and the hoop stress surrounding the wellbore when inducing or opening a fracture.

Yassir & Bell (1994) showed that the pore pressure relates to minimum horizontal stress. They demonstrated that the minimum horizontal stress increased in overpressured zones. Therefore, the pore
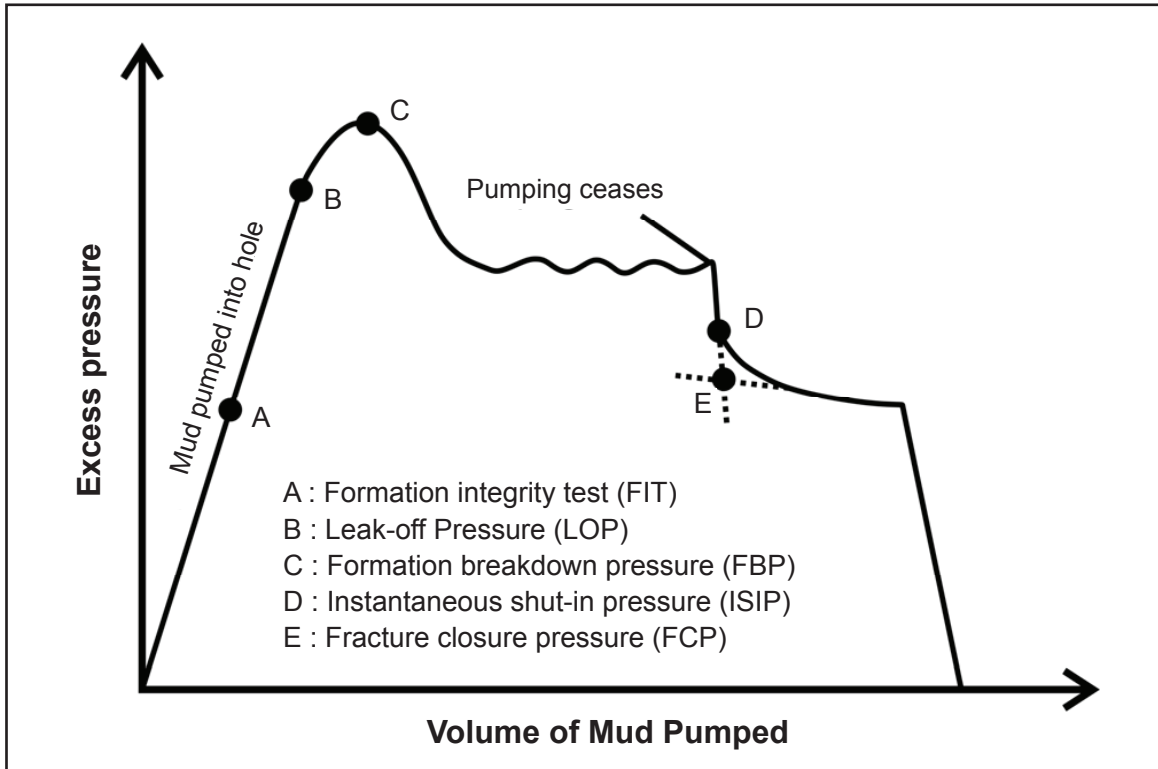
Figure 4
The schematic diagram of LOT (adapted from White *et al.*, 2002).

pressure is analyzed before determining the value of this stress in this study.

Considering the pore pressure condition, the power regression of available LOT data from all wells was used as the proxy for minimum horizontal stress. This method has been used by Breckels & van Eekelen (1982) to establish minimum horizontal stress-depth relation in several sedimentary basins. This method is considered to be realistic in order to avoid factors affecting LOP as discussed above. The available LOT is then related with depth with the following power equation to estimate the minimum horizontal stress (S_{hmin}) value:

$$S_{hmin} = az^b \qquad (3)$$

Where a and b are empirical constants obtained by fitted LOT data with depth.

Maximum Horizontal Stress

Different from the vertical and minimum horizontal stresses, the maximum horizontal stress (S_{Hmax}) cannot be determined directly. However, its orientation can be interpreted from earthquake data, borehole breakouts, and drilling-induced fractures (Binh, *et al.*, 2011).

In this study, the orientation is interpreted from available image log data. Moreover, the magnitude of S_{Hmax} at a given depth is estimated based on drilling -induced tensile fractures using the following equation (Zoback, 2007):

$$S_{Hmax} = 3S_{hmin} - P_b - P_p \qquad (4)$$

Where S_{hmin} is the minimum horizontal stress, P_b is formation breakdown pressure (equal to mud pressure used for inducing tensile fractures), and P_p is pore pressure at the given depth. However, the drilling-induced tensile fractures data in this study are only available in two wells and in a very limited depth interval.

As the vertical and minimum horizontal stresses, the relation between the maximum horizontal stress (S_{Hmax}) and depth (z) is also determined using the power equation:

$$S_{Hmax} = az^b \qquad (5)$$

Where a and b are empirical constants obtained by fitted with depth.

E. Stress Regime

The stress regime of the onshore part of the Northeast Java Basin was determined using Anderson's faulting theory. According to this theory, the stress regime can be classified into three based on the magnitude of the principal stresses (Table 2).

Jaeger & Cook (1979) showed that the value of S_1 (maximum principal stress) and S_3 (minimum principal stress) for a critically oriented fault at the frictional limit as:

$$\frac{S_1 - P_p}{S_3 - P_p} = [(\mu^2 + 1)^{0.5} + \mu^2] \tag{6}$$

Where P_p is pore pressure and μ is the coefficient of friction. For $\mu = 0.6$, the equation from Jaeger & Cook (1979) can be used to estimate the upper bound of in situ stresses using the following equation (Zoback, 2007):

$$\frac{S_v - P_p}{S_{hmin} - P_p} = 3.1 \text{ for normal faulting} \tag{7}$$

$$\frac{S_{Hmax} - P_p}{S_{hmin} - P_p} = 3.1 \text{ for strike-slip faulting} \tag{8}$$

$$\frac{S_{Hmax} - P_p}{S_v - P_p} = 3.1 \text{ for reverse faulting} \tag{9}$$

RESULTS AND DISCUSSION

A. Vertical Stress

As mentioned before, the first thing to do in constructing vertical stress is editing the density log
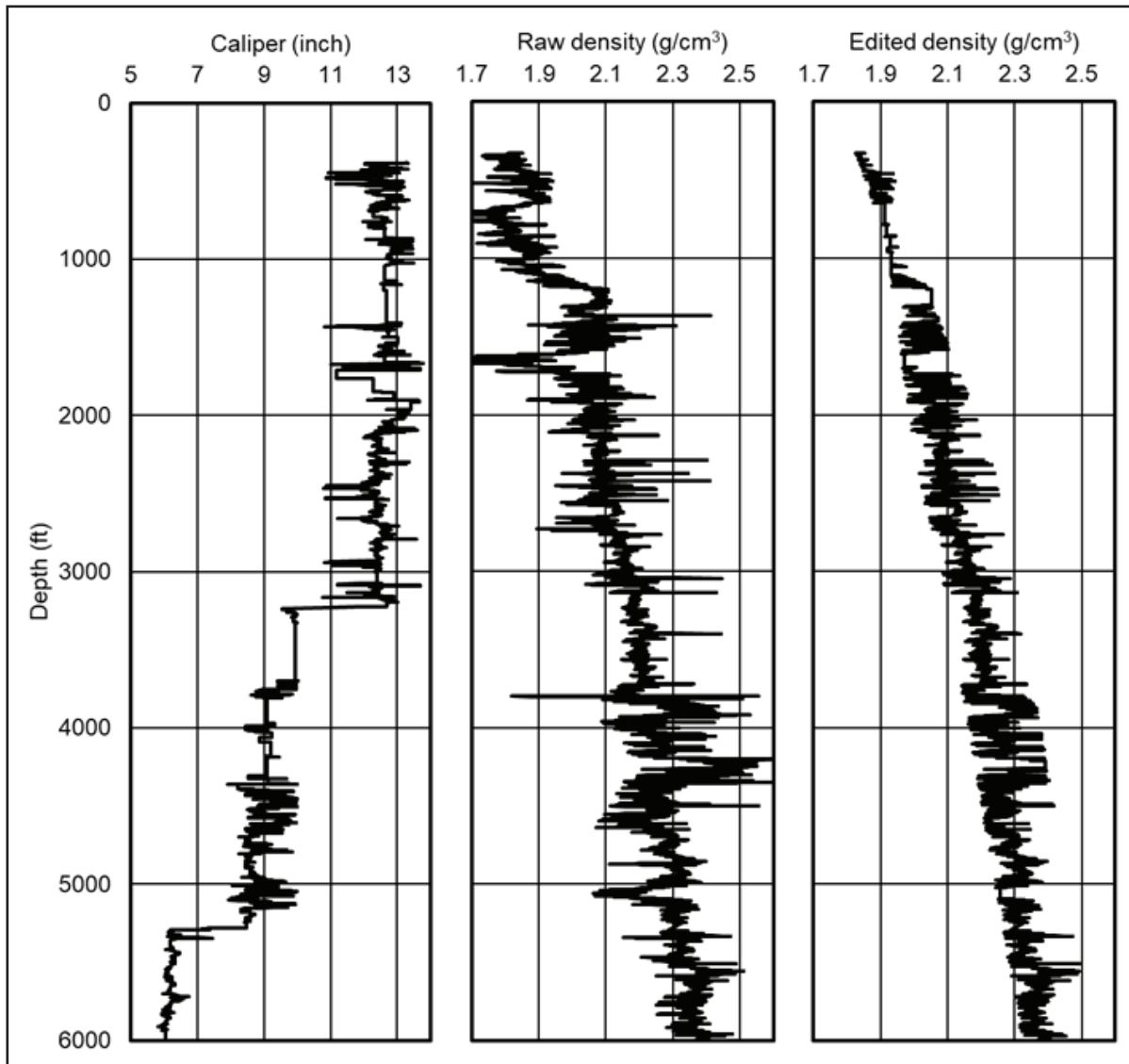
Figure 5
An example of density log editing from well number 4. It can be seen
that the edited density log shows a consistent increase of density value through depth.

based on the caliper log, and filtering it manually for unrealistic values (spikes). An example of density editing is shown in Figure 5. The data is taken from well number 4. The caliper log indicates a good hole condition in general, with some minor hole enlargement in several sections. The raw density data contain some spikes, either unreasonably high or unreasonably low. After editing some bad data points based on the above criteria, we have edited the density log as shown in the right panel of Figure 5.

By using eq. (1), the vertical stress for all wells in the study area is shown in Figure 6a. It can be seen that the vertical stress in the study area is less than one psi/ft, except for well numbers 7 and 9. These two wells have experienced severe erosion that the section with lower density values has been eroded. This is the best explanation for why the vertical stress exceeds the value of one psi/ft in those two wells. Accordingly, it can be inferred that the majority of the wells where the vertical stress is less than one psi/ft have escaped from severe erosion. Ignoring well numbers 7 and 9, the average vertical stress in the study area could be approached by the following equation:

$$S_v = 0.7622z^{1.0201} \qquad (10)$$

Where S_v is in psi, and z is in ft.

B. Minimum Horizontal Stress

As mentioned before, the minimum horizontal stress was determined from LOT data by considering the pore pressure condition. Figure 6b shows the simplified pore pressure profile in the study area. As indicated by the pressure data, the pore pressure

Table 2
The stress regime determination (Zoback, 2007)

Stress Regime	Principal Stress		
	S_1	S_2	S_3
Normal faulting	S_v	S_{Hmax}	S_{hmin}
Strike-slip faulting	S_{Hmax}	S_v	S_{hmin}
Reverse faulting	S_{Hmax}	S_{hmin}	S_v
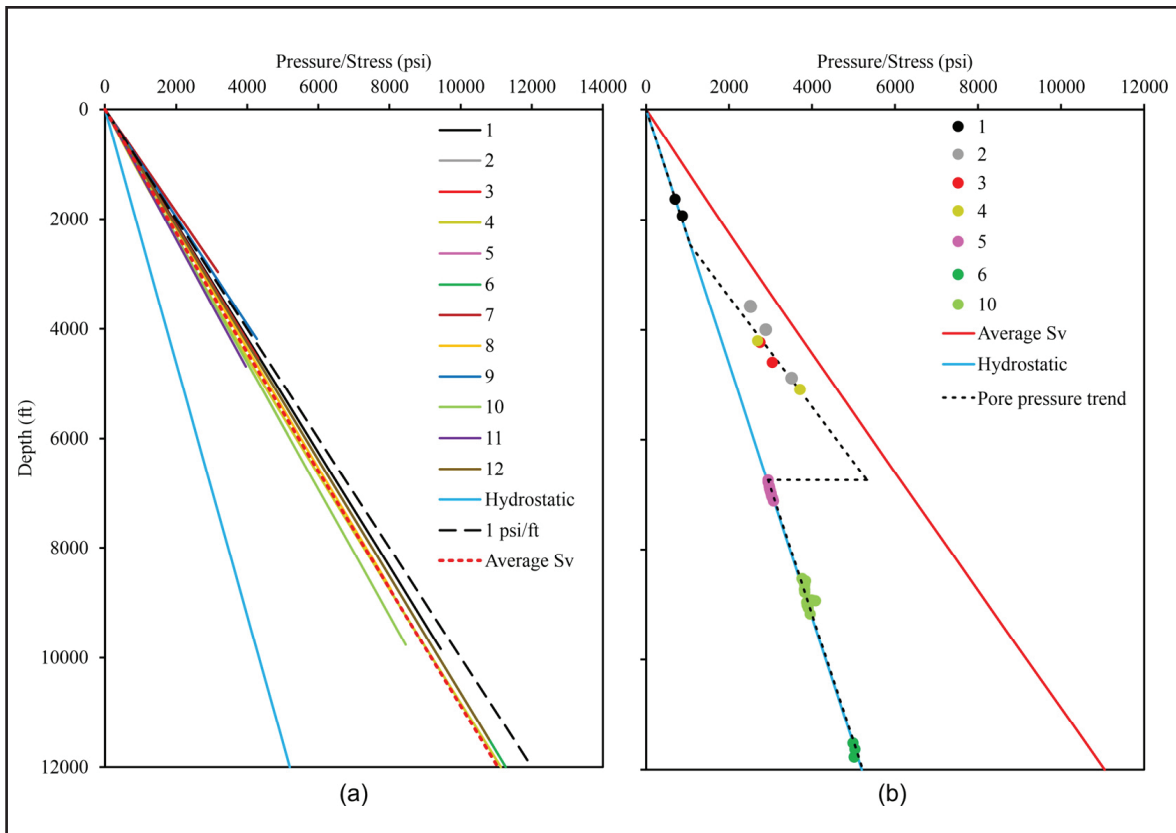
Figure 6
Diagram showing: (a) the vertical stress (S_v) in all wells and their average value (Average S_v), which is less than one psi/ft; (b) pore pressure trend based on available pressure data (colored circle).

from the surface to the depth of ~2,400 ft is hydrostatic. The overpressured zone is found from ~2,400 to ~6,750 ft. After that, the pore pressure is again in hydrostatic condition from ~6,750 ft to the total depth (TD) of wells in the study area.

It seems that the LOT data are not significantly scattered and in the range of nearly touching average vertical stress (Figure 7). The LOT data of well number 7 is greater than LOT data from other wells. It may also be related to severe erosion experienced by this well.

Ignoring LOT data of well number 7 and considering the pore pressure condition, the equations for relating minimum horizontal stress (S_{hmin}) with depth (z) in the study area are:

$$S_{hmin} = 1.0599z^{0.963} \tag{11}$$

$$S_{hmin} = 0.7446z^{1.0228} \tag{12}$$

Where S_{hmin} is in psi and is in ft. Eq. (11) is for hydrostatic zones, while eq. (12) is for the overpressured zone. The ratio of minimum horizontal stress and vertical stress (S_{hmin}/S_v) in hydrostatic zones, from 100 to 2,400 ft and from 6,750 to 12,000 ft, is in the range of 0.89 to 1.07 and 0.81 to 0.84, respectively. Meanwhile, the ratio of minimum horizontal stress and vertical stress (S_{hmin}/S_v) in the overpressured zone (2400 to 6750 ft) ranges from 0.99 to 1.

C. Maximum Horizontal Stress and Stress Regime

In order to estimate the magnitude of using eq. (4), the pore pressure and mud pressure used for inducing tensile fractures must be known. Figure 8 shows the estimated based on drilling-induced tensile fractures
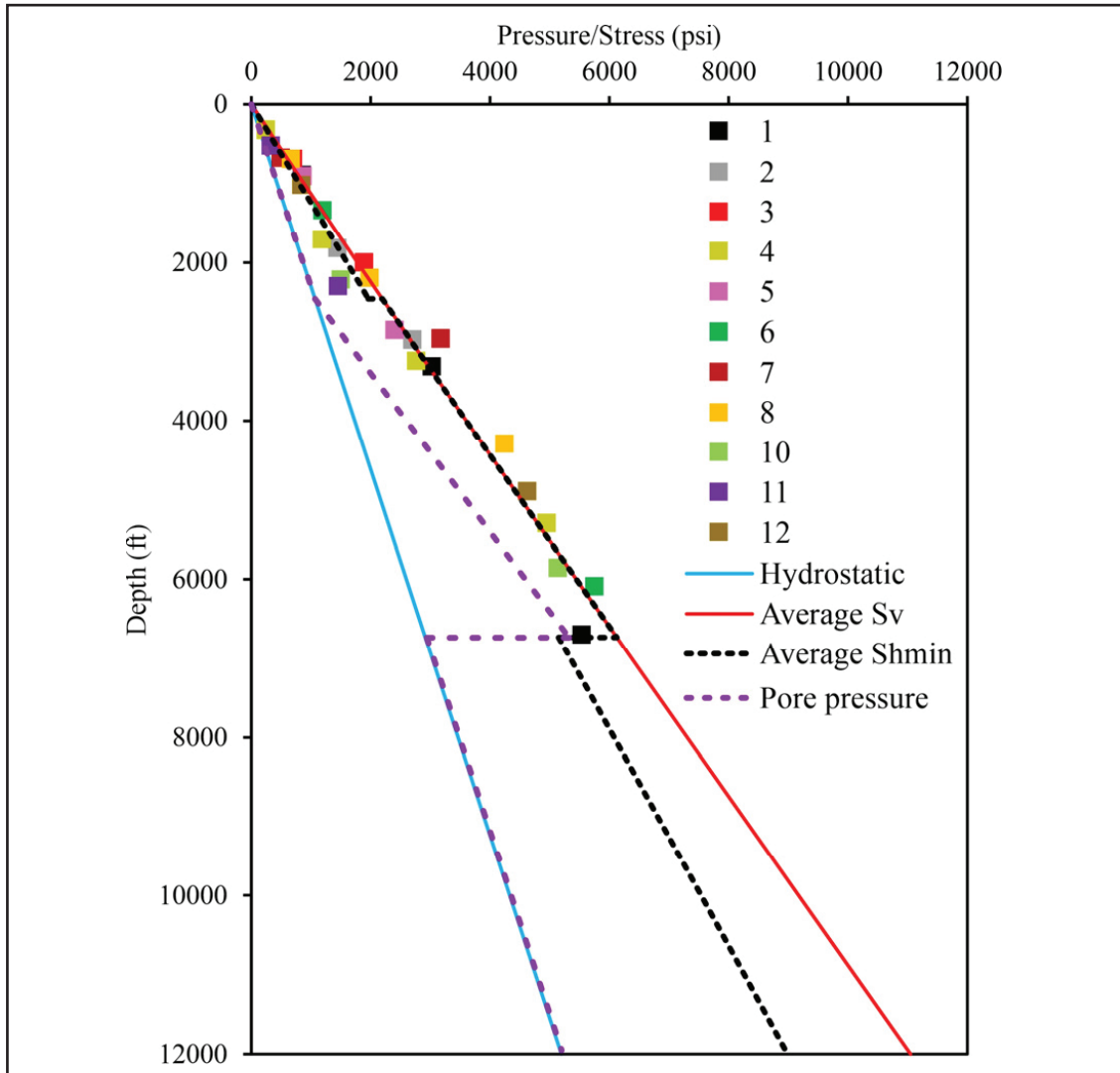
Figure 7
Diagram showing LOT data in all wells (colored box) and
the interpreted average minimum horizontal stress (Average S_{hmin}).
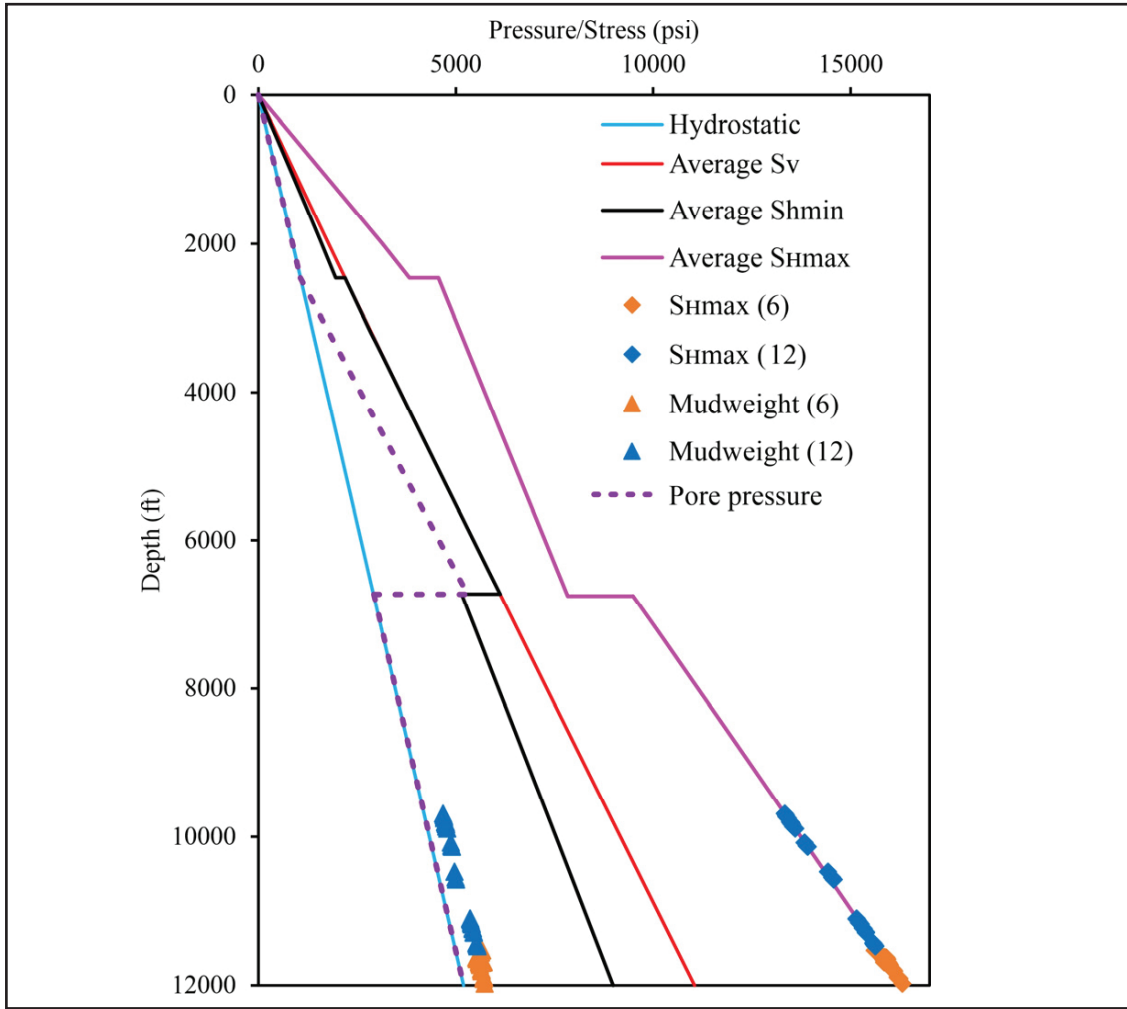
Figure 8
Diagram showing the interpreted average maximum
horizontal stress (Average S_{Hmax}); numbers 6 and 12 indicate well numbers.

(blue and orange diamonds). It is clear that the stress regime is strike-slip faulting since $S_{Hmax} > S_v > S_{hmin}$. Therefore, eq. (8) can be used to estimate the in the depth interval where image log data are not available. Like the vertical and minimum horizontal stresses, the relation of S_{Hmax} and depth (z) can be written as the following equation:

$$S_{Hmax} = 2.4193z^{0.9432} \qquad (13)$$

$$S_{Hmax} = 67.743z^{0.5362} \qquad (14)$$

$$S_{Hmax} = 2.4902z^{0.9396} \qquad (15)$$

Where S_{Hmax} is in psi and z is in ft. Eq. (13) is for the shallow hydrostatic zone (0 to 2,400 ft), eq. (14) is for the overpressured zone (2400 to 6,750 ft), while eq. (15) is for the deep hydrostatic zone (greater than 6,750 ft). The ratio of maximum horizontal stress and vertical stress (S_{Hmax}/S_v) in the hydrostatic zones, from 100 to 2,400 ft and from 6,750 to 12,000 ft, is in

the range of 1.74 to 2.23 and 1.53 to 1.61, respectively. Meanwhile, The ratio of maximum horizontal stress and vertical stress in the overpressured zone (2400 to 6750 ft) ranges from 1.25 to 2.06.

The orientation of the maximum horizontal stress was analyzed based on image log data from two wells, i.e., well numbers 6 and 12 (Figure 9). Both image logs indicate that the orientation is ~NE-SW.

As already mentioned before, well numbers 7 and 9 experienced severe erosion that the section with lower density values has been eroded. This causes the vertical stress of these wells to exceed the value of one psi/ft, while the other wells do not. The average vertical stress (S_v) of these two wells could be approached by the following equation:

$$S_v = 1.0599z^{0.9982} \qquad (16)$$

Where S_v is in psi, and z is in ft.
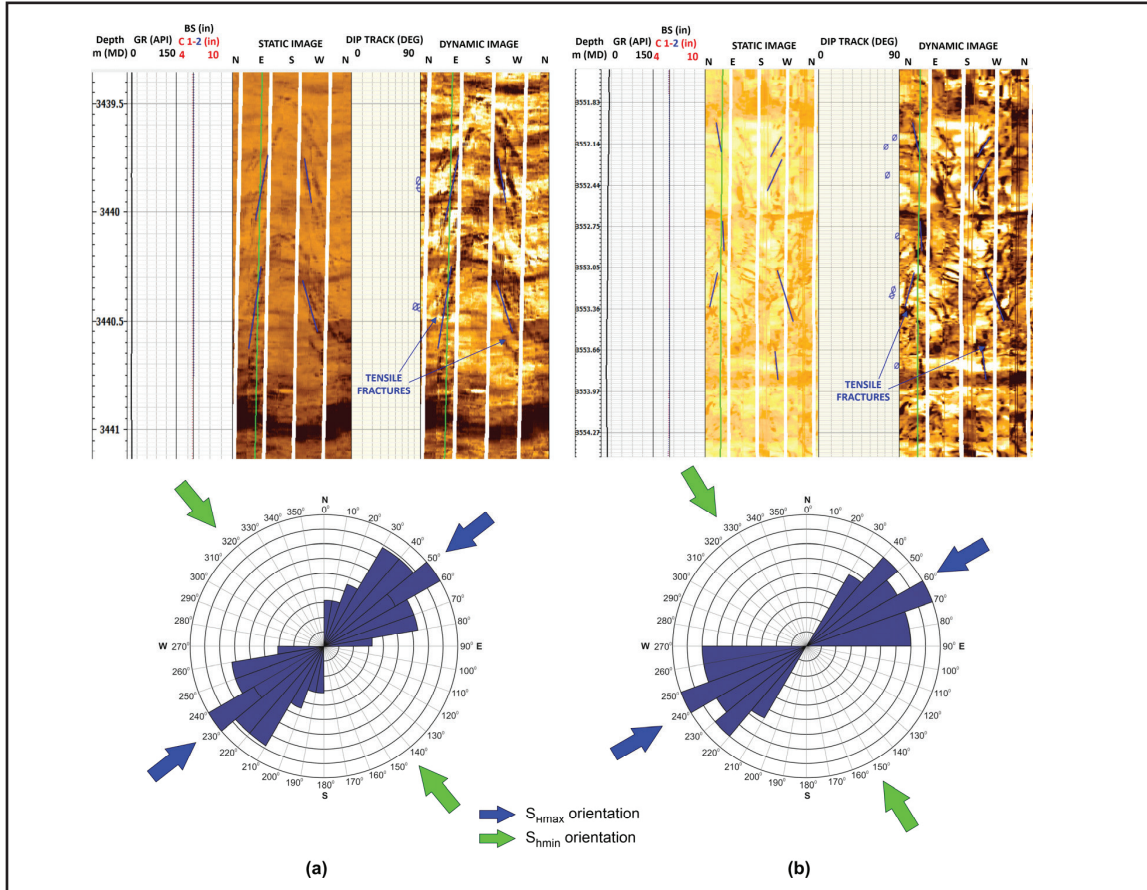
Figure 9
Image log and interpreted S_{Hmax} and S_{hmin} orientation in (a) well number 6 and (b) well number 12.
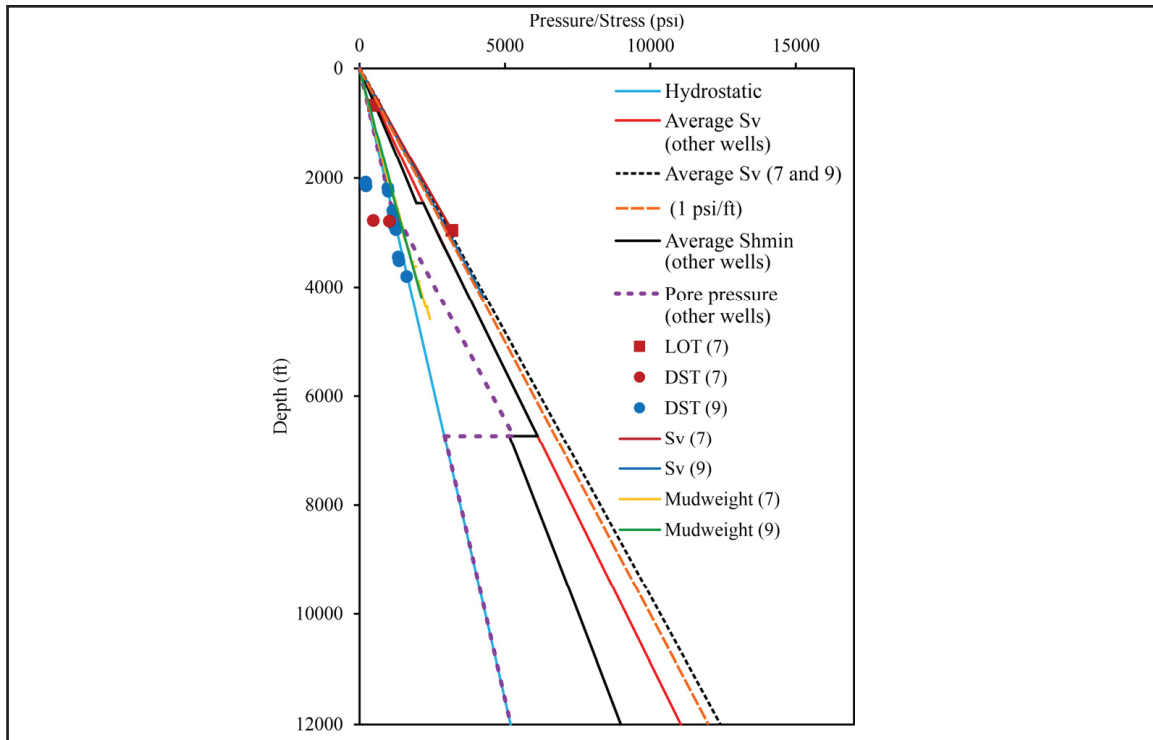
Figure 10
Diagram showing the available LOT, pressure test data (DST), and mudweight
in well numbers 7 and 9 compared to average S_v, S_{hmin}, and pore pressure in other wells.

Figure 10 shows that in these two wells, the reservoir pressure is mostly hydrostatic, though, in some depths, the reservoir pressure is depleted. Nevertheless, the mudweight used during drilling indicates that these two wells experienced slight overpressure. The LOT data of well number 7 still have the same pattern as the average S_{hmin} of other wells, i.e., in the overpressured zone, it coincides with the vertical stress.

Figures 7 and 10 show that there are no leak-off test data in the deep hydrostatic or pressure reversal zone. Thus, the in this interval can not be calibrated. However, Addis (1997) has demonstrated that pore pressure reduction is related to the significant decrease of minimum horizontal magnitude. Therefore, the real average S_{hmin} in this study could be lower than the interpreted average S_{hmin}.

CONCLUSIONS

In the onshore part of the Northeast Java Basin, the vertical stress (S_v) in wells that experienced less erosion is lower than one psi/ft, i.e., can be determined using the following equation: $S_v = 0.7622z^{1.0201}$, where S_v is in psi, and z is in ft. However, wells that experienced severe erosion have a vertical stress gradient higher than one psi/ft ($S_v = 1.0599z^{0.9982}$). The pore pressure condition in this basin can be generalized into three zones, shallow hydrostatic zone from the surface to ~2,400 ft, overpressured zone from ~2,400 to 6,750 ft, and deep hydrostatic zone in depths greater than ~6,750 ft. The minimum horizontal stress (S_{hmin}) in the hydrostatic zone can be estimated as $S_{hmin} = 1.0599z^{0.963}$, while in the overpressured zone, $S_{hmin} = 0.7446z^{1.0228}$. The maximum horizontal stress (S_{hmax}) in the shallow and deep hydrostatic zones can be estimated using equations: $S_{hmax} = 2.4193z^{0.9432}$ and $S_{hmax} = 2.4902z^{0.9396}$, respectively. While in the overpressured zone, $S_{hmax} = 67.743z^{0.5362}$.

The interpreted stress regime in the onshore part of the Northeast Java Basin is strike-slip faulting since the $S_{hmax} > S_v > S_{hmin}$. Moreover, the result of image log analysis indicates that the orientation of S_{hmax} is ~NE-SW.

ACKNOWLEDGEMENT

GLOSSARY OF TERMS

Symbol	Definition	Unit
Bouguer gravity anomaly	the difference between measured gravity and known or modeled gravity values	
Caving	borehole collapse	
Hydrostatic	fluid pressure which is solely depended on the fluid density	
Kick	flux of fluid from formation into the borehole during drilling	
Maximum horizontal stress	the maximum stress in horizontal direction	
Minimum horizontal stress	the minimum stress in horizontal direction	
Mudweight	drilling mud with certain density	
Overpressure	fluid pressure that is greater than hydrostatic	
Pore pressure	the pressure of fluid in the pore space of rocks	
Vertical stress	stress that works in vertical direction due to the overlying material	
Washout	borehole enlargement	

REFERENCES

Addis, M., 1997. *The stress-depletion response of reservoirs.* San Antonio, Texas, Society of Petroleum Engineering (SPE), p. 55-65.

Binh, N. T. T., Tokunaga, T., Goulty, N.R., Son, H.P., & Binh, M.V., 2011. Stress state in the Cuu Long and Nam Con Son basins, offshore Vietnam. *Marine and Petroleum Geology,* 28(5), pp. 973-979.

Binh, N. T. T., Tokunaga, T., Son, H. P. & Binh, M., 2007. Present-day stress and pore pressure fields in the Cuu Long and Nam Con Son Basins, offshore Vietnam. *Marine and Petroleum Geology,* 24(10), pp. 607-615.

Breckels, I. & van Eekelen, H., 1982. Relationship between horizontal stress and depth in sedimentary basins. *Journal of Petroleum Technology,* 34(09), p. 2191–2199.

Gunawan, E. & Widiyantoro, S., 2019. Active tectonic deformation in Java, Indonesia inferred from a GPS-derived strain rate. *Journal of Geodynamics,* Volume 123, pp. 49-54.

Jaeger, J. & Cook, N., 1979. *Fundamentals of Rock mechanics.* 2nd ed. New York: Chapman and Hall.

Koesoemadinata, R. P., 2020. *An Introduction into The Geology of Indonesia, Volume I: General Introduction & Part 1 Western Indonesia.* Bandung: Ikatan Alumni Geologi, Institut Teknologi Bandung.

Mudjiono, R. & **Pireno, G. E.**, 2002. *Exploration of the North Madura Platform, Offshore East Java, Indonesia.* Indonesia, Indonesian Petroleum Association.

Pertamina BPPKA, 1996. *Petroleum Geology of Indonesian Basins: Principles, Methods and Application.* Indonesia: Pertamina-BPPKA.

Pringgoprawiro, H., 1983. *Revisi Stratigrafi Cekungan Jawa Timur Utara dan Paleogeografinya.* Bandung: Institute of Technology Bandung. Unpublished.

Smyth, H. R., Hall, R. & **Nichols, G. J**., 2008. Cenozoic volcanic arc history of East Java, Indonesia: The stratigraphic record of eruptions on an active continental margin. *Geological Society of America Special Paper,* Volume 436, pp. 199-222.

White, A. J., Traugott, M. O. & **Swarbrick, R. E.**, 2002. The use of leak of test as mean of predicting minimum. *Petroleum Geoscience,* 8(2), pp. 189-193.

Yassir, N. A. & **Bell, J. S.,** 1994. Relationships between pore pressures, stresses and present-day geodynamics in the Scotian Shelf. *Offshore Eastern Canada,* Volume 78, p. 1863–1880.

Zoback, M. D., 2007. *Reservoir Geomechanics.* Cambridge: Cambridge.
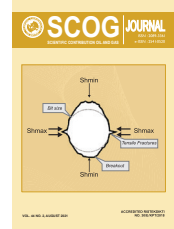
Source Sink Matching for
Field Scale CCUS CO$_2$-EOR Application in Indonesia

Usman Pasarai, Dadan DSM Saputra, and Nurus Firdaus

"LEMIGAS" R & D Centre for Oil and Gas Technology
Jl. Ciledug Raya, Kav. 109, Cipulir, Kebayoran Lama, P.O. Box 1089/JKT, Jakarta Selatan 12230 INDONESIA
Tromol Pos: 6022/KBYB-Jakarta 12120, Telephone: 62-21-7394422, Faxsimile: 62-21-7246150

Corresponding author: usman@esdm.go.id

ABSTRACT - The carbon capture utilization and storage (CCUS) referred in this paper is limited to the use of CO$_2$ to the enhanced oil recovery (CO$_2$-EOR). The CCUS CO$_2$-EOR technology can magnify oil production substantially while a consistent amount of the CO$_2$ injected remains sequestrated in the reservoir, which is beneficial for reducing the greenhouse gas emission. Therefore, this technology is a potentially attractive win-win solution for Indonesia to meet the goal of improved energy supply and security, while also reducing CO$_2$ emissions over the long term. The success of CCUS depends on the proper sources-sinks matching. This paper presents a systematic approach to pairing the CO$_2$ captured from industrial activities with suitable oil fields for CO$_2$-EOR. Inventories of CO$_2$ sources and oil reservoirs were done through survey and data questionnaires. The process of sources-sinks matching was preceded by identifying the CO$_2$ sources within the radius of 100 and 200 km from each oil field and clustering the fields within the same radius from each CO$_2$ source. Each cluster is mapped on the GIS platform included existing and planning right of way for trunk pipelines. Pairing of source-sink are ranked to identify high priority development. Results of this study should be interest to project developers, policymakers, government agencies, academicians, civil society and environmental non-governmental organization in order to enable them to assess the role of CCUS CO$_2$-EOR as a major carbon management strategy.

Keywords: CCUS, source-sink match, CO$_2$-EOR, CO$_2$ emission, carbon management.

How to cite this article:

Usman Pasarai, Dadan DSM Saputra, and Nurus Firdaus, 2021, Source-Sink Matching for Field Scale CCUS CO$_2$-EOR Application in Indonesia, Scientific Contributions Oil and Gas, 44 (2) pp., 97-106.

INTRODUCTION

Indonesia is a long-standing producer of crude oil, though production has fallen steadily for more than 25 years (SKK Migas, 2019). Applying enhanced oil recovery (EOR) techniques in mature oil fields is one of main option of boosting oil production. The only type of EOR that has been deployed in Indonesia so far on a commercial scale is steam flooding. There may be extensive opportunities for EOR in Indonesia, given the maturity of many of the country's oilfields.

Carbon dioxide enhanced oil recovery (CO$_2$-EOR) as variant of EOR technologies that has been practiced for decades worldwide on a commercial scale to improve the recoverable oil is attracting interest for Indonesia recently. By implementing CO$_2$ EOR, it is also will make some CO$_2$ injected become stored in underground formation by the stratigraphic trapping, residual trapping and solubility trapping that happened in the reservoir. The volume of CO$_2$ that can be stored in this way depends on properties of the reservoir and the oil it contains, and on

operational factors of oil production, including well spacing and the relative position of injection and producing wells (OECD/IEA 2015).

CO_2-EOR used with the purpose of storing CO_2 from anthropogenic sources is a type of carbon capture, utilization, and storage (CCUS) technology and has gained confidence as a climate mitigation strategy evidenced by stakeholder acceptance rather recently (International Energy Agency (IEA), 2020). CCUS involves the capture of CO_2 from large point sources, including industrial processes or power generation that use either fossil fuels or biomass for fuel. The captured CO_2 is compressed and transported by pipeline, ship, rail or truck to be used as a feedstock to create valuable products, or injected into oil reservoirs to enhanced oil recovery before being permanently stored. CCUS referred in this paper is limited to the use of CO_2 for enhanced oil recovery, citied here as CCUS CO_2-EOR.

The CCUS CO_2-EOR is a potentially attractive to win-win solution for Indonesia in meeting the goal of increased oil production while also reducing CO_2 emissions over the long term. Energy use and CO_2 as the primary greenhouse gas (GHG) emissions in Indonesia are growing briskly in response to economic and population growth and continuing heavy reliance on coal and other fossil fuels. Under the nationally determined contribution to the United Nations Framework Convention on Climate Change, the Government of Indonesia is committed to reducing national emissions of CO_2 and other GHGs by 29% below a baseline trend by 2030 unconditionally and by up to 41% on the condition that international support for finance, technology transfer, and capacity building is made available.

The development of CCUS CO_2-EOR to date has been concentrated in the United States, which is home to almost half of operating facilities. This is due to in large part to the availability of an extensive CO_2 pipeline network and demand for CO_2-EOR. There are 15 CCUS CO_2-EOR projects in operation around the globe with capacity to capture up to 30 million tone (MtCO$_2$) each year (International Energy Agency (IEA), 2020)**.** Figure 1 shows the relative scale of the capture capacity from various industrial facilities including coal power plants. Most of the CO_2 captured comes from natural gas processing plant. The success of CCUS CO_2-EOR depends on appropriate pairings of sources and suitable oil reservoirs for CO_2-EOR as sinks. A good CO_2 source is able to supply constant CO_2 to the sink within certain period while suitable sink has injectivity correspond to the CO_2 supply rate and sufficient storage capacity (Usman, *et al..*, 2014; Chon, *et al.*, 2019).

Source-sink matching process involves analysis of matching the demand and supply of CO_2 in which the characteristics CO_2 produced from the industrial sources are matched to oil reservoirs properties.
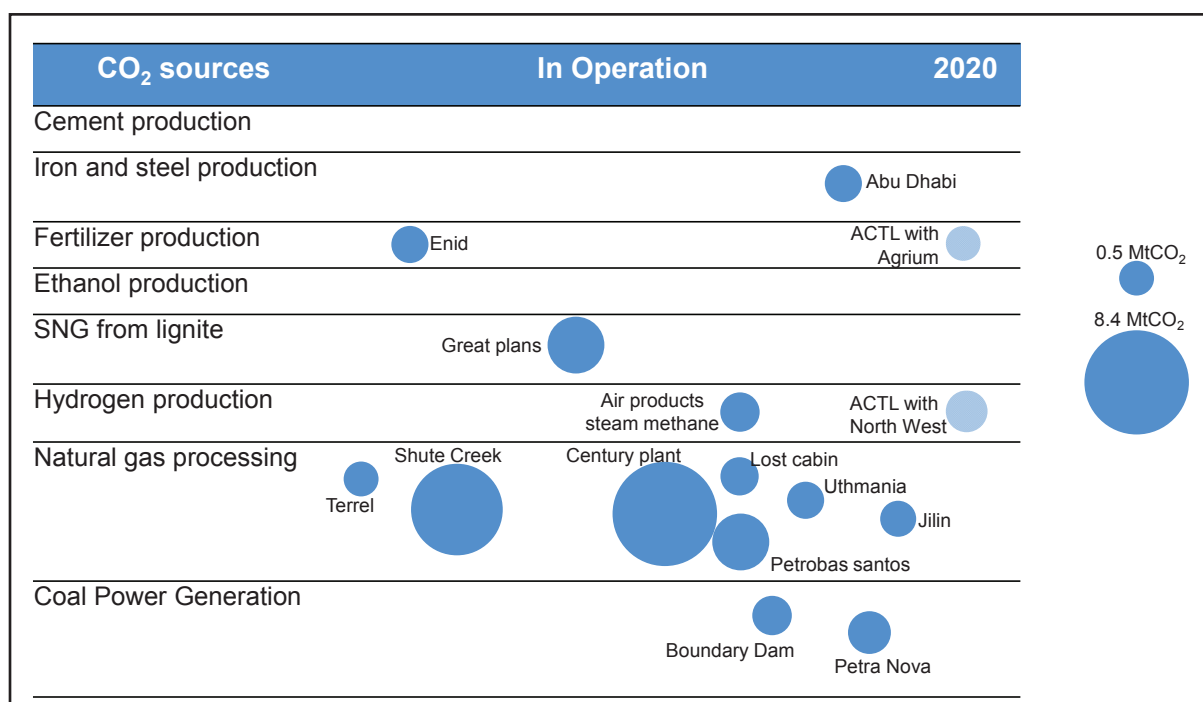
Figure 1
Large-scale commercial CCUS CO²-EOR projects in operation in 2020 (Modified from IEA, 2020).

Although, natural CO_2 fields are currently the dominant sources for the CO_2-EOR market, industrial sources of CO_2 needed in order to ensure adequate CO_2 supplies to facilitate substantial growth in oil production utilizing CO_2-EOR (Advanced Resources International, Inc., 2011). For CCUS CO_2-EOR case, the amount of CO_2 required is increased as the sink converted as CO_2 storage. Several factors affecting source-sink matching include CO_2 content, flow-rate, source type, source temperature, source pressure, formation pressure and fracture pressure. Source-sink matching provides the identification of potential CCUS CO_2-EOR that can be developed to find the least-cost pathway.

DATA AND METHODS

Methodology used in this study includes data collection of the potential fields for CO_2-EOR, screening the CO_2-EOR suitable fields and ranking the fields, data collection for CO_2 sources from oil and gas processing plants, power plants, and other industrial facilities near the potential CO_2-EOR fields, matching between the potential CO_2-EOR candidates and CO_2 sources, and making prioritization for CCUS CO_2-EOR.

Choosing the CO_2-EOR suitable fields is performed using screening criteria provided by Taber, *et al* (1997) and modified by Al Adasani & Bai (2011) as shown in Table 1. The oil fields screened are limited to the fields under operated by Indonesia's state-owned oil and gas company.

This study focuses only on large stationary source CO_2 emitters to which CCUS CO_2-EOR might be applied, such as coal power plant, oil refineries, gathering station, gas flare, industries such as fertilizer, ammonia, iron and steel, cement, and from naturally occurring underground reservoirs. The point sources are technically amenable to CO_2 capture and transportation to oil fields for CO_2 injection. The data inventory is executed through survey, received reports, and interviews to the operators.

Table 1
CO_2-EOR screening criteria (Taber, *et al*., 1997)

No	Oil and Reservoir Characteristics		Recommended	Range of Current Projects
	Crude Oil			
1	Gravity	API	>22	27 to 44
2	Viscosity	cP	<10	0.3 to 6.0
3	Composition		High percentage of intermediate hydrocarbons (especially C_5 to C_{12})	
	Reservoir			
4	Oil saturation	%PV	>20	15 to 70
5	Type of formation		Sandstone to carbonate and relatively thin unless dipping.	
6	Average permeability		Not critical if sufficient injection rates can be maintained.	
7	Depth and temperature		For miscible displacement, depth must be great enough to allow injection pressure greater than Minimum Miscible Pressure (MMP), which increase with temperature [Ref 1] and for heavy oils. Recommended depths for CO_2 floods of **typical Permian Basin** oils follow:	
			Oil Gravity, °API	Depth must be greater than (ft)
	For CO_2-miscible flooding		>40	2,500
			32.0 to 39.9	2,800
			28.0 to 31.9	3,300
			22.0 to 27.9	4,000
			<22.0	Fails miscible, screen for immiscible
	For CO_2-immiscible flooding		13.0 to 21.9	1,800
	(lower oil recovery)		<13.0	All oil reservoirs fail at any depth
	At<1,800 ft, all reservoirs fail screening criteria for either miscible or immiscible flooding with supercritical CO_2			

A source-sink matching process based on Geographical Information Systems (Arc-GIS) is established to facilitate data management, evaluation, modeling and generate information related to location-based CCUS CO_2-EOR implementation then visualize on informative map. The source-sink matching methodology is given in Figure 2, modified from Chen, *et al.*(2011).

Source and sink matching for CCUS CO_2-EOR applied using radial clustering method. For every candidate CO_2-EOR field paired with the potential CO_2 sources within radius of 100 km and 200 km to be a CCUS CO_2-EOR cluster system with the field candidate as sink at the center of radius. Data such as administrative territory boundary, road network, fields location, sources location, pipeline network, and oil and reservoir properties are needed for the Arc-GIS system development. All data is then integrated

and synchronized in the map by making tables to be converted into GIS format. Collection of basic and thematic maps in GIS integrated in vector format. Raster format maps are converted into vector format through the digitization process.

Making prioritization for CCUS CO_2-EOR cluster development is based on the rank of selected oil fields. Ranking oil fields correspond to oil gravity, degree of miscibility as function of minimum miscible pressure (MMP), remaining oil, proximity to CO_2 source, existing infrastructure, and the amount of CO_2 availability. Range of values of those parameters is divided into three classes, which are Class A, B, and C reflects degree of conformity. Class A is least conformity given scored 1, Class B scored 3 has moderate conformity, and Class C is most conformity given a score of 5. Table 2 provides detailed classification of the parameter.
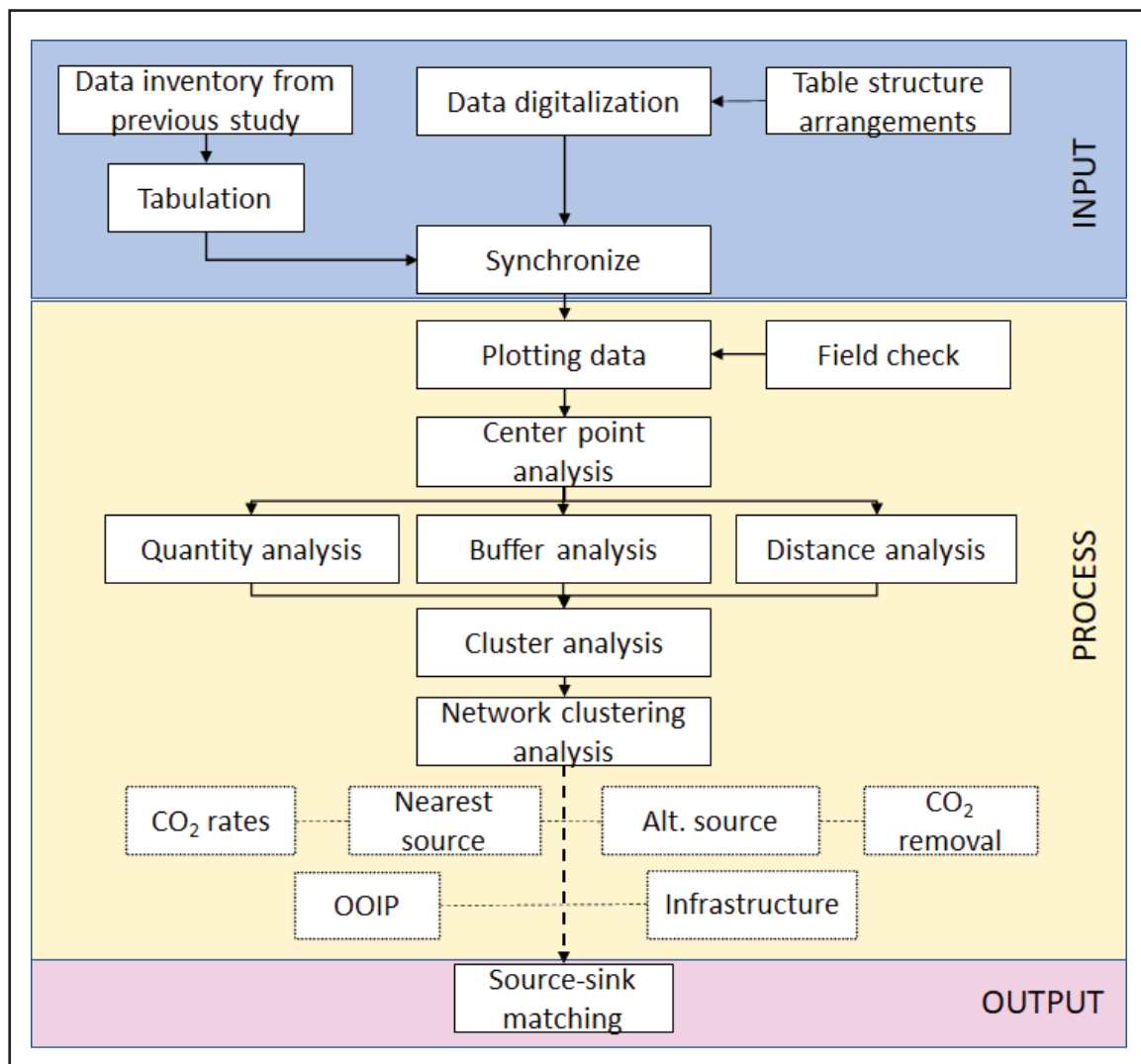
Figure 2
CCUS CO_2-EOR source-sink matching methodology (Firdaus, *et al.*, 2019).

Each parameter is specified a weight that reflects its relative importance among the set of parameters based on expert judgment. Weighting parameter is determined using Pareto Chart method. Total of 40 experts gives their view of which parameters the most importance on making priority list for the source-sink matching process. Number of judgements and weighting scale for each parameter are given in Figure 3. The weighting scale for each parameter is the subtotal for that parameter divided by the total for all categories.

Table 2
Classification parameter (Chon, *et.al*., 2019)

Parameter		Class A	Class B	Class C
Oil gravity	°API	<30	30 - 35	>35
Miscibility		immiscible	near miscible	miscible
Remaining oil	MMstb	<100	100 - 200	>200
Proximity	km	>100	50 - 100	<50
Infrastructure		offshore, far to CO_2 source	onshore, far to CO_2 source	onshore, close to CO_2 source
CO_2 amount	Kt/day	<10	20-Oct	>20
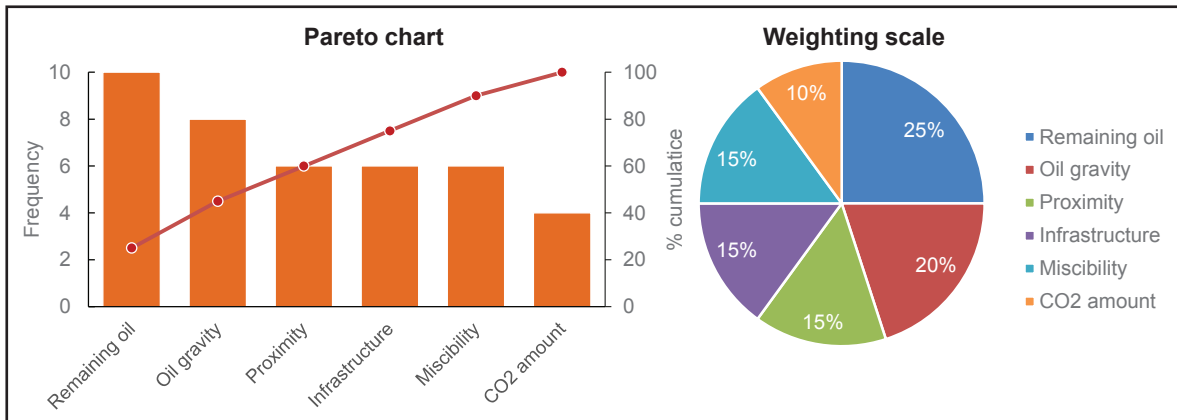
Figure 3
Pareto chart and weighting scale for each of classification parameter.
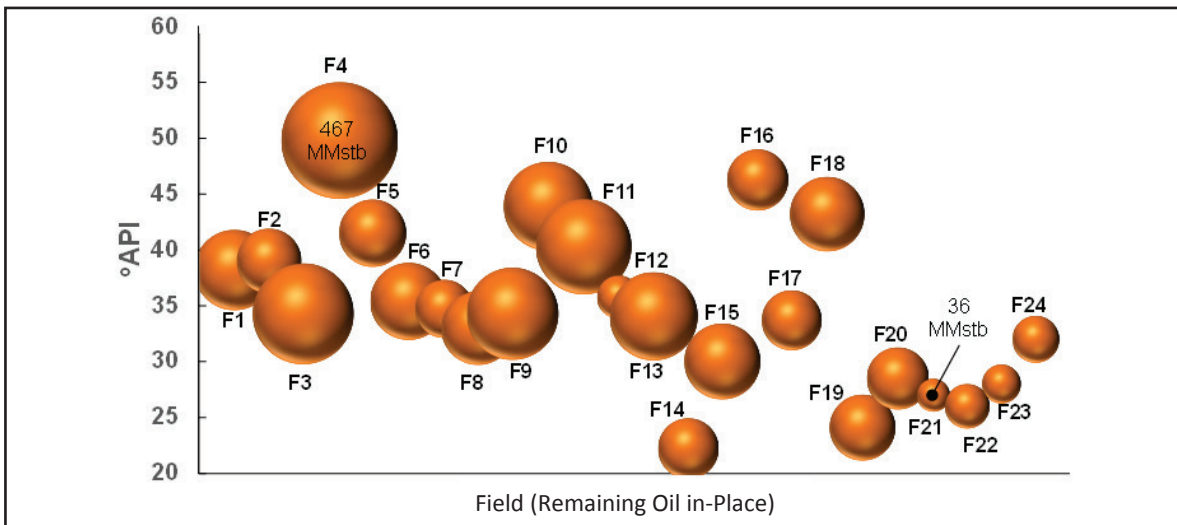
Figure 4
3D bubble map showing relationship between remaining oil in-place with °API gravity from the selected mature oil fields.

Table 3
CO_2 sources from selected industrial activities for CO_2-EOR

CO_2 Source	Method	CO_2 (Mt/year)
Power plant	Data Survey 2018	135.911
Petroleum refinery	Data Survey 2018	2.456
Gas gathering station	Data Survey 2018	5.042
Industry facilities	Data Survey 2018	22.053
Gas flaring	Data Survey 2018	0.897
From underground reservoirs	Data Survey 2018	3.268
TOTAL		169.627
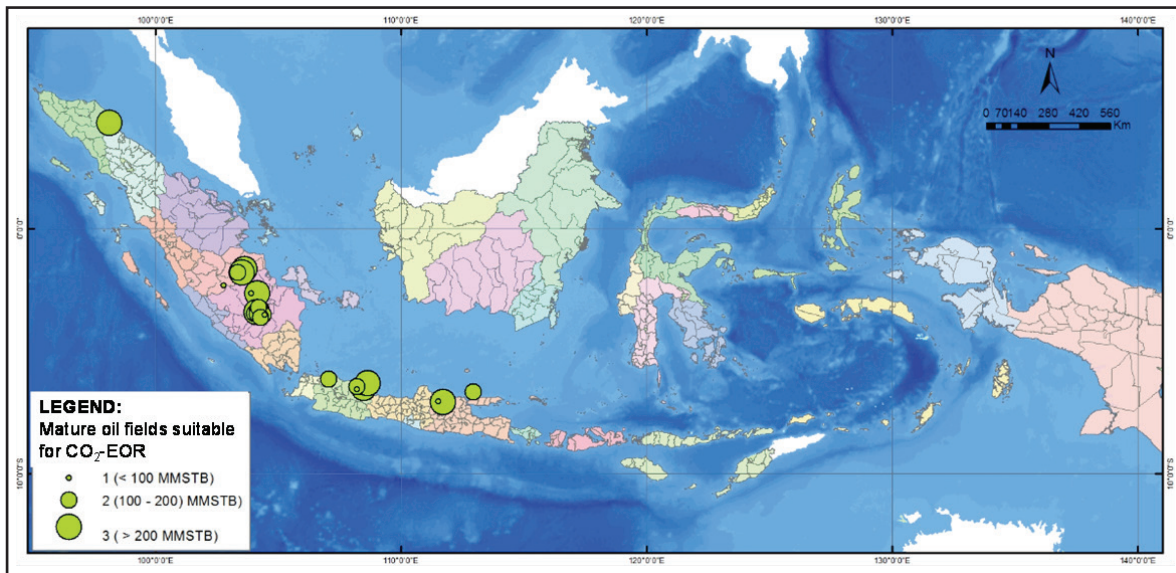
Figure 5
Location of the mature oil field candidates for CO_2-EOR.
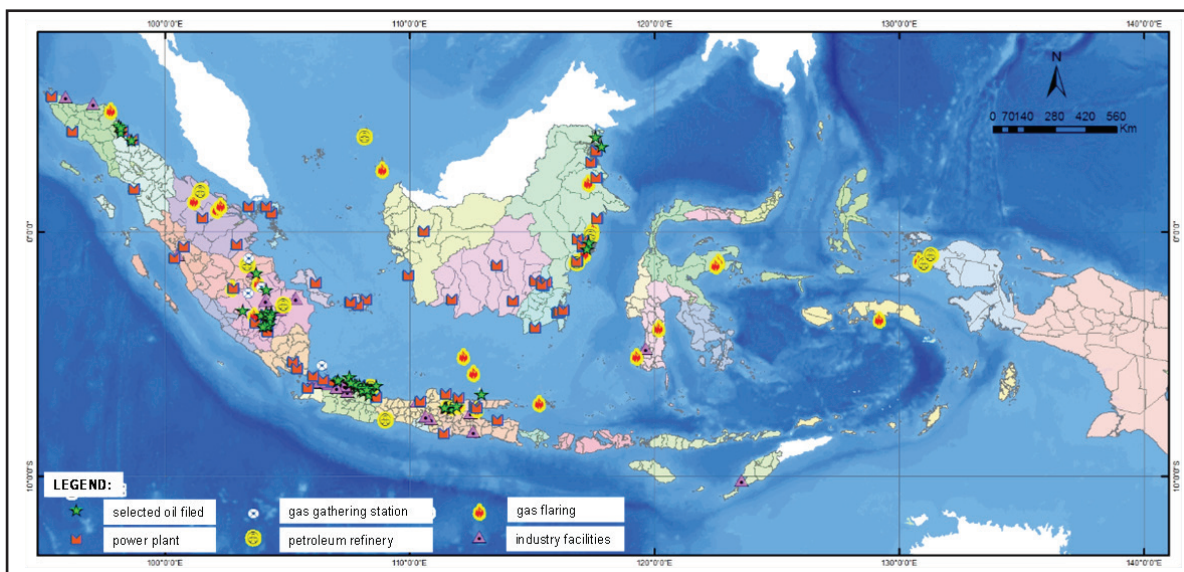
Figure 6
CO_2 source and sinks on GIS map.

RESULTS AND DISCUSSION

There are 24 oil field candidates for CO_2-EOR with the total remaining oil in-place of 4.3 Billion barrel are selected. The range from 36 MMstb to over 467 MMstb of oil and the gravity value ranged from 26 to 50 °API. Of the selected mature oil fields, there of 21 fields would achieve miscible processes, 3 fields would immiscible. Minimum miscible pressure (MMP) calculation using Yellig & Metcalfe (1980) and Lee (1979) correlations which use reservoir temperature parameter are used to determine the miscibility condition in the oil fields. A 3-D bubble map shows relationship between remaining oil in-place with the gravity for 24 selected mature oil fields depicted in Figure 4. Most of the fields concentrated in South Sumatra, West Java, and East Java regions as shown on GIS map in Figure 5.

Totally 176 CO_2 sources are estimated and their emissions amount to around 170 $MtCO_2$/year, with power, industry facilities, and others sharing 80%, 13%, and 7% respectively, as detailed in Table 3. The industries which give abundant amount of CO_2 emission are oil and gas, mining, cement, petrochemical, and also pulp and paper.

Arc-GIS has been established to pair each of selected oil fields with CO_2 sources within the radius of 100 km and 200 km from a selected oil field. All data needed for the source-sink matching process have been integrated into the Arc-GIS make easy to display, consume, and analyze geographically. An example of GIS map with CO_2 sources and sinks is given by Figure 6. It can be seen that within South

Sumatra, West Java, and East Java regions are many large stationary sources of CO_2 that can be captured, therefore promise of CCUS CO_2-EOR cluster deployment.

The field ranking based on the classification parameter and the weighting method presented by Figure 7. The top five cluster highest scoring for CCUS CO_2-EOR implementation are F1, F2, F3, F4, and F5 oil fields. These results are consistent with the operator willingness at the present time in which the operator planned to apply CO_2-EOR in these fields. Highest scoring for those five oil fields due to the proximity to abundant CO_2 sources in addition their suitability for the application of CO_2-EOR, though those five fields are not the fields that have the highest oil remaining.

The F1 oil field which located in South Sumatra surrounded by several potential CO_2 sources in the 100 km and 200 km radius come from petrochemical, fertilizer, pulp and paper facilities, coal power generation, and oil refinery plant. CO_2 can also be supplied from gas processing plant that separated CO_2 from the oil and gas fields production. Within 100 km radius, there are 3 gas processing plants, 1 oil refinery plant, 1 gas power generation plant, 1 petrochemical and fertilizer facility, and 1 ceramic facility. For CO_2 sources in 200 km radius from the F6 field, there are additional potential CO_2 source from 1 coal power plant, 2 pulp and paper facilities, 1 gas refinery, and 2 gas processing plants. Figure 8 shows the candidate of CCUS CO_2-EOR for the F6 cluster.
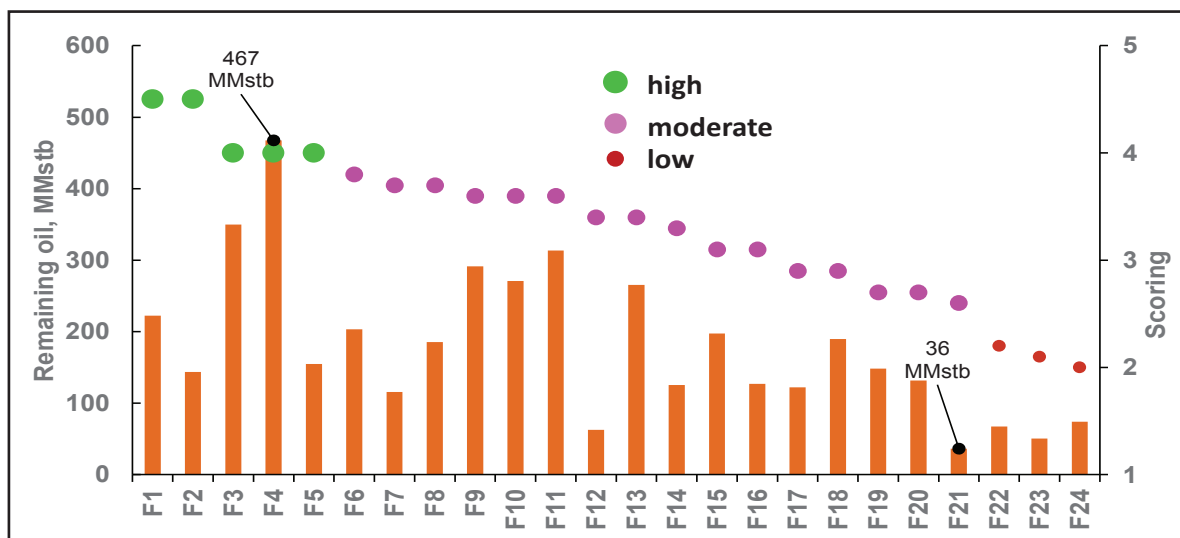
Figure 7
Ranking of candidates for CCUS CO_2-EOR cluster presented in high, moderate, and low priority.
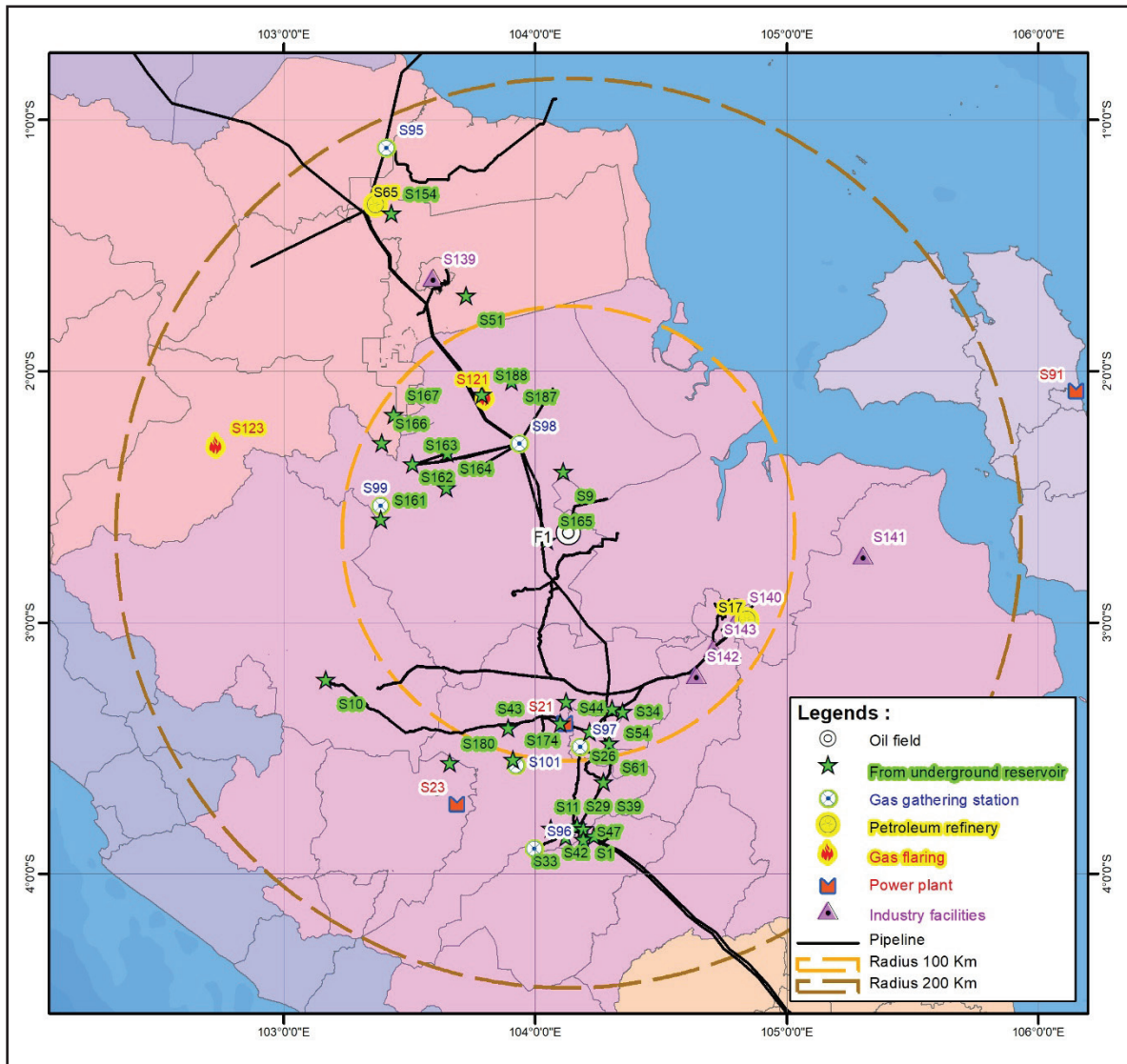
Figure 8
Candidate of F1 CCUS CO_2-EOR cluster.

The F2 oil field is located in East Java and one of the main focus for CCUS CO_2-EOR development in Indonesia. Through the source-sink matching analysis, found that there are several potential CO_2 sources available to be used for the future project. Within 100 km radius of F2 oil field, there are CO_2 sources from pulp and paper, cement, and petrochemical industries, coal power plant, flare, and oil refinery plant. Additional CO_2 sources come from gas fields which will be processed in the nearby gas processing plant with CO_2 separation unit. Extended to 200 km radius, there are coal power plants, and textile and manufacture facilities emitted abundant amount of CO_2. Figure 9 reveals the candidate of CCUS CO_2-EOR for the F24 cluster.

CONCLUSIONS

A source-sink matching process based on geographical information systems (Arc-GIS) has been developed to facilitate data management, evaluation, modeling and generate information for CCUS CO_2-EOR field scale analysis. The top five cluster highest scoring for CCUS CO_2-EOR implementation are identified, which are F1, F2, F3, F4, and F5 oil fields. These results are consistent with the operator willingness at the present time in which the operator planned to apply CO_2-EOR in these fields. CO_2-EOR field priority ranks developed in this study could be used as the supporting assessment for developing future field scale of CCUS
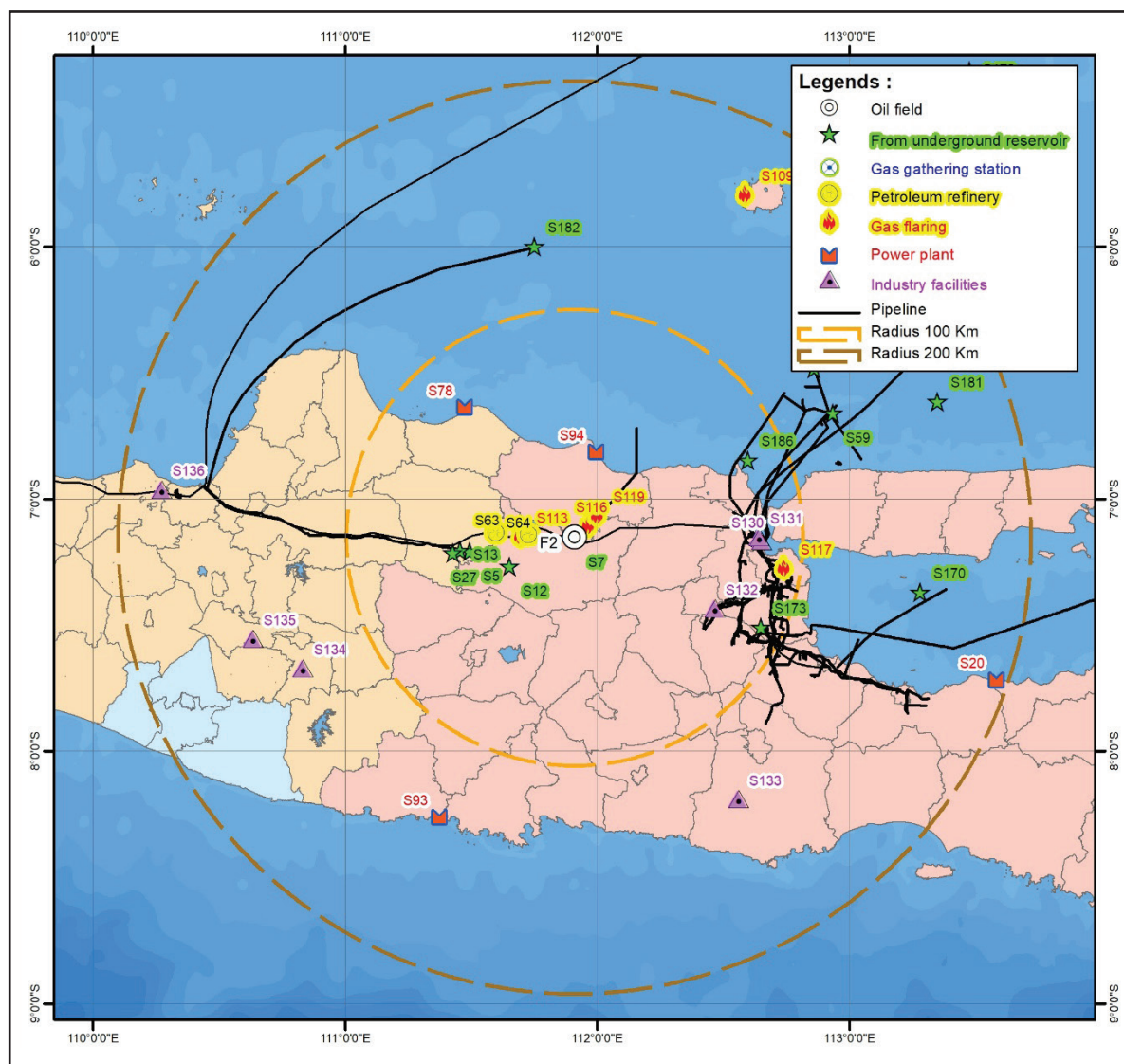
Figure 9
Candidate of F2 CCUS CO$_2$-EOR cluster.

CO$_2$-EOR project. The Arc-GIS map developed in this study should be interested to project developers, policymakers, government agencies, academicians, civil society and environmental non-governmental organization in order to enable them to assess the role of CCUS CO$_2$-EOR as a major carbon management strategy application in Indonesia.

ACKNOWLEDGEMENT

GLOSSARY OF TERMS

Symbol	Definition	Unit
API	American Petroleum Institute	
CCUS	Carbon Capture Utilization and Storage	
EOR	Enhanced Oil Recovery	
GHG	Green House Gas	
GIS	Geographic Information System	

Symbol	Definition	Unit
MMP	Minimum Miscible Pressure	
MMSTB	crude oil volume unit of million stock tank barrels	
OOIP	Original Oil in Place	
SNG	Synthetic Natural Gas	

REFERENCES

Advanced Resources International, Inc., 2011. *Global Technology Roadmap for CCS in Industry: Sectoral Assessment CO$_2$ Enhanced Oil Recovery,* Arlington, VA, USA: United Nations Industrial Development Organization .

Al Adasani, A. & **Bai, B.**, 2011. Analysis of EOR projects and updated screening criteria. *Journal of Petroleum Science and Engineering,* 79(1-2), pp. 10-24.

Chen, W., Huang, L., Xiang, X. & **Chen, J.**, 2011. GIS Based CCS Source-Sink Matching Models and Decision Support System. *Energy Procedia,* 4(5), pp. 5999-6006.

Chon, R. O., Saputra,, D. S. & **Firdaus, N.**, 2019. *Preliminary CO$_2$ Project Implementation Priority with Multicriteria Analysis Approach using CO2 Source-Sink Networking Models in Pertamina EP Fields.* Yogyakarta, Joint Convention Yogyakarta (JCY).

Firdaus, N., Chon, R. & **Saputra, D. S.**, 2019. S*ource-Sink Matching for CO$_2$-EOR Application with Network Clustering Methods in Pertamina EP Fields.* Yogyakarta, Joint Convention Yogyakarta (JCY).

International Energy Agency (IEA), 2015. *Storing CO$_2$ through Enhanced Oil Recovery: Combining EOR with CO$_2$ storage (EOR+) for profit,* Paris: International Energy Agency (IEA).

International Energy Agency (IEA), 2020. *Energy Technology Perspectives 2020: Special Report on Carbon Capture Utilisation and Storage,* Paris: International Energy Agency (IEA).

Lee, J. I., 1979. *Effectiveness of carbon dioxide displacement under miscible and immiscible conditions, Report RR-40,* Calgary, Canada: Petroleum Recovery Institute,.

PPPTMGB "LEMIGAS", 2018. *Laporan Final Studi Pemetaan Potensi Implementasi Injeksi CO$_2$ di Indonesia,* Jakarta: PT Pertamina EP.

SKK MIGAS, 2019. *The 2019 Annual Report SKK MIGAS,* Jakarta: SKK MIGAS.

Taber, J. J., Martin, F. D. & **Seright, R. S.**, 1997. EOR Screening Criteria Revisited - Part 2: Applications and Impact of Oil Prices. *SPE Reservoir Engineering,* 12(3), pp. 199-205.

Usman, Iskandar, U.P., Sugihardjo & **Lastiadi, H.**, 2014. A Systemic Approach to Source- Sink Matching for CO$_2$-EOR and Sequestration in South Sumatera. *Energy Procedia,* Volume 63, pp. 7750-7760.

Yellig, W. F. & **Metcalfe, R. S.**, 1980. Determination and Prediction of CO$_2$ Minimum Miscibility Pressures. *Journal of Petroleum Technology,* 32(01), pp. 160-168.
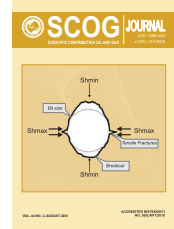
Well Integrity Study for WAG Application in Mature Field X, South Sumatra Area for the Fulfillment as CO_2 Sequestration Sink

Steven Chandra, Prasandi A. Aziz, Muhammad Raykhan Naufal and Wijoyo N. Daton

Petroleum Engineering Study Program, Institut Teknologi Bandung
Jl. Ganesha No. 10, Lb. Siliwangi, Bandung, Jawa Barat 40132
Corresponding author: stevenchandra010@gmail.com; steven@tm.itb.ac.id

ABSTRACT - The most of today's global oil production comes from mature fields. Oil companies and governments are both concerned about increasing oil recovery from aging resources. To maintain oil production, the mature field must apply the Enhanced Oil Recovery method. CO_2 water-alternating-gas (WAG) injection is an enhanced oil recovery method designed to improve sweep efficiency during CO_2 injection with the injected water to control the mobility of CO_2. This study will discuss possible corrosion during CO_2 and water injection and the casing load calculation along with the production tubing during the injection phase. The following study also performed a suitable material selection for the best performance injection. This research was conducted by evaluating casing integrity for simulate CO_2 water-alternating-gas (WAG) to be applied in the X-well in the Y-field, South Sumatra, Indonesia. Corrosion prediction were performed using Electronic Corrosion Engineer (ECE®) corrosion model and for the strength of tubing which included burst, collapse, and tension of production casing was assessed using Microsoft Excel. This study concluded that for the casing load calculation results in 600 psi of burst pressure, collapse pressure of 2,555.64 psi, and tension of 190,528 lbf. All of these results are still following the K-55 production casing rating. While injecting CO_2, the maximum corrosion rate occurs. It has a maximum corrosion rate of 2.02 mm/year and a minimum corrosion rate of 0.36 mm/year. With this value, it is above NORSOK Standard M-001 which is 2 mm/year and needs to be evaluated to prevent the rate to remain stable and not decrease in the following years. To prevent the effect of maximum corrosion rate, the casing material must use a SM13CR (Martensitic Stainless Steel) which is not sour service material.

Keywords: CO_2 Water-Alternating-Gas (WAG), corrosion, casing load

How to cite this article:

Steven Chandra, Prasandi A. Aziz, Muhammad R. Naufal and Wijoyo N. Daton, 2021,Well Integrity Study for WAG Application in Mature Field X, South Sumatra Area for the Fulfillment as CO_2 Sequestration Sink, Scientific Contributions Oil and Gas, 44 (2) pp., 107-121.

INTRODUCTION

A. Background

Most of the current world oil production comes from mature fields. Increasing oil recovery from the aging resources is a major concern for oil companies and authorities. In addition, the rate of replacement of the produced reserves by new discoveries has been declining steadily in the last decades. Therefore, the increase of the recovery factors from mature fields under primary and secondary production will be critical to meet the growing energy demand in the coming years (Alvarado & Manrique, 2010).

To maintain oil production, mature fields have to apply the Enhanced Oil Recovery (EOR) method. CO_2 water-alternating-gas (WAG) injection is an enhanced oil recovery method designed to improve sweep efficiency during CO_2 injection with the

injected water to control the mobility of CO_2 (Chen & Reynolds, 2016). Injecting water and CO_2 into old wells will be difficult and will require careful consideration of a number of factors, one of which is the strength of the tubing in the old well.

This study was conducted to increase oil production by Water Alternating Gas using CO_2. This paper analyzes possible corrosion during CO_2 and water injection and the load calculation along with the production tubing during the injection phase. At the end of this study, the result will be a consideration before injection and the operation ran successfully to do CO_2 water-alternating-gas (WAG) injection.

B. Objectives

This scoping study only focused in X-Well in the Y-field, with objective:

- To evaluate casing integrity X-well in the Y-field for simulating CO_2 water-alternating-gas (WAG)
- To predict corrosion rate on production casing in Y-well for CO_2 water-alternating-gas (WAG)
- To determine suitable tubular material for CO_2 water-alternating-gas (WAG) injection well

C. Basic Theory

When performing Enhanced Oil Recovery (EOR activities, it is imperative that aside from the aspects of chemical interaction between components injected and reservoir aspects are thoroughly investigated, there is an issue of well integrity that must be rectified prior to performing the injection. As most of EOR pilot projects conducted in Indonesia are located in older fields with higher uncertainty in well integrity aspects, this publication tends to answer these questions by investigating several aspects namely tubular integrity against the aspects of burst, collapse, and tension as well as corrosion issue.

1. Water Alternating Gas

CO_2 water-alternating-gas (WAG) injection is a cyclic injection process where water and gas injections are carried out alternately for periods of time to provide better sweep efficiency and reduce gas channeling from injector to producer. This process is used mostly in CO_2 flooding to improve hydrocarbon contact time and sweep efficiency of the CO_2 (Chen & Reynolds, 2016). CO_2-WAG flooding is one of the successful enhanced oil recovery methods for a low permeability reservoir or a reservoir with fractures (Liao, et al., 2013) because WAG results in better mobility control and higher microscopic

miscible displacement efficiency compared to injecting water or CO_2 individually. CO_2-WAG is the preferable method due to the fact it can give higher recovery, better sweep efficiency, and cost effective than other CO_2 injection method (Karimaie, et al., 2017). The WAG parameters consist of slug size, ratio, and cycle (Touray, 2013). The WAG ratio is a comparison between the amount of water injected and the number of solvents injected, both expressed in units of reservoir volume (Juanes & Blunt, 2007). The WAG ratio has a very significant influence on the design of the WAG process. Even so, basically the WAG ratio is very dependent on reservoir wettability and the availability of gas to be injected (Zahoor, et al., 2011).

2. Property of Casing

a. Burst Pressure

Burst pressure is the pressure received from inside the case. Burst occurs when internal pressure is greater than external pressure (Mitchell, et al., 1998). In casing planning it is considered that burst pressure is the formation pressure coming from the next casing route, when the kick casing gets the maximum pressure from the formation. An overview of the burst pressure suffered by the casing can be seen in Figure 1. If the burst pressure that occurs in the case is greater than the strength of the case to hold it, the case will tear. An overview of the bursting case can be seen in Figure 2. Based on the following equation the burst pressure can be calculated (Bourgoyne, 1991):

$$P_{br} = 0.875 \frac{2\sigma_{yield}\, t}{d_n} \qquad (1)$$

Where:

P_{br} = Burst pressure (psi)

σ_{yield} = Minimum yield pressure (psi)

d_n = Outer diameter (inch)

t = Wall thickness (inch)

b. Collapse Pressure

Collapse occurs when external pressure is greater than internal pressure (Mitchell, et al. 1998). In the casing design, as collapse pressure is considered the hydrostatic pressure of cement outside the casing, so the biggest collapse pressure accepted by casing at the bottom of the hole and the worst conditions

occur when the casing is empty or the pressure inside the casing is zero. At zero depth or on the surface of external pressure is zero. If the collapse pressure that occurs in the case is greater than the force to hold it, then the casing will be bent in or collapse. In order to ensure casing not to collapse, the installed casing must have a collapse resistance greater than burst pressure. An overview of the collapse case can be seen in Figure 3. When the axial stress is zero, there are four kinds of range for different collapse pressure regions. They are yield strength collapse, plastic collapse, transition collapse, elastic collapse. Region of collapse pressure determined by outer diameter ratio and wall thickness. The detailed region can be seen in Table 1. The difference between the four regions is the empirical coefficients used for collapse pressure determination. The empirical coefficients for each grade can be seen in Table 2. A transition collapse region between the plastic collapse and elastic collapse regions is defined with this equation (Bourgoyne, 1991):

$$P_{cr} = \sigma_{yield}\left(\frac{F_4}{d_n/t} - F_5\right) \qquad (2)$$

Figure 1
Illustration of burst pressure.

Figure 2
Casing when burst rating is exceeded.

Where:

P_{cr} = Collapse pressure (psi)

σ_{yield} = Minimum yield pressure (psi)

d_n = Outer diameter (inch)

t = Wall thickness (inch)

F_4 = Empirical coefficients

F_5 = Empirical coefficients

c. Tension Load

Tension is a load caused by a series of casings' (Rubiandini, 2004) tension failure will occur when the tension load is greater than the tension rating. An overview of the tension case can be seen in Figure 4. Based on the following equation the tension fore can be calculated (Bourgoyne, 1991):

$$F_{ten} = \frac{\pi}{4} \sigma_{yield}(d_n^2 - d^2) \qquad (3)$$

Where:

F_{ten} = Tensional Force (lbf)

σ_{yield} = Minimum yield pressure (psi)

d_n = Outer diameter (inch)

d = Inner diameter (inch)

3. Corrosion

Corrosion is the destructive attack of a metal by chemical or electrochemical reaction with its environment (Revie, 2008). Corrosion occurs when conditions are as follows (Bellarby, 2011):

- The surface of metal that is exposed to the environment;
- Water or electrolyte;
- A corrodent (something such as oxygen, CO_2, acid, or H_2S to create the corrosion).

For normalized steels of tubing or casing the following equations are applied in the corrosion rate model (Smith & DeWaard, 2005):

$$\log(Vr) = 4.84 - \frac{1119}{t+273} + 0.58\log(f_{CO_2}) - 0.34\left(pH_{actual} - pH_{CO_2}\right) \qquad (4)$$

Where:

t = Temperature (°C)

f_{CO_2} = Fugacity of CO_2 (bar)

pH_{actual} = Actual pH

Figure 3
Collapse casing.
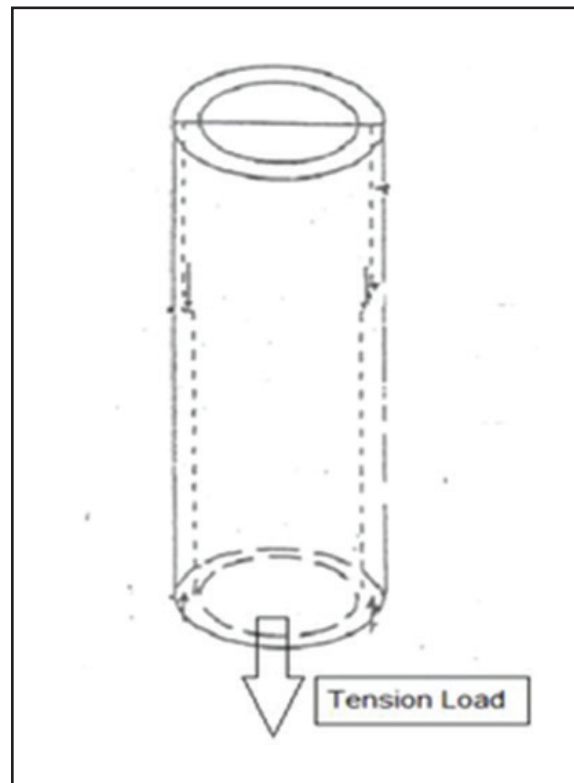
Figure 4
Tension load condition.

Table 1
Range of d_n/t for various collapse-pressure regions when axial stress is zero (reproduced from applied)

API Grade	Yield Strength Collapse	Plastic Collapse	Transition Collapse	Elastic Collapse
H-40	16.4	27.01	42.64	
J-55	14.81	25.01	37.21	
K-55	14.81	25.01	37.21	
C-75	13.6	22.91	32.05	
L-80	13.38	22.47	31.02	
N-80	13.38	21.69	31.02	
C-90	13.01	21.69	29.18	
C-95	12.85	21.33	28.36	
P-105	12.57	20.7	26.89	
P-110	12.44	20.41	26.22	

(Reproduced from Applied Drilling Engineering by Burgoyne, 1991)

pH_{CO_2} = Pure water pH saturated with CO_2 at prevailing pressure and temperature.

The CO_2 fugacity is calculated based on the following equation (Smith & DeWaard, 2005):

$$\log(f_{CO_2}) = \log(p_{CO_2}) + \left(0.0031 - \frac{1.4}{t+273}\right)P \qquad (5)$$

Where:

P_{CO_2} = Partial pressure of CO_2

Table 2
Empirical coefficients used for collapse-pressure determination (reproduced from Applied drilling engineering by Burgoyne, 1991)

API Grade	Empirical Coefficient				
	F1	F2	F3	F4	F5
H-40	2.95	0.047	754	2.063	0.0325
J-55	2.991	0.054	1206	1.989	0.036
K-55	2.991	0.054	1206	1.989	0.036
C-75	3.054	0.064	1806	1.99	0.0418
L-80	3.071	0.0667	1955	1.998	0.0434
N-80	3.071	0.0667	1955	1.998	0.0434
C-90	3.106	0.0728	2254	2.017	0.0466
C-95	3.124	0.0743	2404	2.029	0.0482
P-105	3.162	0.0794	2702	2.053	0.0515
P-110	3.181	0.0819	2852	2.066	0.0532

DATA AND METHODS

The study was completed by following design framework, as can be see in Figure 5, by implementing the following five stages in order to optimize this study:

A. Literature Study

Review the previous research about CO_2 water-alternating-gas (WAG), Corrosion and Corrosion Rate, Standardization of Corrosion Rates, and Load on Production Casing in the several papers and books.

B. Data Preparation

In this section, well data, production casing data, and injected fluid data had been prepared for input to software.

1. Corrosion Rate Prediction

Corrosion rate was calculated using the Electronic Corrosion Engineer (ECE®) corrosion model.

2. Casing Strength Evaluation

At this step, the strength of casing which included burst, collapse, and tension of production casing was assessed using Microsoft Excel.

3. Rating and Tubular Failure Analysis

Last, the output from step before this section was analysed, based on the production casing rating calculation and the result was used to give the
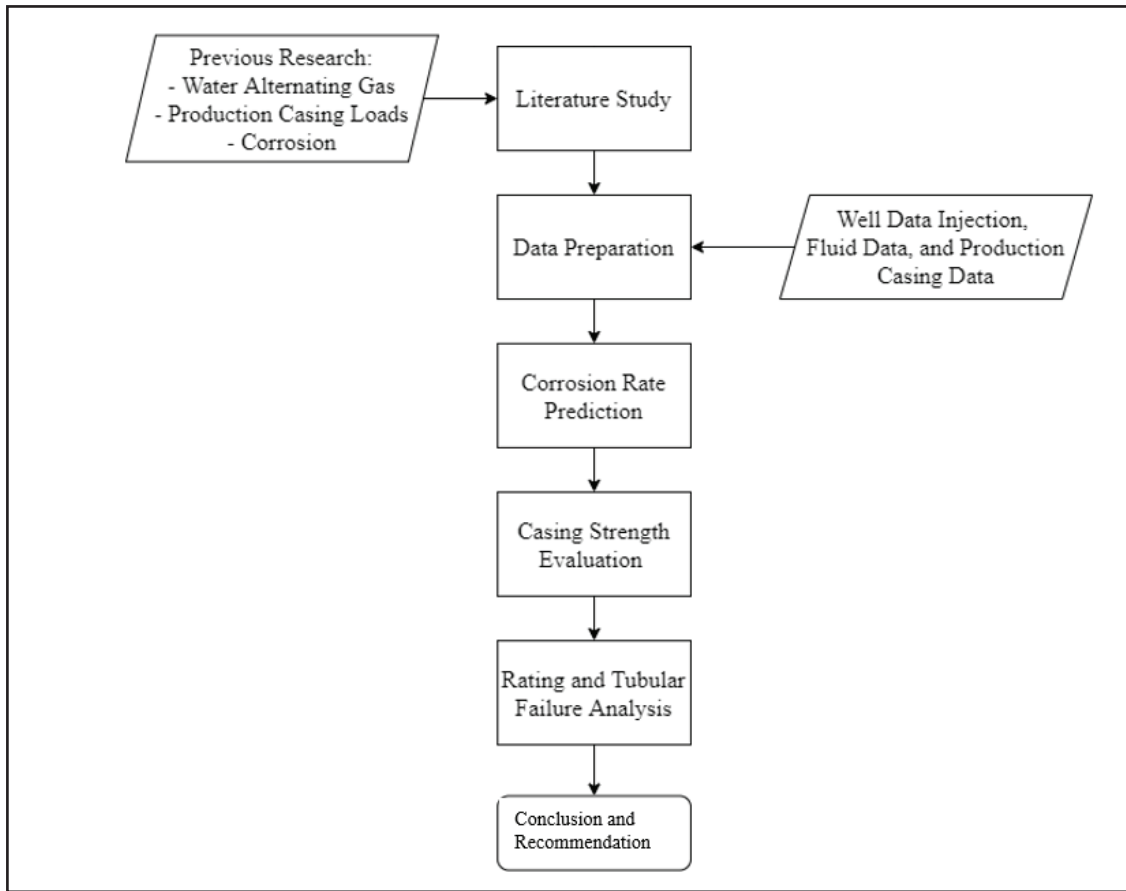
Figure 5
Methodology flowchart.
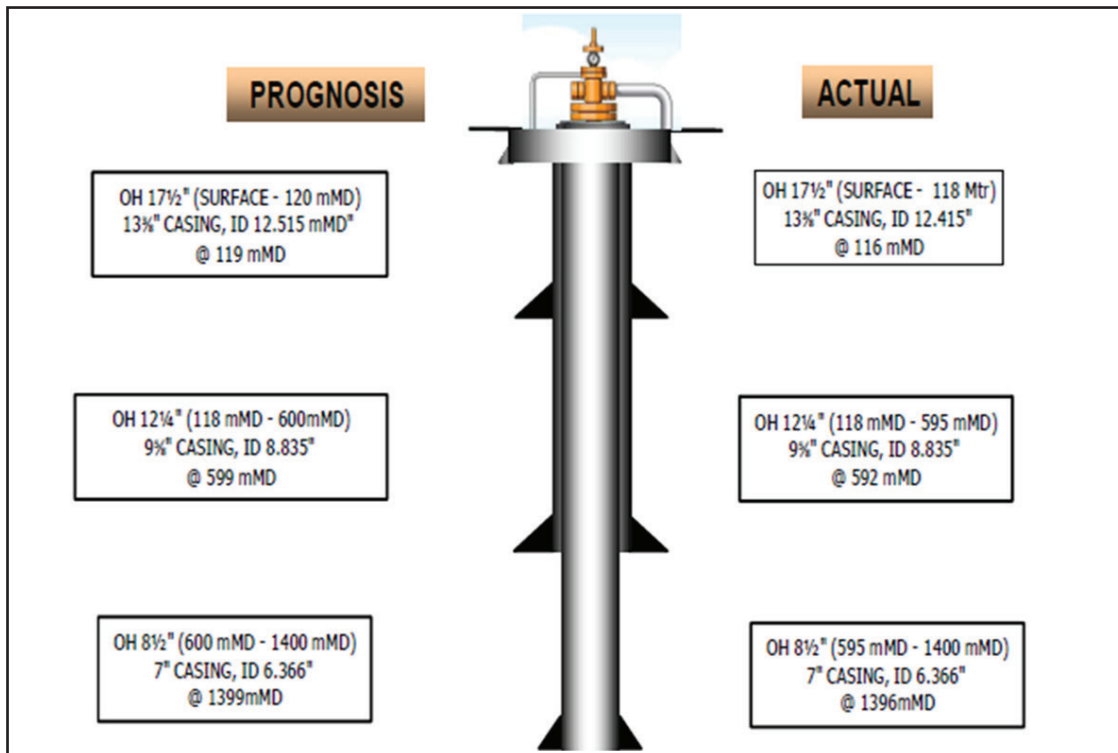
Figure 6
X-Well cross section diagram.

Table 3
Specification of casing

Data	OD (inch)	ID (inch)	Weight (lbm/f)	Wall Thickness (inch)
Surface Casing, K-55	13.375	12.675	54.5	0.38
Intermediate Casing, K-55	9.625	8.835	40	0.395
Production Casing, K-55	7	6.276	26	0.362

best recommendation for what is doing next before CO_2 water-alternating-gas (WAG) be applied.

C. Case Study

1. Well Overview

A mature oil field in Indonesia is known as Y-Field. Some development wells in this field produce oil using various recovery mechanisms. X-Well is one of the wells that has a natural decline. Figure 6 illustrates the vertical well diagram of X-Well. This well wants to use tertiary recovery to enhance oil production using the CO_2 water - alternating - gas (WAG) method in the next development.

X-Well consists of surface casing, intermediate casing, and production casing without using tubing. Table 3 lists the specifications for each casing. For inject this well using production casing. Table 12 shows the rating of each casing.

2. Production Casing Data

The production casing used in X-Well has a K-55 grade with OD size of 7" with 26 ppf for weight and for the type of connection is BTC with type of casing length range is R3, the casing was installed to a depth of 4,980 ft, additional data used in this case study shown by Table 4.

3. Injected Fluid Description

Enhanced Oil Recovery will be used on this well. CO_2 is injected, followed by an alternating brine. The CO_2 water-alternating-gas (WAG) procedure is for case 1, Injection of brine (composition is 8,600 ppm, with no bicarbonate and acetic acid containing) injection 1,500 BWPD with pump pressure is 500 psi, followed by case 2, Injection (99%; H_2S pollutant 5 ppm) as much as 7 MMSCFD with compressor pressure is 800 psi. Table 5 illustrates the detailed scenario of case 1 and Table 6 illustrates case 2.

4. Case Overview

Before doing the injection, it is necessary to evaluate the strength of the casing due to increased

Table 4
Detailed specification of production casing

Production Casing Data

Production Casing Grade	K-55
Type of Connection	BTC
Weight of Production Casing, lbm/ft	26
Type of Casing Length Range	R3
Production Casing OD, inch	7
Production Casing ID, inch	6.276
Wall Thickness, inch	0.362
Minimum Yield Pressure, psi	55000

Table 5
Data input of case 1 for ECE

Case 1

Wellhead Pressure, psia	515
Bottomhole Pressure, psia	2322
Temperature at Wellhead, F	77
Temperature at Bottomhole. F	120
CO_2 Composition, %	0
H_2S Composition, ppm	0
Water Salinity, ppm	8600
Rate Crude oil, bopd	0
Gas Rate, MMSCFD	0
Water Rate at Wellhead, bwpd	1500
Measured Depth, m	1400
OD, inch	7
Wall Thickness	0.362

production and corrosion effects which will put a load on the casing. With some assumption such as the
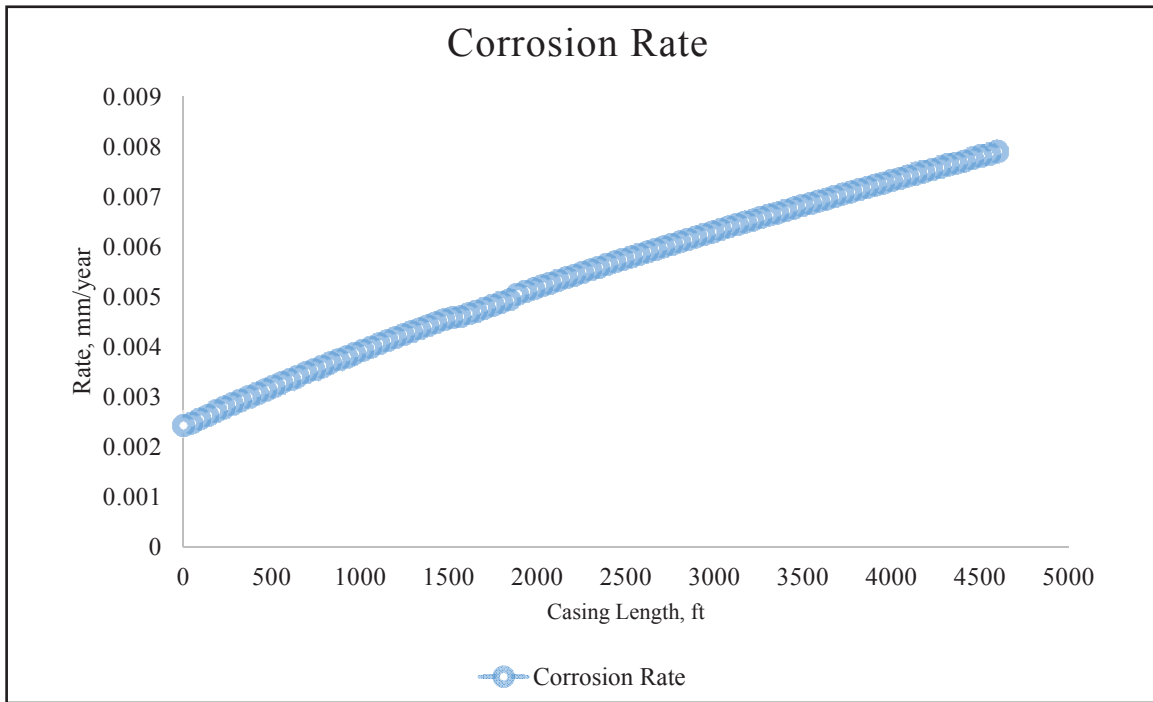
Figure 7
Case 1 corrosion rate.
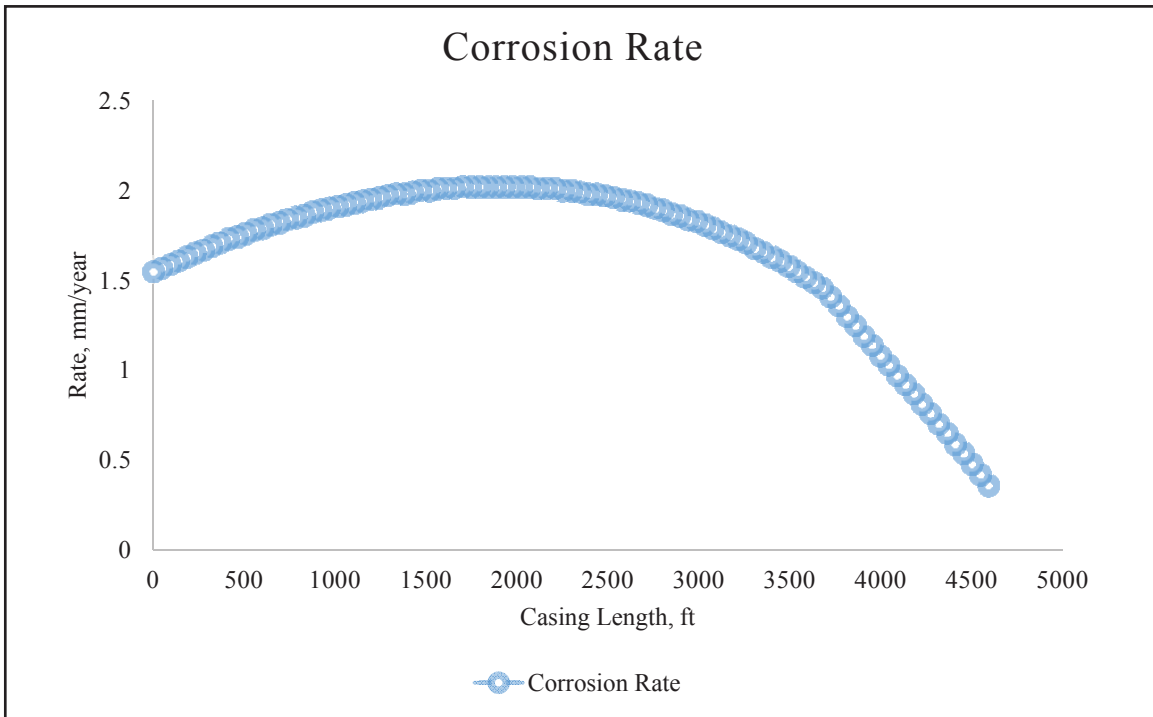
Figure 8
Case 2 corrosion rate.

well is not used production tubing and well is vertical so does not have any deviation. For the purpose of assessing tubing failure, data, and assumptions based on the injection scenario, The API 5 CT (American Petroleum Institute, 2005) rating was used.

RESULTS AND DISCUSSION

A. Corrosion

In CO_2 water-alternating-gas (WAG) injection which is injecting brine and CO_2 alternately can

have an effect on the material of the case. One of the effects is corrosion. By knowing the potential corrosion that will occur, it can be avoided by selecting the appropriate casing material and able to withstand the rate of corrosion that occurs due to the injection.

The Result of the potential corrosion for two cases shown in Table 7. The corrosion rate are 0.008 mm/year maximum and 0.0025 mm/year minimum in the first case, which is brine injection with the following data is in Table 5. Figure 7 shows the corrosion rate along the production casing. Because there is no chemical lead to corrosion, the corrosion rate is low. This value, it is still within the safe limit for corrosion rate which far below NORSOK Standard M-001 of 2 mm/year.

For the second case using CO_2 injection, which the detailed data is in Table 6. The result obtained the maximum corrosion rate is 2.02 mm/year and the minimum corrosion rate is 0.36 mm/year. From the data, it can be concluded that corrosion rate for the second case can be said to fail because it is above NORSOK Standard M-001 which is 2 mm/year and needs to be evaluated to prevent the rate to remain stable and not decrease in the following years.

Tubing material selection is important to ensure well integrity in this case production casing, so it can deliver fluids safely for the entire injection life and there are no minor/major problems that can impact the injection. Based on Table 13, Table 14, and Figure 15, the casing material that will be used to inject CO_2 is SM13CR (Martensitic Stainless Steel) which is not sour service materials because there is small amount of H_2S in two different condition which is in Wellhead and Bottomhole condition.

B. Production Casing Load

With the input data shown by Table 8, it can be seen that at the Burst load, the internal pressure comes from wellhead pressure, which is assumed to be compressor pressure, and the column pressure of brine in the casing. The external pressure is generated by pore pressure, which is assumed to be 0.465 psi/ft (Bourgoyne, 1991). The burst calculation gave a pressure of 600 psi at 0-meter depth and 426.96 psi at 4,580 ft depth, the tubing's end. This value must meet the 4977.5 psi rating of K-55 production casing. Table 9 shows the details of the calculation. Figure 9 represents the graph of burst pressure. Figure 10 illustrates the burst rating.

Table 6
Data input of case 2 for ECE

Case 2	
Wellhead Pressure, psia	815
Bottomhole Pressure, psia	2322
Temperature at Wellhead, F	77
Temperature at Bottomhole. F	120
CO_2 Composition, %	99
H_2S Composition, ppm	5
Water Salinity, ppm	0
Rate Crude oil, bopd	0
Gas Rate, MMSCFD	7
Water Rate at Wellhead, bwpd	0
Measured Depth, m	1400
OD, inch	7
Wall Thickness	0.362

Table 7
Corrosion rate each case

Scenario	Corrosion Rate, mm/year	
	Minimum	Maximum
Case 1 (Brine)	0.0025	0.008
Case 2 (CO_2)	0.36	2.02

Table 8
Data input for production load calculation

Properties	Value
Depth of Production Casing, ft	4580
Injection Pressure, psi	500
Pore Pressure Gradient, psi/ft	0.465
Water Density, lb/ft^3	62.4
Water Gradient, psi/ft	0.43333333
Mud Weight, lb/gal	9.75
Weight of Production Casing, lbm/ft	26
Safety Factor Burst	1.2
Safety Factor Collapse	1.2
Safety Factor Tension	1.6

When it comes to the collapse load, this calculation must be done when the external pressure
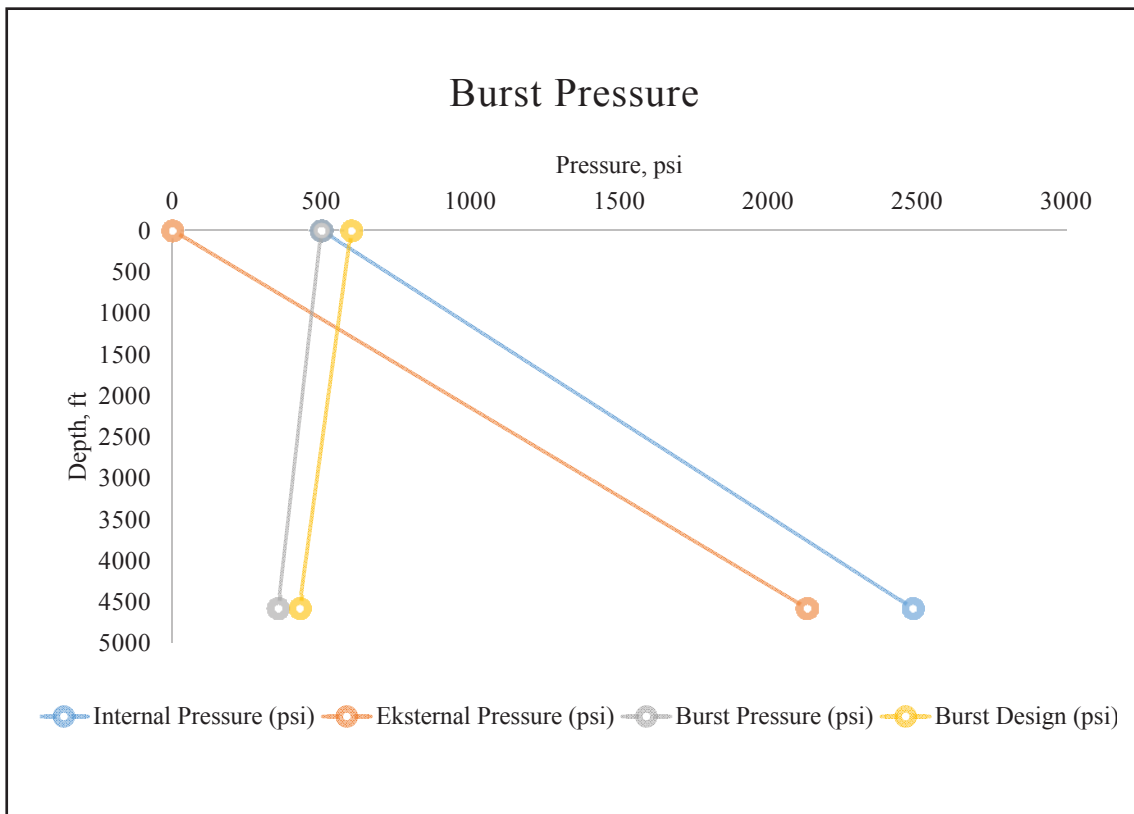
Figure 9
Burst load of production casing.
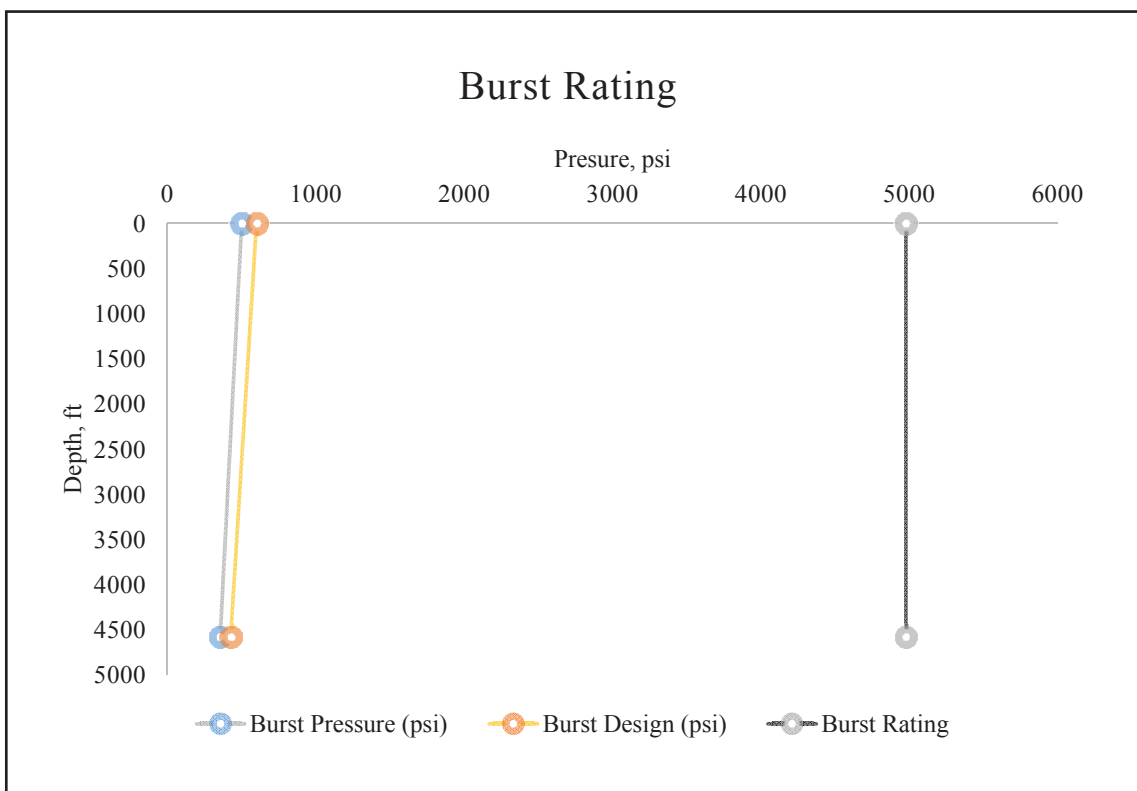
Figure 10
Burst rating of production casing.
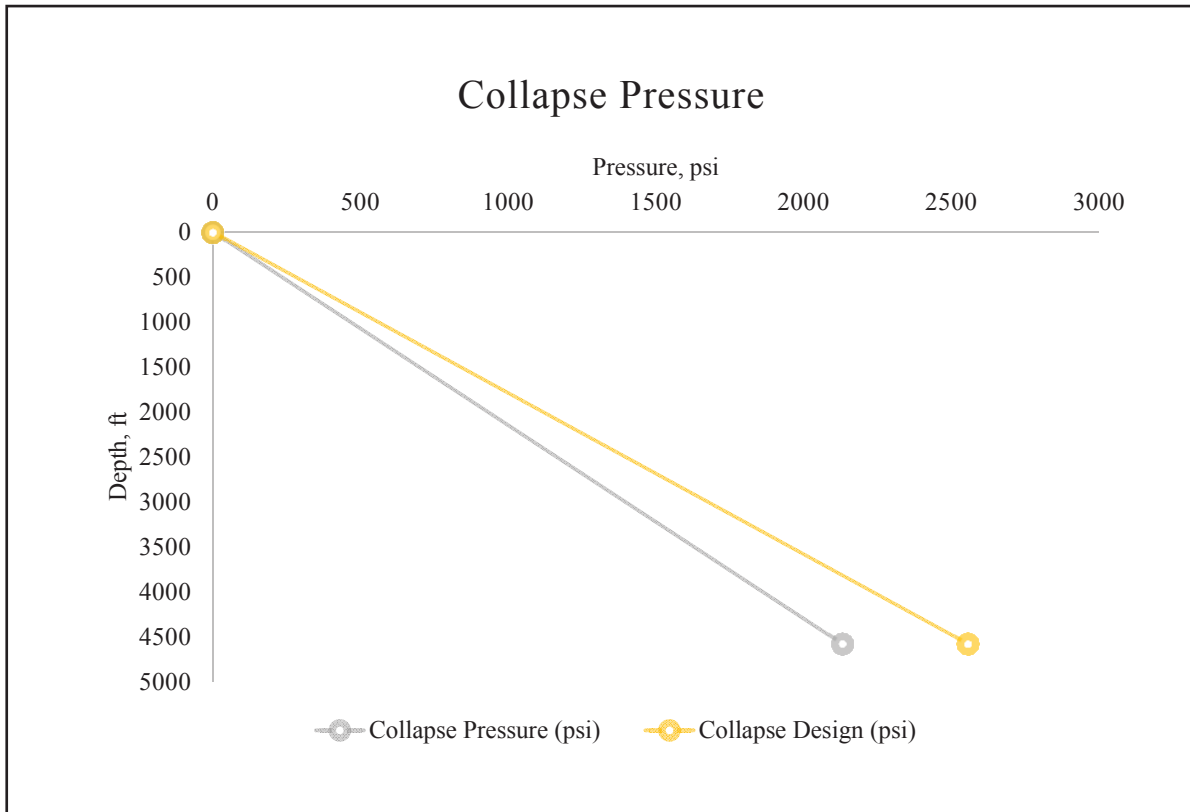
Figure 11
Collapse load of production casing.
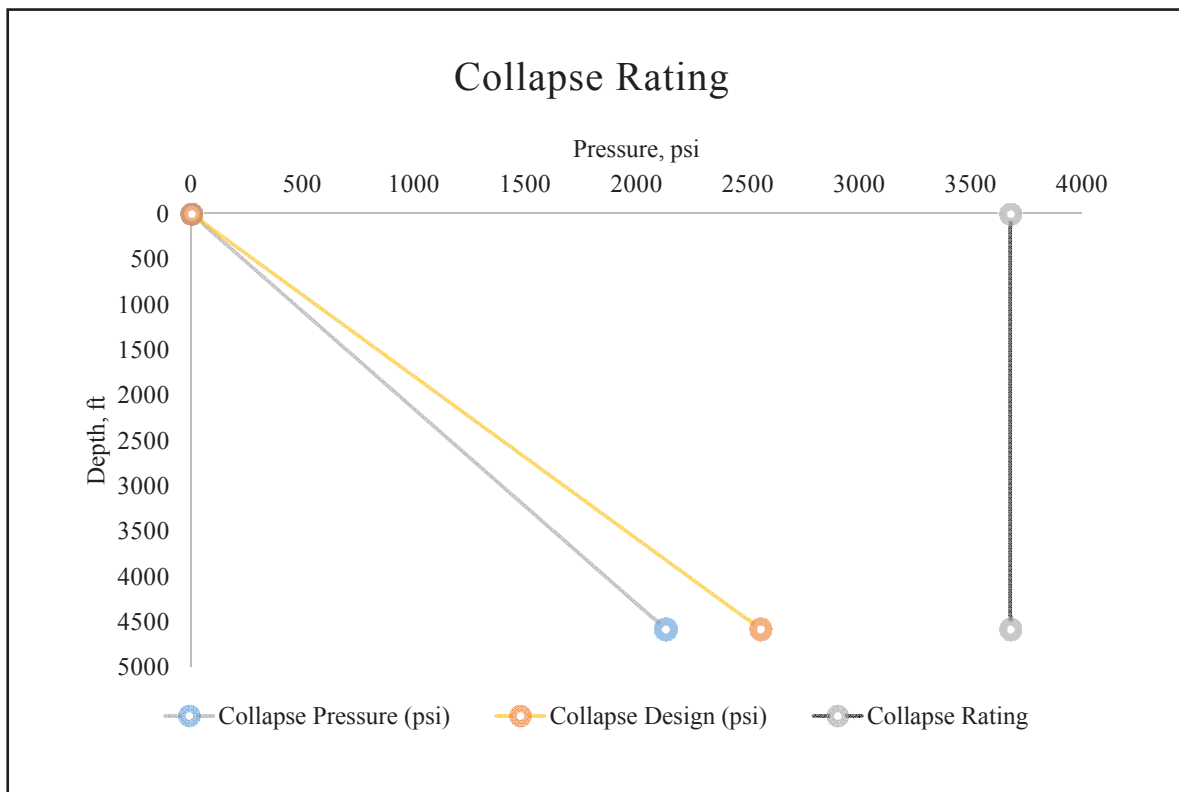
Figure 12
Collapse rating of production casing.

Table 9
Burst pressure calculation

Depth (ft)	Internal Pressure (psi)	External Pressure (psi)	Burst Pressure (psi)	Burst Design (psi)
0	500	0	500	600
4580	2484.67	2129.7	354.97	425.96

Table 10
Collapse pressure calculation

Depth (ft)	Internal Pressure (psi)	Eksternal Pressure (psi)	Collapse Pressure (psi)	Collapse Design (psi)
0	0	0	0	0
4580	0	2129.7	2129.7	2555.64

Table 11
Tension load calculation

Depth (ft)	Pounder (ppf)	Tension (lbf)	Tension Design (lbf)
0	26	119080	190528
4580	26	0	0

Table 12
Result of casing rating calculation

Casing Rating	Surface Casing K-55, 13-3/8", 54.5 ppf	Intermediate Casing K-55, 9-5/8", 40 ppf	Production Casing K-55, 7", 26 ppf
Burst Rating	4977.5	3950	2734.579439
Collapse Rating	3677.284286	2509.457143	1128.04486
Tension Rating	415200.9904	629957.6567	787695.453

is high, but the internal pressure is zero. 2,555.64 psi is the result of the collapse pressure. The collapse rating of production tubing K-55 is 3,677.28 psi, and this result meets that requirement. Table 10 shows the details of the calculation. Figure 11 captures the collapse pressure graph. The rating of collapse is presented in Figure 12.

For the tension load. This calculation calculates the weight of production tubing per feet and the tubing's true vertical depth. 190,528 lbf tension load calculation results. This value is equal to the 415,200.99 lbf rating of production tubing K-55. Table 11 shows the tension load calculation. Figure 13 illustrates the tension load graph. The rating of tension is presented in Figure 14.

All of this value when compared to its rating for burst, collapse and tension, the loads do not exceed the calculated rating limit.

Based on the calculations performed, it can be seen that the tubular configuration proposed in this publication could hold against the loads of injection as well as the corrosion effects from injecting a combination of CO_2 and brine. However, it has to be noted that further works should assume on declining tubular properties and routine monitoring is required to ensure the longevity of the operation.

CONCLUSIONS

Based on the analysis above, several conclusions can be taken to comply with this study objectives:

The production casing K-55 tubing used in X-well in the Y-field has a lower risk of failure due to CO_2 water-alternating-gas (WAG) because all of the production casing loads meets requirements with burst pressure 600 psi, collapse pressure 2,555.64, and the tension of 190,528 lbf.

In the second case, while injecting CO_2, the maximum corrosion rate occurs. It has a maximum corrosion rate of 2.02 mm/year and a minimum corrosion rate of 0.36 mm/year. With this value, it is above NORSOK Standard M-001 which is 2 mm/year and needs to be evaluated to maintain the rate to remain stable and not decrease in the following years.

Table 13
General reservoir data
for material selection in the Wellhead

Properties	Value
Reservoir Pressure, psia	815
Reservoir Temperature, F	77
CO2 Partial Pressure, psia	806.85
H2S Partial Pressure, psia	0.004

Table 14
General reservoir data
for material selection in the bottomhole

Properties	Value
Reservoir Pressure, psia	2322
Reservoir Temperature, F	120.2
CO_2 Partial Pressure, psia	2298.78
H_2S Partial Pressure, psia	0.12

Figure 13
Tension load of production casing.

Figure 14
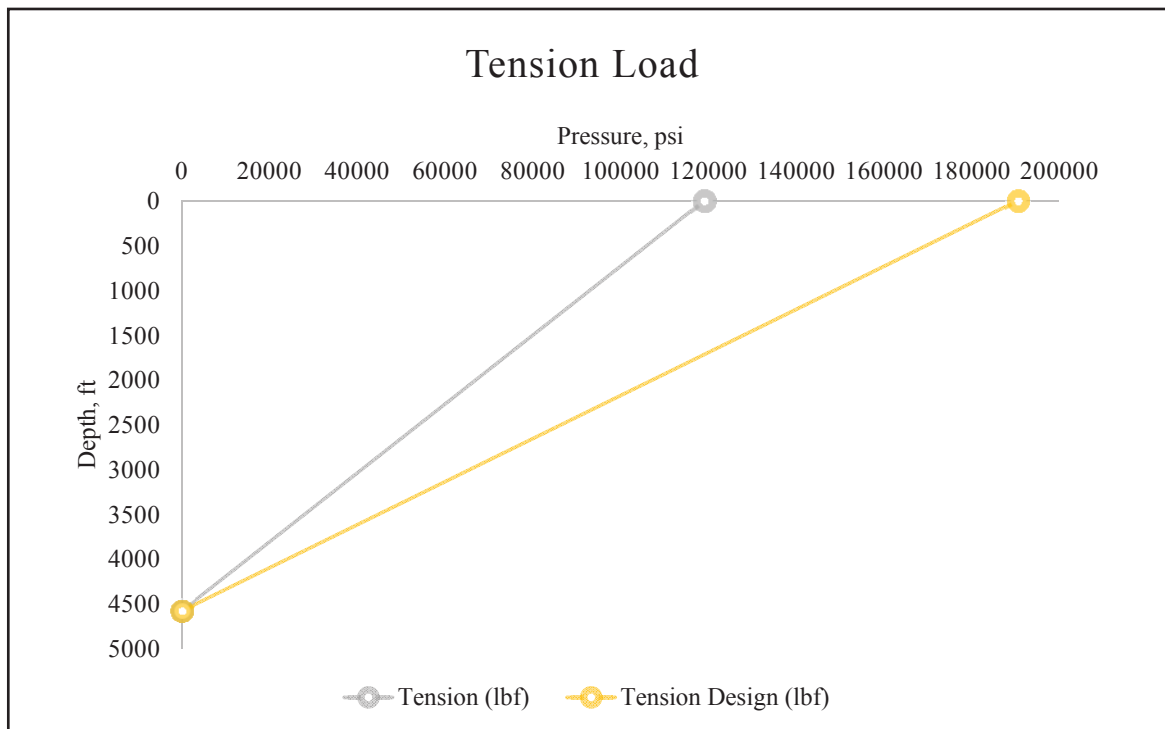Tension rating of production casing.
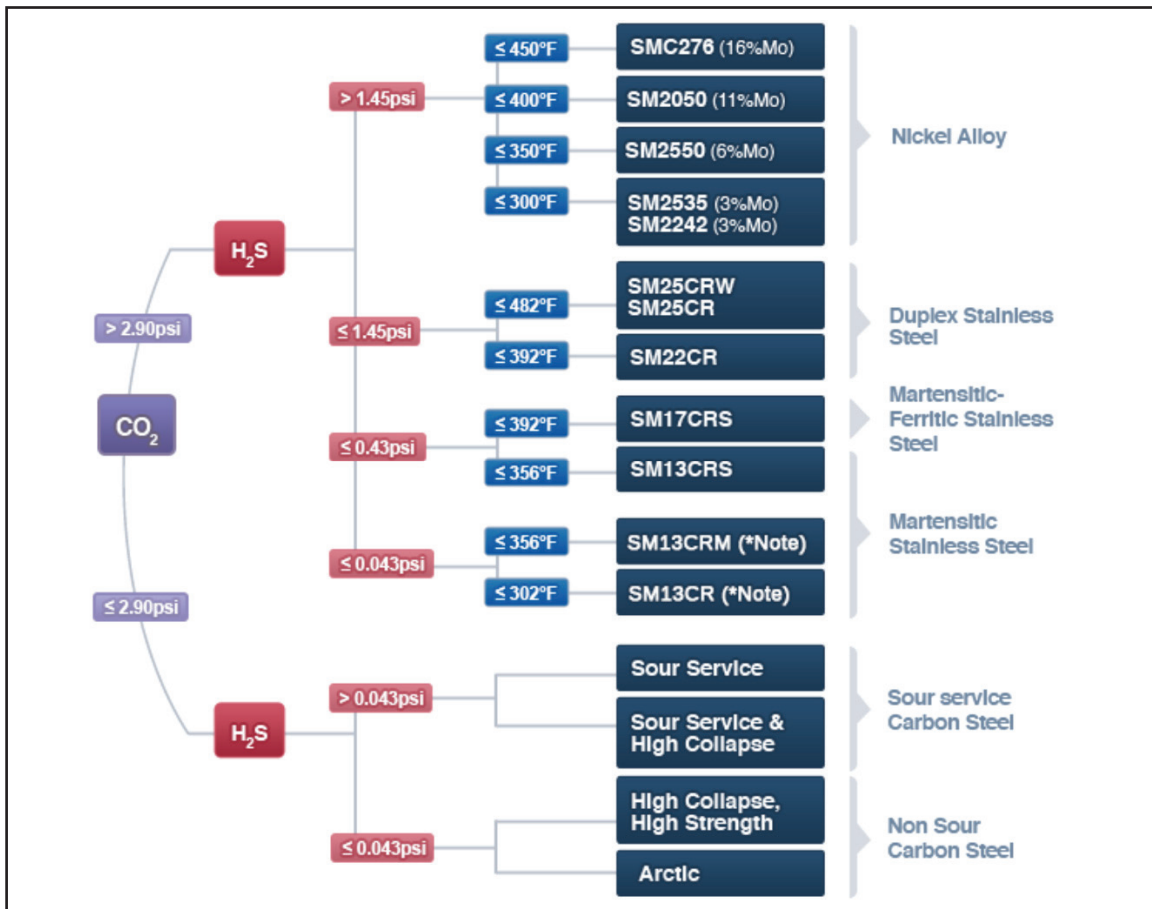
Figure 15
Material selection chart by Nippon Steel
(http://www.tubular.nipponsteel.com/productservices/octg/materials/materials/).

To prevent the effect of maximum corrosion rate, the casing material must use a SM13CR (Martensitic Stainless Steel) which is not sour service material.

Some recommendations can be applied for further development of this studies to gain more understanding and increase the implementation reliability in this field:

To reduce the impact of CO_2 injection, in addition to using the appropriate material, in this case SM13CR (Martensitic Stainless Steel) which is not sour service material can also use other alternatives for example injecting corrosion inhibitor either pre-flush or post-flush or it can also be by coating the tubing with corrosion resistance material before CO_2 injection.

GLOSSARY OF TERMS

Symbol	Definition	Unit
WAG	water-alternating-gas	
ECE	Electronic Corrosion Engineer	
P_{br}	Burst pressure	psi
d_n	outer diameter	inch
t	wall thickness	inch
σ_{yield}	Minimum yield pressure	psi
F_{ten}	Tensional Force	lbf
f_{CO2}	Fugacity of CO2	bar

REFERENCES

Alvarado, V. & Manrique , E., 2010. Enhanced oil recovery: An update review. *Energies,* 3(9), pp. 1529-1575.

American Petroleum Institute, 2005. *API Spec-5CT-2005: Specification for casing and tubing,* Washington DC: American Petroleum Institute.

Bellarby, J., 2011. *Well completion design.* Amsterdam: Elsevier.

Bourgoyne, A. T., 1991. *Applied drilling engineering.* Richardson, TX: Society of Petroleum Engineers.

Chen, B. & Reynolds, A. C., 2016. Ensemble-Based Optimization of the Water-Alternating-Gas-Injection Process. *Society of Petroleum Engineers (SPE) Journal,* 21(3), pp. 786-798.

Juanes, R. & Blunt, M. J., 2007. Impact of Viscous Fingering on the Prediction of Optimum WAG Ratio. *SPE Journal,* 12(4), pp. 486-495.

Karimaie, H., Nazarian, B., Aurdal, T., Nokleby, P.H., & Hansen, O., 2017. Simulation Study of EOR and Storage Potential in a North Sea Reservoir. *Energy Procedia,* Volume 114, pp. 7018-7032.

Liao, C., Xin-wei, L., Xiao-liang, Z. & Ning, L., 2013. *Study on Enhanced Oil Recovery Technology in Low Permeability Heterogeneous Reservoir by Water-Alternate-Gas of CO Flooding*, Society of Petroleum Engineers (SPE).

Mitchell, R. F., Miska, S. & Wagner, R. R., 1998. Casing and tubing design. In: *Petroleum well construction, Chapter 7.* s.l.:s.n., pp. 175-214.

Nippon Steel Tubular Products, 2021. *Nippon Steel Tubular Products*. [Online] Available at: http://www.tubular.nipponsteel.com/product-services/octg/materials/materials/ [Accessed 20 July 2021].

Revie, R. W., 2008. *Corrosion and Corrosion Control.* 4th ed. New Jersey: Wiley Interscience.

Reza, H., Arman, A. & Ghazal, H., 2016. Comparative Study on Oil Recovery Enhancement by WAG Injection Technique in a Fractured Oil Reservoir in the South-west of Iran. *Journal of Petroleum & Environmental Biotechnology,* 7(1), pp. 1-6.

Rubiandini, R., 2004. *Diktat Kuliah Perancangan Pemboran.* Bandung: Institut Teknologi Bandung (ITB).

Smith, L. & DeWaard, C., 2005. *Corrosion prediction and materials selection for oil and gas producing environments.* Houston, Texas, NACE.

Touray, S., 2013. *Effect Of Water Alternating Gas Injection,* USA: Dalhousie University.

Zahoor, M. K., Derahman, M. N. & Yunan, M. H., 2011. WAG Process Design – An Updated Review. *Brazilian Journal of Petroleum and Gas,* 5(2), pp. 109-121.

Utilization of Crude Oil as an Alternative Oil Base Mud Drilling Operation by "VICOIL" Standard Drilling Simulation Rig in MGTM Well UPN "Veteran" Yogyakarta Education Park Mineral Geotechnology Museum Field

KRT Nur Suhascaryo[1], Endah Wahyurini[2], and Yuan Cahyo Guntoro[1]
[1]Department of Petroleum Engineering,
Faculty of Mineral Technology, Universitas Pembangunan Nasional "Veteran" Yogyakarta
Jl. SWK 104 Condongcatur, Sleman, Yogyakarta, Indonesia 55281
[1]Department of Agrotechnology,
Faculty of Agriculture, Universitas Pembangunan Nasional "Veteran" Yogyakarta
Jl. SWK 104 Condongcatur, Sleman, Yogyakarta, Indonesia 55281
Corresponding author: nur.suhascaryo@unpyk.ac.id, endaywahyurini@yahoo.com

ABSTRACT - Shale is one of the rocks that often causes drilling problems because shale tends to swell or swell when in contact with mud filtrate, mainly Water-base Mud (WBM). This study aims to determine how the performance of Oil-base Mud (OBM) based on Crude Coconut Oil (CCO) in overcoming the swelling problem. The methodology used consists of drilling simulation and cutting analysis in the X-Ray Diffraction (XRD) laboratory. The series of activities in the study began with the preparation of rock layers, followed by testing the penetration rate using Water-base Mud as a comparison. After cutting analysis was carried out in the XRD laboratory of UPN "Veteran" Yogyakarta with the Rigaku tool, then replaced the type of drilling fluid Oil-base Mud with basic materials alternative to Crude Coconut Oil (CCO) and followed by a penetration test. Rate of Penetration (ROP) test results from WBM with Rheology 1 at interval A or a depth of 1.96 ft-4.92 ft is 442.8 ft/h, Rheology 2 at interval B or a depth of 4.92-10.5 ft is 118.5 ft/hr on the first day. Swelling occurred and resulted in pipe sticking at depth of 6.5 ft. Based on the Bulk Mineral analysis, clay mineral content is 23.84%. Based on the Clay Oriented, smectite dominates the clay by 29.09%. Based on MBT, shale belongs to class B (illite and mixed-layer montmorillonite illite), where this mineral can expand. Based on a Geonor As test, 5.18% of the cutting can develop when exposed to water. The drilling fluid was replaced with Oil-base Mud based on alternative Crude Coconut Oil (CCO), and obtained ROP Rheology 1 at Interval A of 492 ft/h and Rheology 2 at Interval B of 480 ft/h. The results of the Compressive Strength test interval A on the first, third, and fifth days were 31,699 psi, 42,265 psi, and 52,831 psi. The results of the Compressive Strength test interval B on the first, second, and third days were 31,496 psi, 41,517 psi, and 52,971 psi. Based on clay mineral analysis and magnitude of ROP value, is known that Crude Coconut Oil (CCO) based Oil-base Mud is effective because during the simulation, there are no drilling problems, and the resulting ROP value is greater than the first day Water-base Mud.

Keywords: Swelling, Minerals, Crude Coconut Oil, Oil Base Mud, Rate of Penetration

How to cite this article:

KRT Nur Suhascaryo, Endah Wahyurini, and Yuan C. Guntoro, 2021, Utilization of Crude Oil as an Alternative Oil Base Mud Drilling Operation by "VICOIL" Standard Drilling Simulation Rig in MGTM Well UPN "Veteran" Yogyakarta Education Park Mineral Geotechnology Museum Field, Scientific Contributions Oil and Gas, 44 (2) pp., 123-139.

INTRODUCTION

Each type of drilling fluid has character, mainly in controlling hydrostatic pressure, which will affect the rate of penetration or Rate of Penetration (ROP) and its role in minimizing problems during drilling.

Two drilling mud systems, namely water-base mud and oil-base mud. Some of the categories include air, water, and oil. Drilling mud depends on its physical and chemical properties. Problems are often found in the water-base mud (WBM), mainly in the shale

zone. Drilling-grade bentonite is a naturally occurring clay containing the clay minerals of smectite. It can also contain accessory minerals, such as quartz, mica, feldspar and calcite. Shale layer swells or peels off when it comes into contact with water-based drilling mud. By definition, a high performance water-based system is supposed to emulate the performance of an invert fluid while eliminating most, if not all, of the risk and cost associated with managing wastes generated while drilling with invert emulsion systems.

Rate of penetration (ROP) is the volume of rock crushed per unit area (ft) per unit time (hours), or it can also be interpreted as the bit rate destroying the rock to be penetrated and in general ROP measures the speed or progress of the bit when drilling. The compressive strength is equal to the sum of the uniaxial compressive stresses, when the element under consideration is completely disconnected. Shale is a type of rock whose constituent minerals are mostly clay minerals. Swelling and sloughing are influenced by the mineral content in shale itself and the reactivity value of the clay. It is agreed on by many researchers that the methylene test is one of the most accurate and quickest methods in detecting clay minerals in aggregate fines. In drilling operation, there is direct contact between the circulating mud and the walls of the wellbore, resulting in a reaction that affects the properties of the mud, especially in drilling on shale or clay formation (argillaceous). The hydration phenomenon is caused by the interaction between drilling mud and argillaceous formation, which causes an increase in bulk volume of rock and expansion pressure. The conditions identified include the occurrence of sloughing, heaving, expansion (tight hole) and gradual hole enlargement and caving.

The use of oil-base mud has an unfavorable environmental impact, so that in several countries, regulations regarding its use have been enacted. Oil-base mud is more expensive than water-base mud. Coconut Crude Oil (CCO) or coconut oil is used as an alternative to mud oil-base hoping that the drilling operation process can be more effective. Coconut Oil or Crude coconut oil (CCO) is a processed product from coconut meat in the form of a clear liquid, tasteless liquid with a distinctive coconut odor. Crude coconut oil does not require expensive, because the raw materials are easy to obtain at low prices and simple processing. Pure coconut oil has chemical-physical properties, including organoleptic (colorless and needle-like crystals) and odor (there is a slightly sour smell plus a caramel smell). The solubility of CCO is insoluble in water, but soluble in alcohol (1:1). The specific gravity is 0.883 at 20°C. The percentage of evaporation is that CCO does not evaporate at a temperature of 21°C (0%). The melting point is 20-25°C, boiling point: 225°C, and the density of air (Air=1): 6.91. Vapor pressure (mmHg) is one at 121°C. CCO processing methods include fermentation methods, gradual heating, centrifugation, acidification and inducement.

X-Ray Diffraction (XRD) is an analytical method that is effective in describing rocks and certain chemical compounds in solid form by using X-ray diffraction/reflection. The basic law of using X-ray diffraction refers to Bragg's Law which is written with the formula $n\lambda = 2d \sin$ where n is the order of fraction (1,2,3,...n), is the wavelength (Å), d is the thickness of the unit cell , and is the diffraction angle.

This research aims to determine the performance of Crude Coconut Oil as an alternative material Oil-base Mud in overcoming swelling problems. The methodology used consists of drilling simulation and cutting analysis. The series of activities in the study began with the preparation of rock layers, penetration rate using Water-base Mud, cutting analysis was conducted in the X-Ray Diffraction Laboratory, Methylene Blue Test, and Geonor As analysis, then replaced the type of drilling fluid Oil-base Mud with alternative base material Crude Coconut Oil and continued with the penetration rate test.

A. Literature Review

1. Drilling Mud

Drilling mud or fluid is a fluid that circulates in rotary drilling, which has various functions required in drilling operations. The type of drilling mud that is in accordance with the characteristics of the well will support the success of the drilling operation, especially on the flow pattern and drilling speed and the successful removal of cuttings to the surface (Coussot *et al.*, 2004; Saasen *et al.*, 2002).

There are two drilling mud systems, namely water base mud and oil base mud. Zaba & Doherty (1970) classified drilling mud mainly based on the fluid phase: water (water base), oil (oil base) or gas.

Utilization of Crude Oil as an Alternative Oil Base Mud Drilling Operation by "VICOIL"
Standard Drilling Simulation Rig in MGTM Well UPN "Veteran" Yogyakarta Education
Park Mineral Geotechnology Museum Field (Suhascaryo, *et al.*)

2. X-Ray Diffraction (XRD) – Bulk Mineral

X-ray diffraction is a tool used to determine the mineralogy of sedimentary rocks. Monocormatic x-ray rays that penetrate the mineral grains, will be scattered by the atoms that make up the mineral. At a certain angle, the scattered x-ray beam will produce a secondary beam. This phenomenon is called diffraction. This relationship is written in the Bragg equation:

$$N\lambda = 2d \sin \theta$$

Description:

d = Basal spacing.

n = Fraction order (1, 2, 3,…..n)

λ = Wave length, Å

θ = Shooting angle, º

Furthermore, to calculate the percentage of minerals in the sample, the following equation is used:

$$A = I_A/(I_A + I_B + ... I_n) \times 100\% \qquad (1)$$

Description:

A = Percent mineral (%)

I = Shooting intensity (cps)

3. Coconut Crude Oil (CCO)

Coconut Oil or Crude coconut oil (CCO) is a processed product from coconut meat in the form of a clear, tasteless liquid with a distinctive coconut odor. The manufacture of Crude coconut oil does not require expensive costs, because the raw materials are easy to obtain at low prices and simple processing. Pure coconut oil has chemical-physical properties, including organoleptic (colorless and needle-like crystals) and odor (there is a slight sour smell plus a caramel smell). The solubility of CCO is insoluble in water, but soluble in alcohol (1:1). The specific gravity is 0.883 at 20ºC. The percentage of evaporation is that CCO does not evaporate at a temperature of 21ºC (0%). The melting point is 20-25ºC, boiling point: 225ºC, and the density of air (Air=1): 6.91. Vapor pressure (mmHg) is 1 at 121ºC.

4. "VICOIL" Standard Drilling Simulation Rig

The "VICOIL" standard drilling simulation rig consists of a power system using a Honda C70 engine and a Dexta Cam Starter generator type QS5-15P/3. The Honda C70 engine has 71.8 cc engine specifications, type OHC, 4 stroke air conditioning, performance 6 hp @ 9000 rpm (power), 0.53 kg.m @ 7000 rpm (torque). The generator has 500V and 15A specifications. The supporting structure made of steel construction with a height of 3 meters, an area of 4 m² (bottom) and 2 m2 (top). The substructure is made of an arrangement of 24 iron pipes measuring 1.25 inches with an area of 16 m2. The substructure is equipped with a cat walk with a height of 4 m and an iron construction ladder consisting of 15 steps. Rig floor has an area of 16 m² of iron plate. On the hoisting equipment there is a modified drawwork made of the Honda C70 frame with dimensions of 1,805 mm (length), 685 mm (width), 995 mm (height). Suspension in the form of swing arm, double shockbreaker (front), leading link, and 2.2 inch travel (rear). Drum type brakes to help control speed. Rear tire size 2.50 – 17 - 6 PR. The overhead tool consists of a 12 cm diameter crown block, a modified hook with a direct drilling line belay, a modified traveling block with a rectangular shape measuring 1 m long, 15 cm wide and 30 cm high. The drilling line consists of a fast line made of steel rope. The rotary assembly consists of a square turntable with a side length of 30 cm. The turntable is connected to the generator via a belt on a 15 in diameter gear. The master bushing is square with a side length of 16 cm. kelly bushings are rectangular in shape with a side length of 4 cm. The drill pipe series consists of a rectangular kelly with a length of 9.8 ft, a drill pipe in the form of a 1.25 inch steel pipe with a length of 5.58 ft, and a modified drill collar in the form of a steel pipe thread measuring 1.25 inch with a length of 8.2 ft. The chisel (bit) is a modified drag bit with a steel cutter bit type with a three-blade design with a diameter of 4 inches. The preparation area for the circulation system consists of a tandone brand mud tank with a capacity of 350 liters equipped with a dynamo-powered agitator to stir the drilling fluid in the mud tank. Modern brand dynamo with type JY09A-4 with specifications HP, 220V, 50 HZ, 2.36A, 1400 RPM. The circulation equipment consists of a Shimizu brand mud pump model PS-226 BIT in the form of a water pump with a specification rate of 0.069 bpm to 0.176 bpm. The conditioning area consists of a rectangular shale shaker with a double-layered iron wire filter measuring 30 cm wide and 40 cm long. There are setting tanks with a capacity of 70 liters used to accommodate mud during the conditioning area. The settling tanks are equipped with an International type DB-125 water pump with a specification rate of 0.176 bpm.

DATA AND METHODS

The method in this research is drilling simulation and laboratory test with the following steps:

1. Arrangement of rock layers

   The preparation of this layer is intended to determine the effect of rock layer compactness on the penetration rate with drilling mud.

2. Preparation of WBM

   Preparation of water-base mud (WBM) which will be used for drilling and acts as a comparison for OBM made from CCO.

3. Rate of penetration

   This test was carried out using a standard drilling simulation rig, VICOIL, located at the Mineral Geotechnology Museum Park, UPN "Veteran" Yogyakarta. The drilling simulation tower is equipped with four drilling systems with modifications.

4. Cutting analysis

   Cutting analysis was carried out using the X-Ray Diffraction method with the Rigaku tool.

X-ray diffraction bulk mineral analysis

X-ray diffraction analysis using bulk minerals is used to see the mineral content contained in the sample. X-ray diffraction is a tool used to determine the mineralogy of sedimentary rocks. Monochromatic x-ray rays that penetrate the mineral, will be scattered by the atoms that make up the mineral. At a

Figure 1
"VICOIL" standard drilling simulation rig.

Utilization of Crude Oil as an Alternative Oil Base Mud Drilling Operation by "VICOIL"
Standard Drilling Simulation Rig in MGTM Well UPN "Veteran" Yogyakarta Education
Park Mineral Geotechnology Museum Field (Suhascaryo, *et al.*)

certain angle, the scattered x-ray will produce a secondary ray.

X-ray diffraction clay oriented

After the mineral content based on bulk, minerals is known and if there is clay content, it must be continued with X-ray diffraction analysis using bulk minerals to see the clay content in bulk minerals.

Methylene blue test

The methylene blue (MBT) test was carried out to determine the cations that could be found and had indications of flake reactivity and swelling tendency. Based on the MBT value, the value of the cation exchange capacity will be obtained, which will later be used determine the appropriate type of shale.

Geonor As

The mechanism of this test is sedimentation to see the large percentage of clay to swell when in contact with water.

5 . Analysis of drilling problems is carried out based on data obtained during cutting analysis in the laboratory.
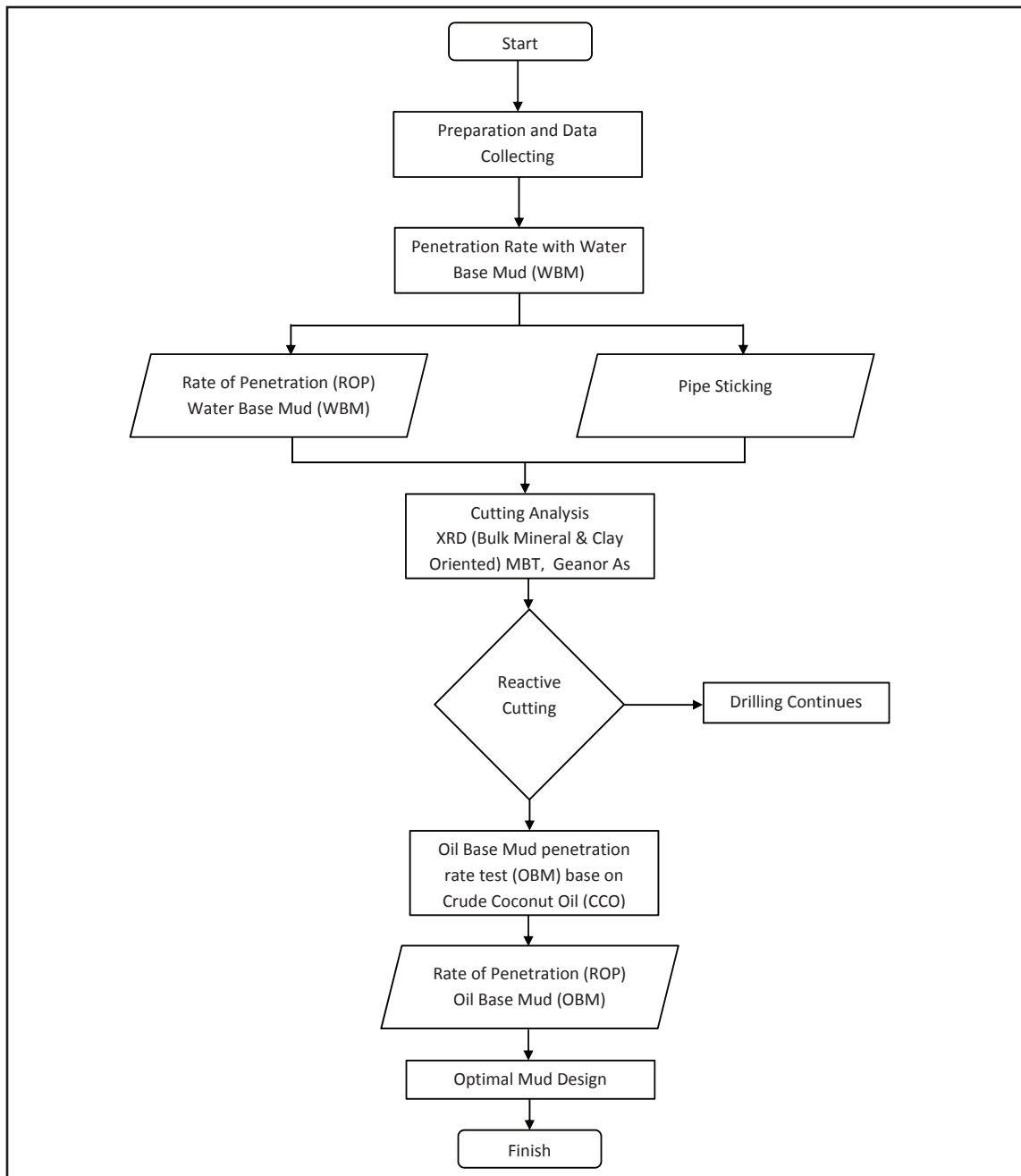
Figure 2
Flow chart.

6. Change of oil-base mud drilling mud type and determination of drilling mud composition

Change a drilling mud and determine the composition of the drilling mud by identifying the potential problems seen from the XRD readings and also the target physical properties of the drilling mud to be achieved.

7. The physical properties of an effective Coconut Crude Oil-based oil-based mud can be determined based on the results of the penetration rate test with the "VICOIL" standard drilling simulation tower.
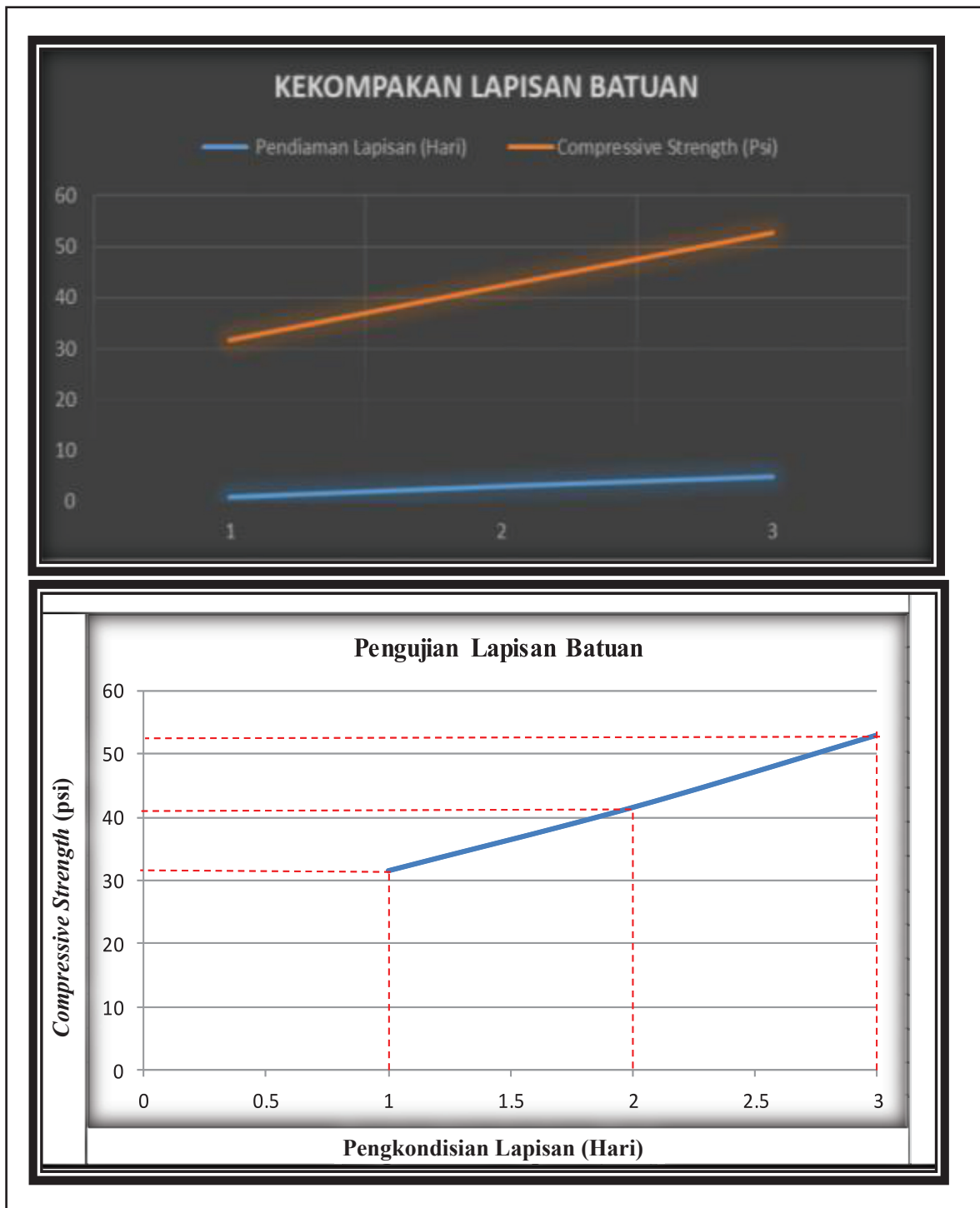
Figure 3
Comparison of compressive strength to well Layer A (left) and B (right) conditioning.

Utilization of Crude Oil as an Alternative Oil Base Mud Drilling Operation by "VICOIL"
Standard Drilling Simulation Rig in MGTM Well UPN "Veteran" Yogyakarta Education
Park Mineral Geotechnology Museum Field (Suhascaryo, *et al.*)

RESULTS AND DISCUSSION

A. Drilling Simulation by "VICOIL" Standard Drilling Simulation Rig

1. Arrangement of Rock Layer

In the simulation well, there are 2 rock layers were arranged in the form of shale and sandstone. First rock layers or interval A on depth 1.96-4.92 ft with a composition consisting of 6.6 kg or 37 % bentonite, 5.5 kg or 49 % sand, and 1.7 kg or 14 %. Second rock or interval B layer on depth 4.92-10.5 ft with a composition consisting of 23.1 kg or 41% bentonite, 27.5 kg or 42% sand, and 8.5 kg or 17% cement. This simulation areonducted 6 shale layers, where 2 insert shale lies at the middle and bottom of interval A and 4 layers of shale on interval B at of 6 ft - 6.6 ft, 6.8 ft - 7.5 ft, 7.7 ft - 8.3 ft, and 8.5 ft - 8.8

ft. The results of the Compressive Strength interval A testing on the first, third and fifth day is 31,699 psi, 42,265 psi, and 52,831 psi. The results of the CS interval B testing on the first, second and third day is 31,496 psi, 41,517 psi, and 52,971 psi. Composition WBM of A and B listed on Table 1.

2. Penetration Rate Testing with Water Base Mud (WBM)

The rock layer testing was carried out after the rock layers were arranged in the simulation well using "VICOIL" standard drilling simulation rig. The fixed WOB value used is 7.136 lb for interval A and 32.34 lb for interval B, the RPM fixed value is 147 rpm. The drilling pump used has a rate of 0.069 bpm. The volume of drilling mud used in this simulation is 17.85 liters interval A and 38.92 liters interval B. During testing with WBM, a pipe sticking problem

Table 1
Composition of water base mud (WBM) simulation

Composition Of Water Base Mud A and B				
Interval A			**Interval B**	
Ingredients		Amount		
Water	17.85	liter	38.92	liter
Bentonite	1147.5	gram	2502	gram
KOH	25.5	gram	55.6	gram
PAC-L	127.5	gram	336.6	gram
PAC-R	127.5	gram	336.6	gram
KCL	255	gram	667.2	gram

Table 2
Comparison of WBM rheology test results

No.	Properties	Rheology 1	Rheology 2	API Spec	Unit
Rheology Water Base Mud Comparison by "VICOIL" Drilling Simulation Rig					
1	*Mud Weight*	8.6	8.9	8.8 - 9.6	ppg
2	*Plastic Viscosity*	13	10	10-Aug	cp
3	*Yield Point*	12	14	< 24	lb/100 ft2
4	*Gel Strength* (10 sec/ 10 min)	2-Jan	4-Feb	2-3/ 4-5	lb/100 ft2
6	*Filtration loss*	6.8	6.2	< 15	ml/30 min
7	*Filter Cake Thickness*	0.285	0.22	< 4	mm
8	**pH**	9	10	9.5 - 11.5	

occurred in the bottom of interval A and at a depth of 7 ft and 8 ft from the surface. There are WBM rheology 1 for interval A and rheology 2 for interval B are shown on Table 2.

3. Cutting Sample Analysis

Cutting analysis is carried out to determine the type of rock layer that is penetrated. The cuttings tested in this simulation show an indication of swelling, this can be seen in Figure 4 which shows the reaction of swelling when the sample is dropped with water.

XRD Bulk Mineral Analysis

Cutting analysis was carried out using a Rigaku tool with a firing angle of 3º–90º. A figure 6 is obtained after shooting the cutting sample, where this figure is a comparison between the intensity and the angle of shooting.

From this figure, it is known that the peak of the cutting interval is at a shooting angle of 26.68º with an intensity of 192.647196 cps. Then the calculation is carried out using the Bragg equation as follows:

$$d = \frac{\lambda}{2\sin\left[\frac{2\theta(deg)}{2}\right]}$$
$$d = \frac{1,5406 \; nm}{2\sin\left[\frac{26.68}{2}\right]}$$
$$d = 3.34 \; Å$$

It is known that the peak size indicates the percentage of minerals, it can be calculated by the following equation:

$$= \frac{Quartz \; Intensity(cps)}{Total \; Intensity} \times 100\%$$

$$= \frac{192.647196}{365.24989} \times 100\%$$

$$= 56.97 \; \%$$

Calculation from those above equation is tbaulation, the presectation of table 5 various minerals in the analyzed cuttings were obtained. The mineral content of Clay in the cutting drilling by the "VICOIL" Driling Simulation Rig is quite large, namely 23.84 %, Quartz mineral content is 56.97 %, Kaliophilite mineral content is 6.75 %, Pyrite mineral content is 6.69%, and Dolomite mineral content is 5.75 %. So we can take the conclussion the high clay minerals can be examination with Clay Orientation.

Table 3
Results of WBM rheology 1
and 2 penetration rate on the first daytable

Depth (ft)	ROP Day 1 by Rheology WBM 1 (ft/h)	Depth (ft)	ROP Day 1 by Rheology WBM 2 (ft/h)
2.94	944.64	7	1069.7
3.94	235.2	9	360
4.92	176.4	10.5	131.7

Table 4
WBM rheology 1 and 2 total of penetration rate results

WBM Testing			
Rheology	Day	Depth (ft)	ROP Total (ft/h)
1	1	4.92	442.8
2	1	5.58	295.4

XRD Bulk Mineral Analysis

Based on Clay Oriented, clay content dominated by smectite or montmorillonite 29.09 %. Cation Exchange Capacity from smectite is high, there are 80-120 meq/ 100 gr.

Methylene Blue Test (MBT)

From MBT analysis, titration every 2 ml of methylene blue to sampel of cutting. The result is 16 meq/ 100 gr so the shale include a B class (illite and mixed layer), from that, the shale can be swelling.

Geonor As

Based on the swelling test with the geonoor as tool, then if the cutting sample is in contact with water it will produce a swelling percentage of 5.18%.

4. Testing the Penetration Rate Using OBM made from CCO

The penetration rate test uses Oil Base Mud (OBM) drilling fluid with alternative base materials of Crude Coconut Oil (CCO) or Coconut Oil. The volume of drilling mud used in this simulation is 38.92 bbl.

In testing the penetration of rock layers using Oil Base Mud based on alternative CCO, the results obtained are different Rate of Penetration (ROP). The longer the rock layer is left in place, the higher the

Utilization of Crude Oil as an Alternative Oil Base Mud Drilling Operation by "VICOIL"
Standard Drilling Simulation Rig in MGTM Well UPN "Veteran" Yogyakarta Education
Park Mineral Geotechnology Museum Field (Suhascaryo, *et al.*)
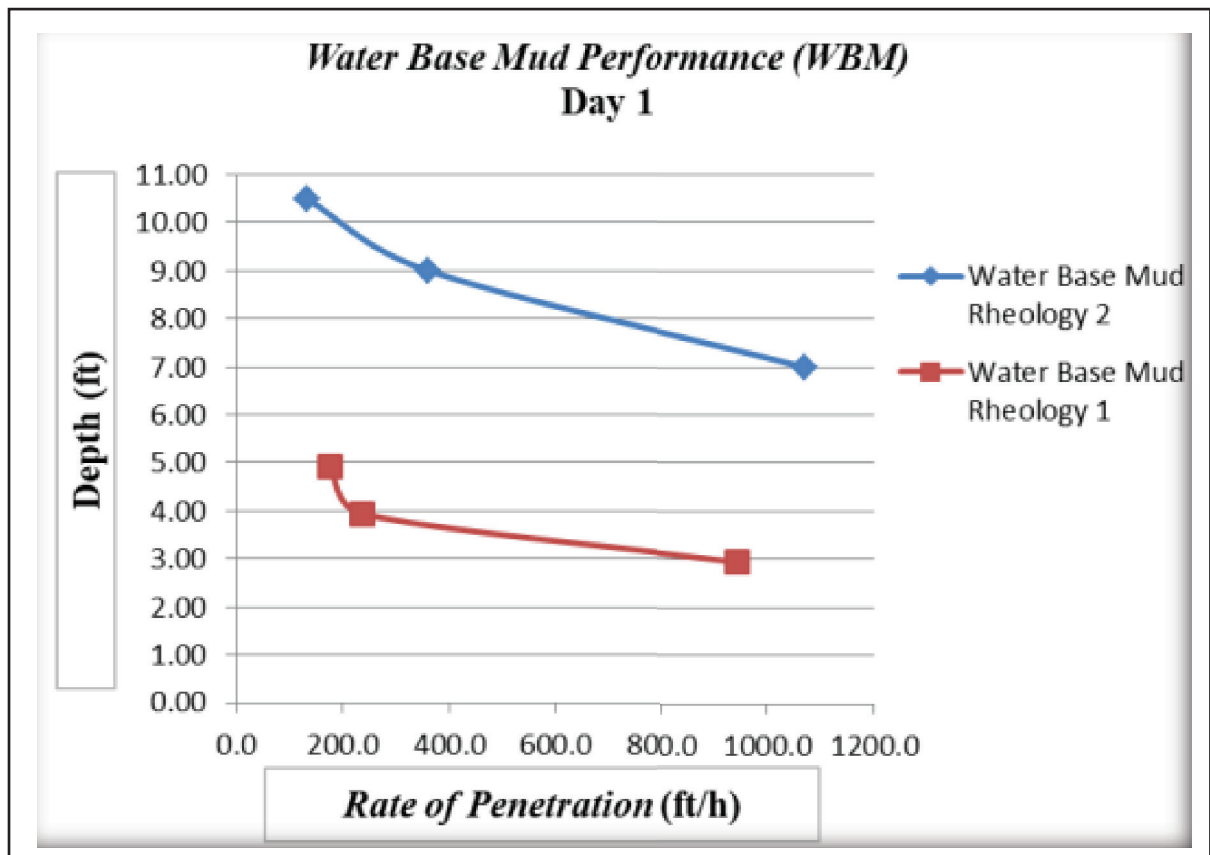
Figure 4
Comparison of depth with rate of penetration day 1 by rheology.

Figure 5
Sample of cutting dropped by water.
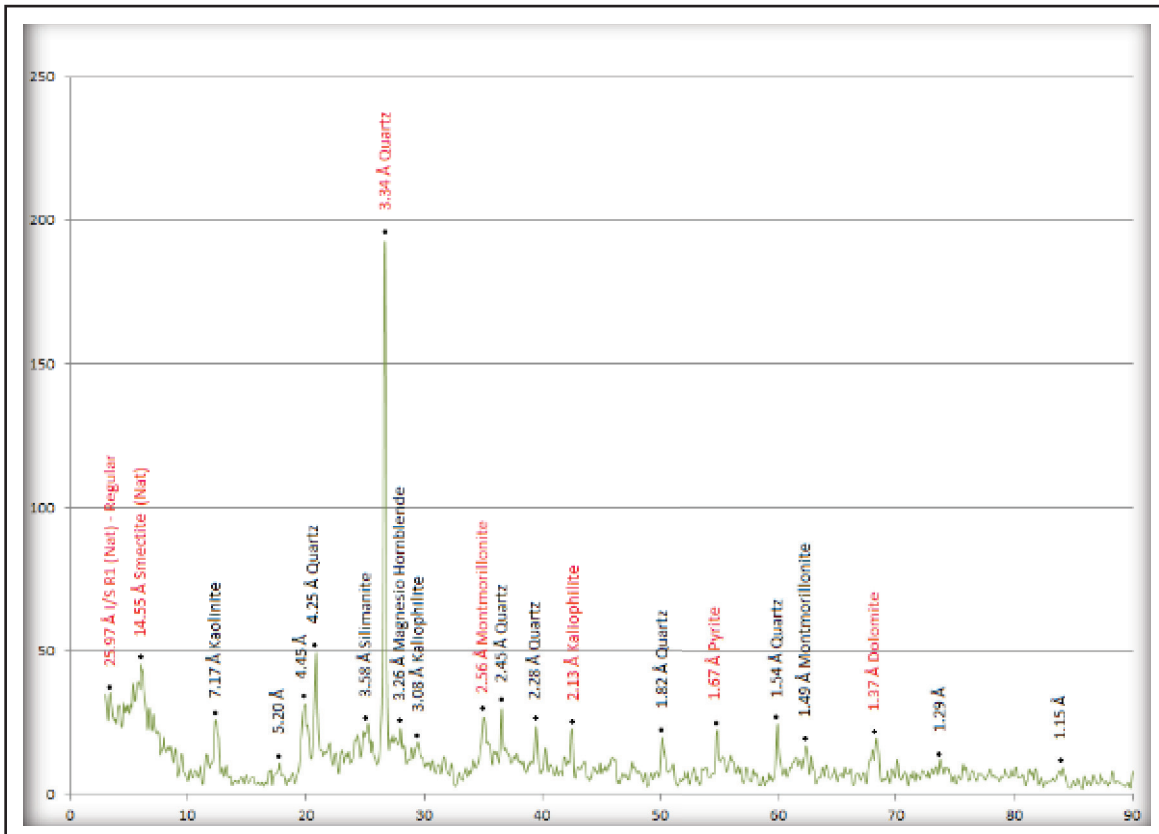
Figure 6
Results of bulk mineral analysis

Table 5
Cutting analysis results of bulk mineral XRD

2 θ (deg)	Intensity (cps)	2 θ/2	d	Mineral	Percent (%)
3.4	35.371654	1.7	25.97	I/S R1 (Nat) - Regular	10.46
6.07	45.259733	3.035	14.55	Smectite/ Monmorillonite	13.38
26.68	192.647196	13.34	3.34	Quartz	56.97
42.5	22.821814	21.25	2.13	Kaliophilite	6.75
54.89	22.620702	27.445	1.67	Pyrite	6.69
68.34	19.459853	34.17	1.37	Dolomite	5.75

Compressive Strength value is due to the influence of the cementation level of the rock and the load on the rock, so the rate of penetration will be smaller.

The total Rate of Penetration (ROP) value generated while using OBM Rheology 2 on the first day of testing was 589.1 ft/h, the second day of testing was 164.7 ft/h, and the third day of testing was 71.7 ft/h. The rate of penetration produced by OBM on the first day is greater than the use of WBM Rheology 2. When the drilling simulation with OBM was carried

Utilization of Crude Oil as an Alternative Oil Base Mud Drilling Operation by "VICOIL"
Standard Drilling Simulation Rig in MGTM Well UPN "Veteran" Yogyakarta Education
Park Mineral Geotechnology Museum Field (Suhascaryo, *et al.*)
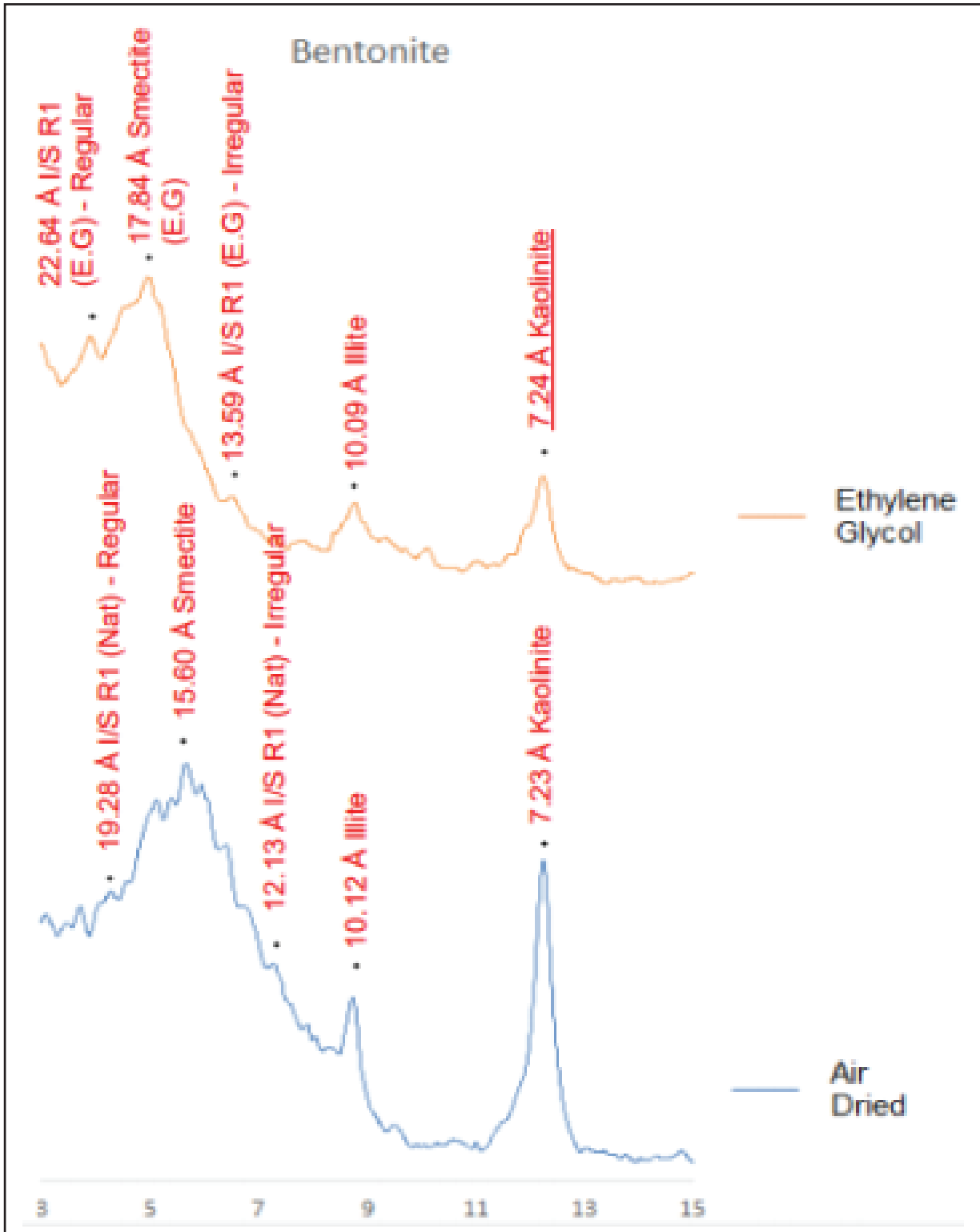
Figure 7
Results of clay oriented analysis.

out, no problems were found. Based on the value of the penetration rate with OBM, it can be seen that the rate of penetration will decrease with increasing days which is in line with the increase in the compressive strength value of the rock layer.

CONCLUSIONS

First day ROP data obtained using WBM interval A with Rheology 1 is 442.8 ft/h, Rheology 2 is 295.4 ft/h and OBM Rheology 1 is 492 and Rheology 2
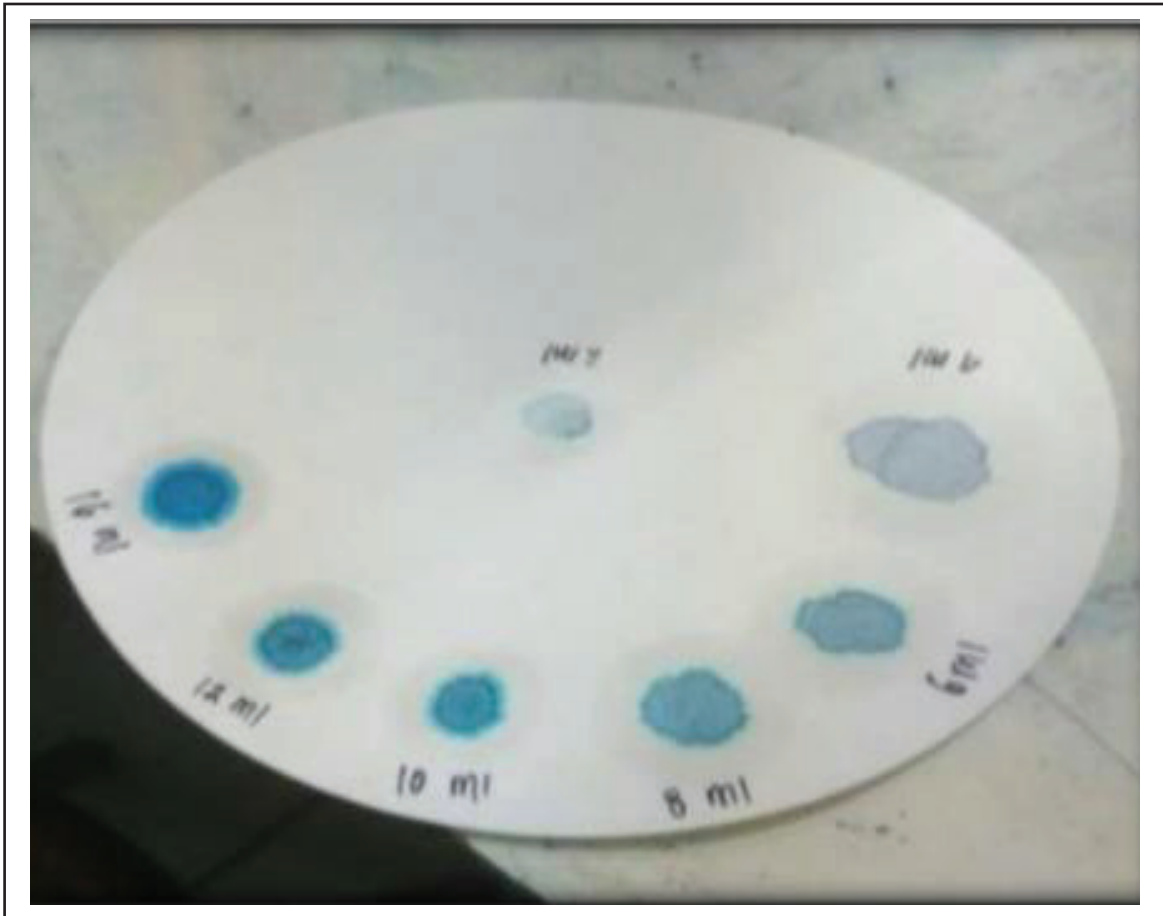
Figure 8
Results of MBT test.
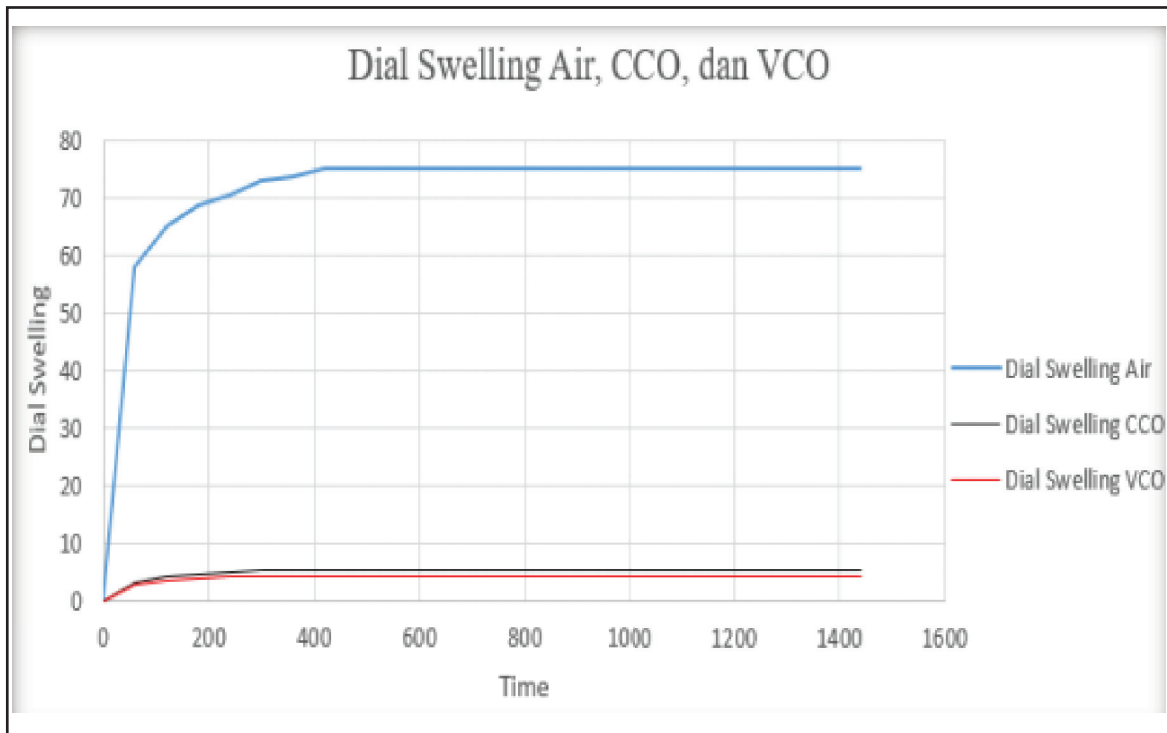
Figure 9
Dial swelling cutting.

Utilization of Crude Oil as an Alternative Oil Base Mud Drilling Operation by "VICOIL"
Standard Drilling Simulation Rig in MGTM Well UPN "Veteran" Yogyakarta Education
Park Mineral Geotechnology Museum Field (Suhascaryo, *et al.*)
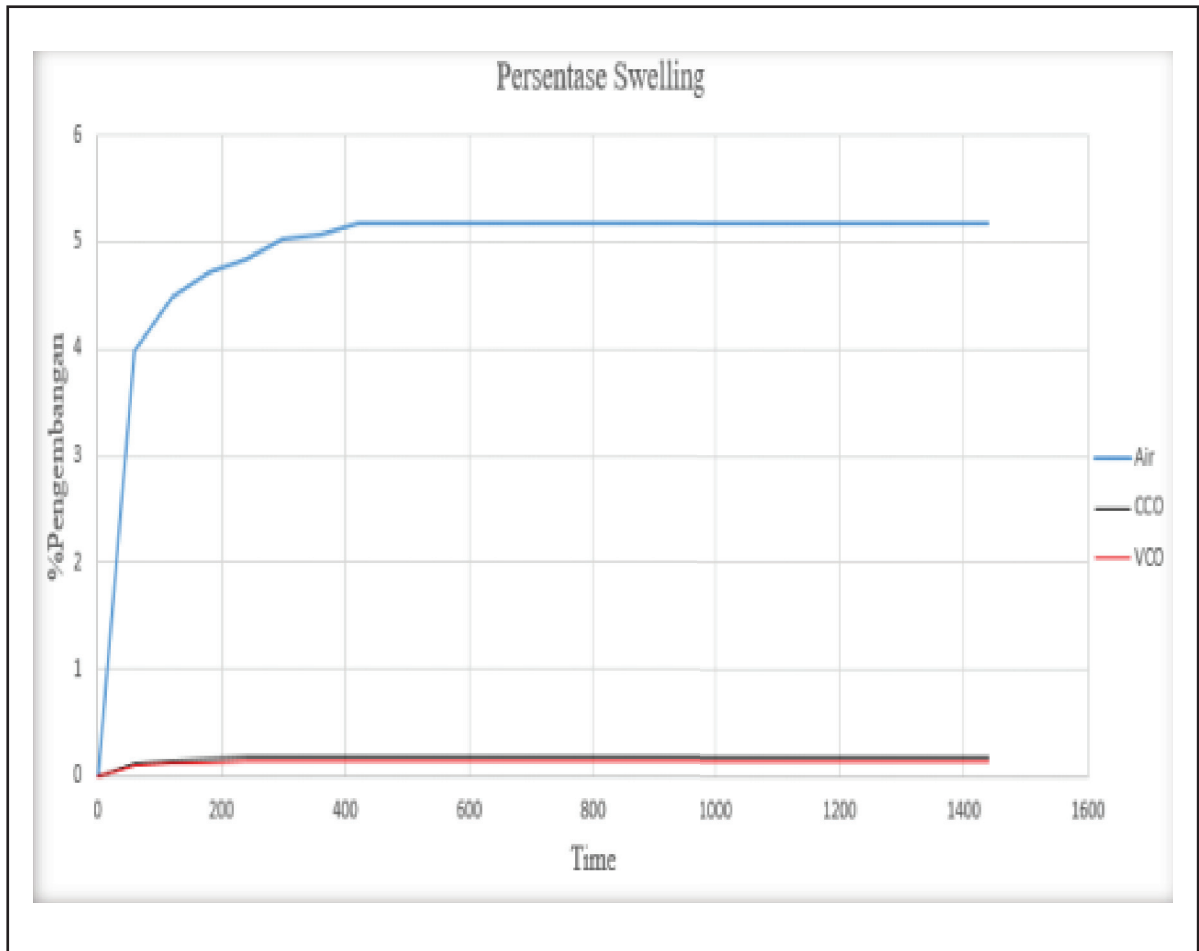
Figure 10
Percentage swelling cutting.

Table 6
Composition of oil base mud (OBM) simulation by "VICOIL" standard simulation rig

Composition of Oil Base Mud interval A and B			
Interval A		**Interval B**	
Ingredient	Amount	Amount	
CCO	12.495 liter	31.136	liter
Water	5.355 liter	7.8	liter
CaCl2	1530 gram	3892	gram
H-*Lime*	255 gram	556	gram
Barite	5100 gram	11120	gram
Geltone	153 gram	333.6	gram
Carbotrol	255 gram	667.2	gram
Invermul	0.255 liter	0.6	liter
EZ Mul	0.102 liter	0.2	liter

Table 7
Comparison of rheology test results by "VICOIL" drilling standard simulation rig

No.	Properties	Rheology 1	Rheology 2	API SPEC	Unit
	Rheology Oil Base Mud				
1	**Mud Weight**	10.3	10.1	11-Oct	ppg
2	**Plastic Viscosity**	19	18	< 35	cp
3	**Yield Point**	32	24	15 – 25	lb/100 ft2
4	**Gel Strength (10 sec/ 10 min)**	16-Dec	15-Aug	6-10/ 13-18	lb/100 ft2
6	**Filtration loss**	3	3.8	< 4	ml/30 min
7	**Filter Cake Thickness**	1.7	1.8	< 2	mm
8	**pH**	8	6	8.5 - 9.5	
9	**MBT**		12	≤ 12.5	meq/ ml of fluid

Table 8
First, second and third day penetration rate results with OBM rheology 1 and 2

Rheology	Depth (ft)	Day 1 ROP (ft/h)	Day 3 ROP (ft/h)
	2.94	944.64	248.5
1	3.94	271.3	160.3
	4.92	196	135.6
	7	1152	195.8
2	9	595	73.2
	10.5	348.4	37.6

Table 9
Total penetration rate results

Rheology	Total Penetration Rate OBM by Rheology 2		
	Day	Depth (ft)	ROP (ft/h)
1	1	4.92	492
	3	4.92	264.3
2	1	5.58	589.1
	3	5.58	71.7

Utilization of Crude Oil as an Alternative Oil Base Mud Drilling Operation by "VICOIL"
Standard Drilling Simulation Rig in MGTM Well UPN "Veteran" Yogyakarta Education
Park Mineral Geotechnology Museum Field (Suhascaryo, *et al.*)
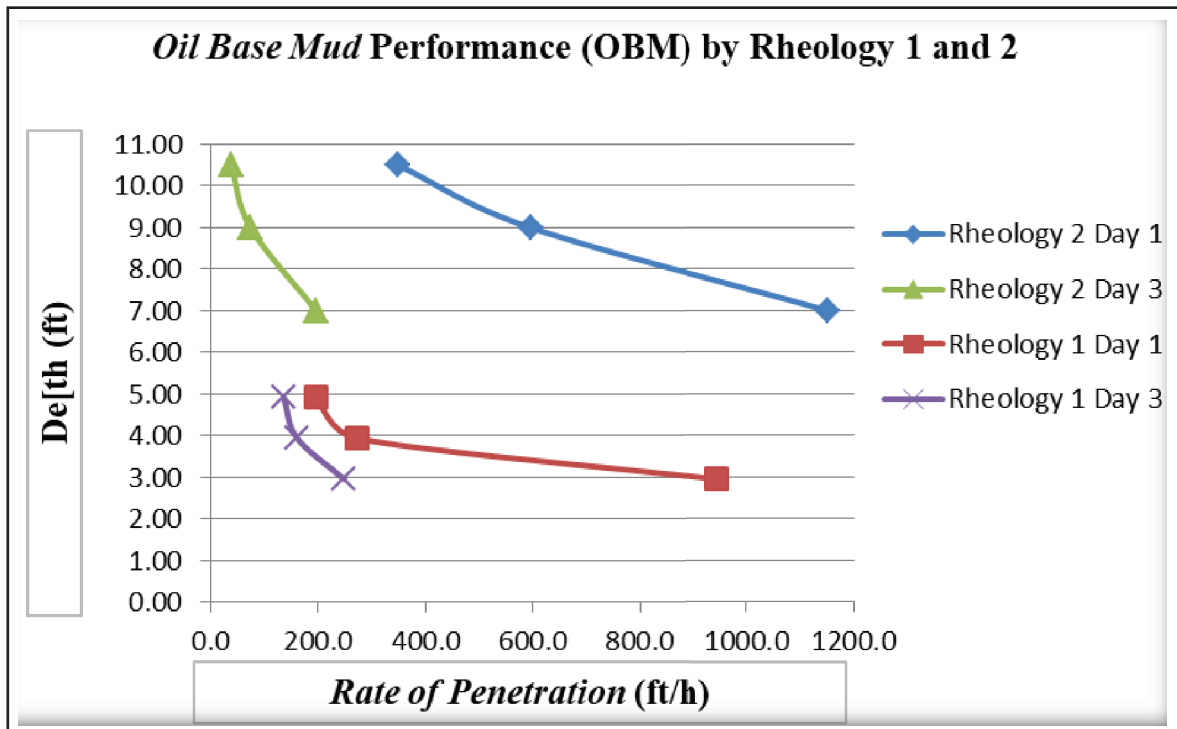
Figure 11
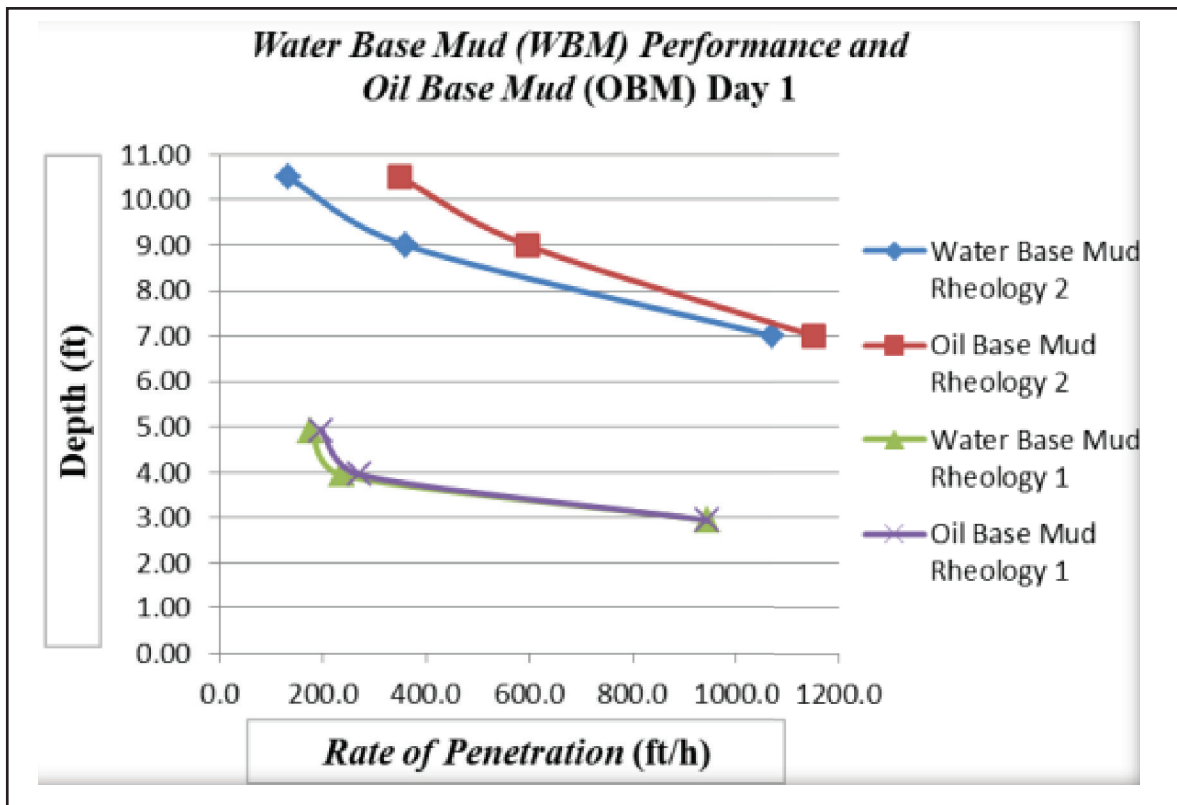Oil base mud (OBM) performance of rheology 1 and 2.

Figure 12
Comparison of the performance of water base mud (WBM)
and oil base mud (OBM) on the first day of Rheology 1 and 2.

is 589.1 ft/h. The smaller ROP WBM results were caused by a swelling problem that resulted in pipe sticking.

Based on cutting analysis, from bulk mineral analysis it is known that the mineral content clay minerals are 23.84 %. Based on Clay Oriented, the cotent of clay mineral dominated by smectite 29.09 %, Based on MBT test, shale include in the B class (illite and mixed layer) where this mineral can be swelling. Based on Geonoor As, there are 5.18% the cutting can be swelling if contact with water.

Compressive Strength interval A testing on the first, third and fifth day is 31,699 psi, 42,265 psi, and 52,831 psi. The results of the CS interval B testing on the first, second and third day is 31,496 psi, 41,517 psi, and 52,971 psi.

Based on the results of the clay mineral analysis and the magnitude of the ROP value, it can be seen that the use of Crude Coconut Oil (CCO) based Oil Base Mud is effective because during the simulation there are no drilling problems and the resulting ROP value is greater than the first day Water Base Mud.

ACKNOWLEDGEMENTS

GLOSSARY OF TERMS

Symbol	Definition	Unit
Cation	A cation is an ion with fewer electrons than protons. Therefore, it has a positive charge.	
Compressive strength	The maximum compressive stress that, under gradually applied load, a given solid material can sustain without fracture.	
Crude Coconut Oil	Coconut Oil or Crude coconut oil (CCO) is a processed product from coconut meat in the form of a clear, tasteless liquid with a distinctive coconut odor.	

Symbol	Definition	Unit
Cutting	Drill cutting are broken bits of solid material removed from a borehole drilled by rotary, percussion, or auger method and brough to the surface in the drilling mud.	
Diffraction	The spreading of waves around obstacles.	
Hydration	A substance that contain water.	
Mineral	A solid chemical compound with a fairly well-defined chemical composition and a specific crystal structure that occurs naturally in pure form.	
Montmorillonite	A very soft phyllosilicate group of mineral that form when they precipitate from water solution as microscopic crystals, known as clay.	
Mud	A heavy viscous fluid mixture that is used in oil and gas drilling operation to carry rock cuttings to the surface and also to lubricate and cool the drill bit.	
Oil Base Mud	Drilling fluid in drilling engineering, composed of oil as the continuous phase and water as the dispersed phase in conjunction with emulsifiers, wetting agents and gellants.	
Pipe Sticking	A drill pipe is stuck in a borehole and cannot be recovered from the bore without damage to the drill pipe.	
Rate of Penetration	The speed at which a drill bit breaks the rock under it to deepen the borehole.	
Rheology	The study of relationship between force (stress) and deformation (strain) of engineering materials under a set of loading and environtmental conditions.	

Utilization of Crude Oil as an Alternative Oil Base Mud Drilling Operation by "VICOIL"
Standard Drilling Simulation Rig in MGTM Well UPN "Veteran" Yogyakarta Education
Park Mineral Geotechnology Museum Field (Suhascaryo, *et al.*)

Symbol	Definition	Unit
Rig	The machine components used to drill a wellbore.	
Sloughing	The collapse of the borehole wall due to the nature of the formation that it easy to collapse, brittle and the presence of cracking in the hole.	
Swelling	A part of the body of rock increase in size, typically as a result of injury, inflammation, or fluid retention.	
Water Base Mud	A drilling fluid composed os water and bentonite and heavy minerals which are also added for weight.	
Weight on Bit	The amount of downward force exerted on the drill bit and is normally measured in thousands of pounds.	
Wellbore	A hole that is drilled to aid in the exploration and recovery of natural resources, including oil, gas, or water.	
X-Ray Diffraction	A method or tool used to determine the atomic and molecular structure of a crystal by diffracting a beam of x-ray in all directions.	

REFERENCES

Bourgoyne Jr, A. T., Millheim, K., Chenevert, M. & Young Jr., F., 1991. *Applied Drilling Engineering.* United States of America: Society Of Petroleum Engineers.

Davarpanah, A., Zarei, M. & Mehdi-Nassabeh , S., 2016. Assessment of Mechanical Specific Energy Aimed at Improving Drilling Inefficiencies and Minimize Wellbore Instability. *Journal of Petroleum & Environmental Biotechnology,* Volume 2.

Halliburton Fluid Systems, 2006. *Baroid Fluid Services Fluids Handbook*: Halliburton Fluid Systems.

Herianto & Askeyanto, D., 2015. *Analisa Swelling Clay Formasi Telisa Untuk Perencanaan Lumpur Pemboran.* Yogyakarta, FTM UPN "Veteran" Yogyakarta.

Pitre, B. T., 2012. *Application of the modified Methylene Blue Test to detect clay minerals in coarse aggregate fines.* Texas: Texas A&M University.
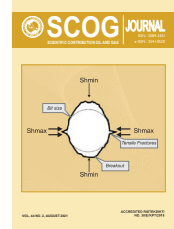
Suhascaryo, K. N., Herlambang, S. & Pasaribu, H., 2020. *The Effects of VICOIL Bopanprog Usage as a Substitute for Crude Oil for Oil-Based Drilling Fluids.* Yogyakarta, LPPM UPN "Veteran" Yogyakarta Conference Series, pp. 284-294.

Suhascaryo, K. N. & Yudiantoro, A., 2020. *Proses Aktivasi Dalam Peningkatan Kualitas VICOIL BOPANPROG Desa Bojong, Kecamatan Panjatan, Kabupaten Kulonprogo.* Yogyakarta: Uwais Inspirasi Indonesia.

Wicaksono, D. D., Setiawan, N. I., Wilopo, W. & Harijoko, A., 2017. *Teknik Preparasi Sampel Dalam Analisis Mineralogi Dengan XRD (X-Ray Diffraction) - Di Departemen Teknik Geologi, Fakultas Teknik, Universitas Gadjah Mada.* Yogyakarta, Fakultas Teknik, Universitas Gadjah Mada.

Prediction of Hydraulic Fractured Well Performance using Empirical Correlation and Machine Learning

Kamal Hamzah[1,2)], Amega Yasutra[2)], and Dedy Irawan[2)]
[1]PT. Medco E&P Indonesia
The Energy Building 36th Floor, SCBD Lot 11A
Jl. Jendral Sudirman, Kav. 52-53, Jakarta 12190, Indonesia
[2]Institut Teknologi Bandung
Jl. Ganesha 10, Lb. Siliwangi, Kec. Coblong, Bandung, Jawa Barat 40132 Indonesia
Corresponding author: humas@itb.ac.id

ABSTRACT - Hydraulic fracturing has been established as one of production enhancement methods in the petroleum industry. This method is proven to increase productivity and reserves in low permeability reservoirs, while in medium permeability, it accelerates production without affecting well reserves. However, production result looks scattered and appears to have no direct correlation to individual parameters. It also tend to have a decreasing trend, hence the success ratio needs to be increased. Hydraulic fracturing in the South Sumatra area has been implemented since 2002 and there is plenty of data that can be analyzed to resolve the relationship between actual production with reservoir parameters and fracturing treatment. Empirical correlation approach and machine learning (ML) methods are both used to evaluate this relationship. Concept of Darcy's equation is utilized as basis for the empirical correlation on the actual data. The ML method is then applied to provide better predictions both for production rate and water cut. This method has also been developed to solve data limitations so that the prediction method can be used for all wells. Empirical correlation can gives an R^2 of 0.67, while ML can give a better R^2 that is close to 0.80. Furthermore, this prediction method can be used for well candidate selection means.

Keywords: Hydraulic Fracturing, Well Performance, Empirical Correlation, Machine Learning.

How to cite this article:

Kamal Hamzah, Amega Yasutra, and Dedy Irawan, 2021, Prediction of Hydraulic Fractured Well Performance using Empirical Correlation and Machine Learning, Scientific Contributions Oil and Gas, 44 (2) pp., 141-152.

INTRODUCTION

Hydraulic fracturing is a stimulation treatment to enhance well productivity and improves the economic value of well reserves. It have been widely applied to both low and moderate permeability reservoirs. In low permeability reservoir, it greatly contributes both to well productivity and to well reserves, while in moderate permeability reservoirs, it accelerates production without impacting the well reserves (Holditch & Ma, 2016).The production

improvement and additional reserve (if any) have to be justified economically because hydraulic fracturing jobs requires high cost and involve large scale equipment.

Meanwhile, hydraulic fracturing in some fields in South Sumatra has been implemented on more than 200 wells since 2002. Year by year, it becomes more challenging due to increasingly limited well candidates with good reservoir properties and decreasing trend in production results. Thus, hydraulic fracturing optimization both in planning

that include well candidate selection/design and job execution has to be applied. The objective is to increase fracturing job success ratio and therefore contribute to more oil production.

However, the production results from hydraulically fractured wells looks scattered and has no clear correlation to individual well parameters (Azhari, 2015). It gets even more challenging due to the decreasing trend in production result of hydraulic fracturing job that make the job economics becoming marginal. There are hundreds of data sets that are potentially useful for the evaluation. The data covers the reservoir parameters from primary log data, petrophysical analysis, and dynamic parameters from well-testing analysis. Hydraulic fracturing parameters both the treatment data and fracture geometry result are also utilized.

To ensure that hydraulic fracturing job can give additional value for the field, there is a need to estimate and quantify conclusively the result of hydraulic fracturing job in order to minimize unsuccessful job. Thus, the prediction tool has to be developed to determine well candidate based on reservoir and well properties. Two (2) methods to develop the prediction tools are presented in this paper.

The first method is empirical correlation equation. It contains a mathematical equation based on some parameters from a given set of empirical data that will be used for predicting other data (Ribarič & Šušteršič, 2017). In this paper, the empirical correlation equation is used to predict the hydraulic fracturing result based on combined parameters of reservoir pressure, transmissibility data and dimensionless productivity index from hydraulic fracturing treatment.

The second method is machine learning approach. Machine learning is the study of computer algorithms that can improve automatically through experience by discovering general rules in large data sets to meet the user's interest (Mitchell 1997). Temizel, *et al.* (2021) has described the applications of machine learning in oil & gas industry and provide its capability and limitations in unconventional reservoir engineering and well completion calculations. In many cases, machine learning was proven able to predict the output that has problem in data limitation and data quality (Makhotin, *et al.*, 2019).

Finally, both two (2) approaches are expected to yield a robust prediction tool that can be easily applied to all wells using common primary data as input parameters. The prediction tool is then utilized in well candidate selection to determine the good well candidates and eliminate non-potential well candidates in the future hydraulic fracturing job campaign. It's also expected to ensure and guide the fracturing treatment optimization to maximize the production result.

DATA AND METHODS

The workflow in developing this study consist of 5 major phases that represents the whole process and details of working procedure. It is shown on Fig.1 that consists of data preparation, empirical correlation approach, machine learning approach to predict production and water cut, and its application on well candidate selection. Actual data field will be incorporated in the discussion of each step to ensure that this methodology is applicable.

A. Data Preparation

Data from actual hydraulic fracturing job were collected and tabulated that including input and output data. The output data is the production performance whereas input data covers well data including well completion data such as perforating length and wellbore size, and reservoir data including several parameters such as reservoir pressure, open-hole log and petrophysical data. Hydraulic fracturing parameters also covers actual treatment data and calculated fracture geometry.

The data was evaluated to become a ready-to-use data set. It consists of several steps that includes data conversion, ignoring & filling missing values and outlier data elimination. The data set is tested by using Pearson correlation coefficient (Pearson, 1920) to measure the direction and strength of the linear relationship between input parameters and output parameter.

B. Empirical Correlation Approach

The empirical correlation approach utilizes the Darcy equation in radial condition as shown in equation (1). This equation need reservoir properties that are represented by transmissibility and reservoir pressure and fracture parameters. Transmissibility can be defined from petrophysical analysis and well testing. The latter method is preferred because it represents the reservoir quality at certain radius. This method utilizes the pre-frac data obtained in mini-fall-off test and analyzed using short
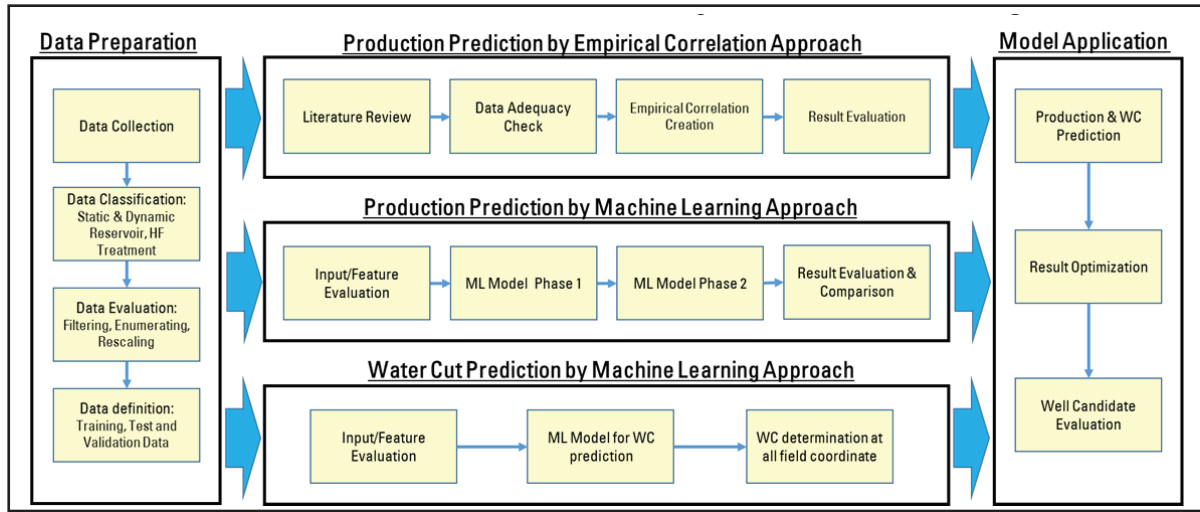
Figure 1
Workflow for performance prediction of hydraulic fractured well.

impulse injection test to obtain reservoir permeability (Abousleiman *et al*., 1994). Through this method, we can also estiamte the reservoir pressure.

$$q = \frac{kh(P_r - P_{wf})}{141.2 \; \mu B \ln(\frac{r_e}{r_w} + S)} \qquad (1)$$

Fracture parameter is represented by dimensionless productivity index (PI) or J_D as shown in equation (2). This parameter can be calculated based on a simulated result of fracture geometry using equivalent wellbore radius concept and unified fracture design method thru proppant number.

$$J_D = \frac{1}{\ln(\frac{r_e}{r_w} + S)} = \frac{1}{\ln(\frac{r_e}{r_w^r})} \qquad (2)$$

Prats (1961) first introduce the idea of the effective wellbore radius ($r_{w'}$). It based on a simple balancing of flow areas between a wellbore and a fracture gives the equivalent value of $r_{w'}$ for a propped fracture. Cinco-Ley *et al*. (1978) later integrated this into a full description of reservoir response, including transient flow. For pseudoradial flow, rw´ is expressed as a function of fracture length (X_f) and dimensionless fracture conductivity (C_{fD}).

The unified fracture design methodology provided by Economides, Oligney, and Valkó (2002), expands the above approach to include fracture and well drainage area dimensions that will not reach pseudoradial flow before the onset of pseudosteady state. The key of this approach is the idea that for a given proppant volume and well drainage area, there is a fracture half length, width, and conductivity that

maximize the well productivity. For a given proppant volume, square well drainage area, and values for both proppant and reservoir permeability, the dimensionless proppant number, Np, is defined as

$$N_p = \frac{4k_f x_f w}{k x_e{}^2} = \frac{4k_f x_f wh}{k x_e{}^2 h} = \frac{2k_f V_{prop}}{k V_{res}} \qquad (3)$$

All above parameters are combined based on equation (1) and then plotted versus production result (in BFPD) at pseudosteady state regime. The correlation of this cross plot can be utilized in a form of empirical correlation to predict the result of next hydraulic fracturing job.

C. Machine Learning Approach

Machine learning (ML) is a broad subfield of artificial intelligence aimed to enable machines to extract patterns from data set. It is based on mathematical statistics, numerical methods, optimization, probability theory, discrete analysis, geometry and etc (Smola & Vishwanathan, 2008). There are three main components in ML that consists of data, features or parameters and algorithms or method.

Nowadays there are four main directions in machine learning that consist of classical ML, ensemble methods, reinforcement learning and neural networks & deep learning (www.vas3k.com). Classical ML utilizes pure statistics method and consist of supervised (e.g. linear regression) and unsupervised (e.g. clustering). Ensemble methods construct a set of classifiers and then classify new data points by taking a (weighted) vote of their

143

predictions (Dietterich, 2000). Some wellknown ensemble method are Random Forest (Breiman, 2001), Gradient Boosting (Friedman, 2001) and Ada-Boost (Dietterich, 2000). Reinforcement learning is used in case no data input but it have an environment to live in. Neural Networks and Deep Leaning is used for replacement of all previous algorithms. It often used in object identification, speech recognition and synthesis, image processing and etc.

In this paper, ML is used to create relationship between production result as output and reservoir/hydraulic fracturing parameters as input. The ML approach is divided into two phases. In phase 1, the input data is limited to pressure, transmissibility and PI dimensionless data, similar to the empirical correlation approach. It aims to compare the result of empirical correlation and ML methods, and to evaluate the importance of each parameter in machine learning. In phase 2, the input used in phase 1 is replaced by primary data such as open-hole log, petrophysical parameters, and fracturing treatment. This phase is proposed to make the ML model usable practically by using parameters that almost all wells have.

The ML model that used in this phase is supervised machine learning (linear regression) and ensemble method that consist of Random Forest, Gradient Boosting and Adaboost. The best model is chosen based on mean absolute error (MAE), coefficient of determination (R^2) and Pearson correlation coefficient (R) on actual production rate and prediction based on ML model.

Beside production rate prediction, the ML is also used to predict the water cut (WC) and net oil production. In this case, the k-Nearest Neighbor (k-NN) model is utilized due to the similarity of its base concept with the WC prediction based on

geographical coordinates. The main concept of kNN is to predict the label of a query instance based on the labels of k closest instances in the stored data (Kang, 2021). The stored data in our case is the WC data of each producer wells.

D. Application on Well Candidate Selection

The best ML model on production rate and water cut predictions are implemented in well candidate selection for future hydraulic fracturing job. Economic value is determined for each well based on the net oil prediction. This method can eliminate wells with low oil production potential that yields low economic value.

Moreover, the ML model can be utilized to optimize the fracturing treatment plan in order to have more oil production. The optimization can be conducted by tuning the proppant type, proppant volume and other parameters.

RESULTS AND DISCUSSION

This section presents results of empirical correlation and ML approaches to establish the relationships between actual production and reservoir/fracturing parameters.

A. Empirical Correlation Approach

There are 45 hydraulic fractured wells that have complete data as required by the Darcy's equation. Products of pressure, transmissibility data, and dimensionless productivity index is plotted against the actual production rate to get the trend and empirical correlation as well.

Two (2) correlations have been developed based on two methods to define the dimensionless PI. The first method is the Cinco-Ley correlation using
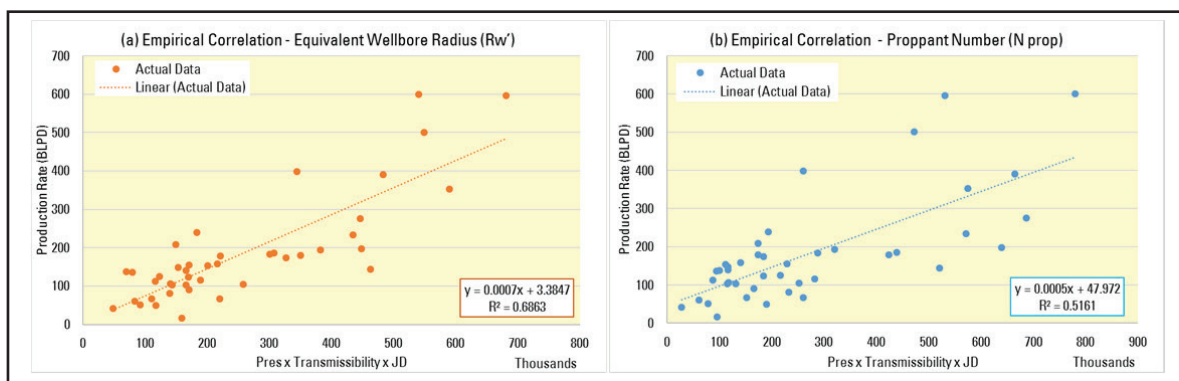

Figure 2
Empirical Correlation based on (a) Cinco Ley Correlation
using equivalent wellbore radius and (b) Unified Fracture Design using proppant number.

the equivalent wellbore radius whereas the second method is unified fracture design using proppant number. The empirical correlation results for each method are shown on Figure 2.

The empirical correlation shows that there is a linear correlation between the product of pressure, transmissibility, and dimensionless PI to the production rates. It complies basic Darcy's equation. Empirical correlation based on dimensionless PI using wellbore equivalent radius gives better result than empirical correlation based on proppant number. The R^2 of the first method is 0.67 which is higher than R^2 from the second method of 0.57. So is the Pearson correlation coefficient, it shows that the first method give +0.82 which is higher number than the second method of only +0.72. The cross plot between actual production and production result based on empirical correlation is shown in Figure 3. At production rate of more than 400 BLPD, the plot starts to deviate from line $R^2=1$, resulting in R^2 of lower than 0.7.

B. Machine Learning Approach

Machine learning phase 1 was carrying out using input as same input as for the empirical correlation approach. The objective is to assess and ensure that ML can be utilized for the production prediction of hydraulic fractured well. The result then will be compared to the empirical correlation approach.

Input evaluation has been applied by assessing the input using feature engineering and feature importance for each ML model. As described on Figure 4, reservoir transmissibility appears to be the most influential parameters to the production rate result. It is represented by the Pearson correlation coefficient value of +0.72, which is the highest among the parameters. Then it is followed by reservoir pressure and dimensionless PI.

Consistent with the feature importance evaluation, reservoir transmissibility becomes the most important for all ML models with values between 0.5 and 0.6. Reservoir pressure and J_D have ranging values within $0.1 - 0.3$ for all ML models.

The 45 wells data is then divided into two groups of 80% data for training and 20% data for testing. As previously mentioned, the ML models used to predict production results is Linear Regression, Random Forest, Gradient Boosting and AdaBoost.

Training and testing result evaluations for each ML model are shown in Table 1. The ML model that has R^2 consistent above 0.7 are Random Forest and Gradient Boosting. AdaBoost has a tendency for overfitting in the training, having testing R^2 of only 0.67. Linear regression shows not too robust as the testing R^2 is larger than the training value. As described on Fig. 5, the cross plot between actual production and prediction from ML model that follow the $R^2=1$ are Random Forest and Gradient Boosting. Linear regression shows scatter and AdaBoost clearly shows overfitting in the training data set but scatter in the testing data set.
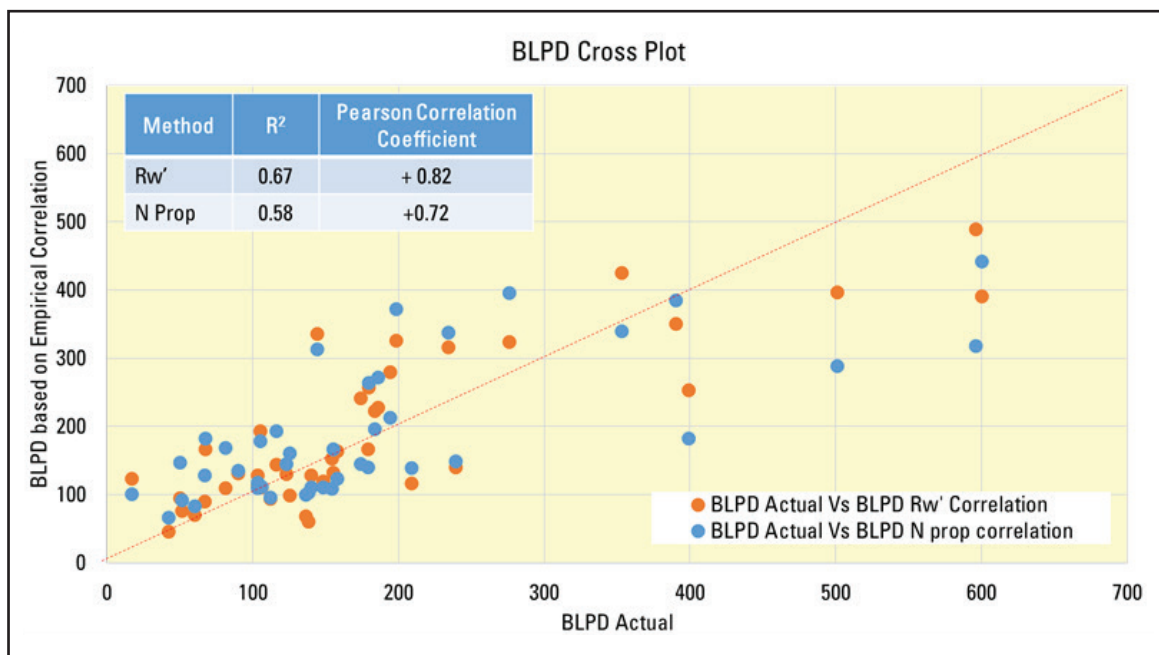

Figure 3
Cross Plot between production actual Vs production from empirical correlation.

Through this approach, it can be concluded that ML can be used to estimate the production result of hydraulic fractured well. Transmissibility from mini-fall-off test becomes the most important parameter in machine learning. However, the main concern is that the ML model cannot be applied to other well because of:

- The availability of transmissibility data from mini-fall-off test are limited to only 45 wells. It required high effort/cost to obtain this data.

- The correlation between actual transmissibility and petrophysical analysis is low at $R^2 = 0.597$. The utilization of transmissibility of petrophysical analysis will lead to lower R^2 in the correlation and produce more error. Thus, it cannot replace the actual transmissibility.

C. Machine Learning with Primary Data Set

In order to have ML model that is practically able to be used for well candidate selection, ML model based on the primary data set is then developed. This ML model will utilize common parameters that almost all of wells have. The input parameters will consist of basic well data, open-hole log, petro-physical analysis and fracturing treatment. Fracturing treatment data are preferred to be used because lack of validation on fracture geometry data. Only limited number of wells that have temperature log to validate the simulated fracture geometry.

Feature engineering is applied to both reservoir properties and fracturing treatment to select the parameters that can be input as feature in ML model. The value of Pearson correlation coefficient to production data that higher than +1 and lower than -1 are selected to feature in ML. Some important parameters were also selected to be input feature in ML. Finally, the parameters that were selected to be the input feature in ML model are shown in Table 2.

There are 140 wells data set to be analyzed by ML. They are divided into two groups consisting of 80% data for training and 20% data for testing. Same as previous, ML model used to predict the production result are Linear Regression, Random Forest, Gradient Boosting and AdaBoost.

The training and testing results of each ML model are shown in Table 3. The ML models that show R^2

Table 1
ML phase 1 result evaluation

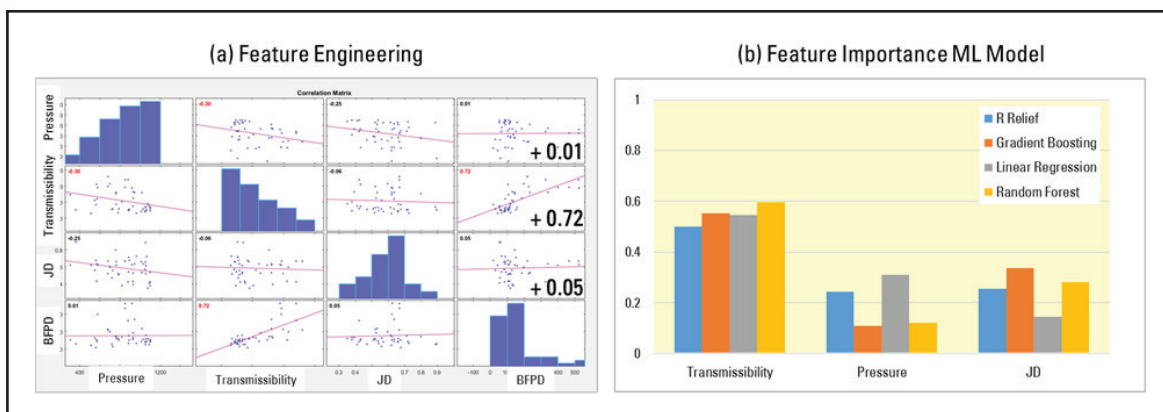| ML model	Training : 80%			Testing: 20%		
	MAE	R^2	R	MAE	R^2	R
Random Forest	32	0.88	0.94	29	0.76	0.95
Linear Regression	64	0.57	0.75	19	0.87	0.96
Gradient Boosting	2.1	1	1	26	0.83	0.91
AdaBoost	0.1	1	1	33	0.67	0.95

Figure 4
Input evaluation using (a) feature engineering and (b) feature importance for each ML Model.

consistent above 0.7 are Random Forest, AdaBoost and Gradient Boosting. Random Forest and Gradient Boosting give satisfying results based on R^2 and Pearson Correlation coefficient. AdaBoost tend to have over-fitting in the training but also give good result in the testing, whereas Linear Regression's R^2 value is the lowest one.

Figure 6 also describes the cross plot between actual production and prediction result from each ML model. Training and testing data that follow the $R^2=1$ was shown in gradient boosting and random forest. However, both Random Forest and Gradient Boosting exhibit deviation from line $R^2=1$ at rate higher than 500 BLPD. This might be caused by the small data population in this production rate range. So the ML model does not have adequate data for having accurate prediction at this range production rate.

However, Linear Regression model shows scattered correlation between actual and prediction result both for traninig and testing data set. Linear Regression does not seem fit with the typical data with many input and have an issue in the quality. AdaBoost tend to have over fitting in training data set so that looks scatter in testing data set.

Finally, we can inferred that Gradient Boosting is the most reliable ML model to predict the production rate of hydraulic fractured well. Gradient Boosting has stable R^2 both in training and testing data set that indicates the robustness of this model. This model is then recommended to be applied in the production rate prediction.

D. Water Cut (WC) Prediction

ML can also be utilized to predict the water cut of each well by position. For this purpose, k-Nearest Neighbors (k-NN) is used for the water cut prediction based on XY coordinate as well as vertical position of the bottom zone. The dataset is taken from all producer wells with the updated WC and is also divided into two sets, training and testing. This partition to ensure that the model has good robustness and consistency.

Table 2
Input evaluation result for ML phase 2

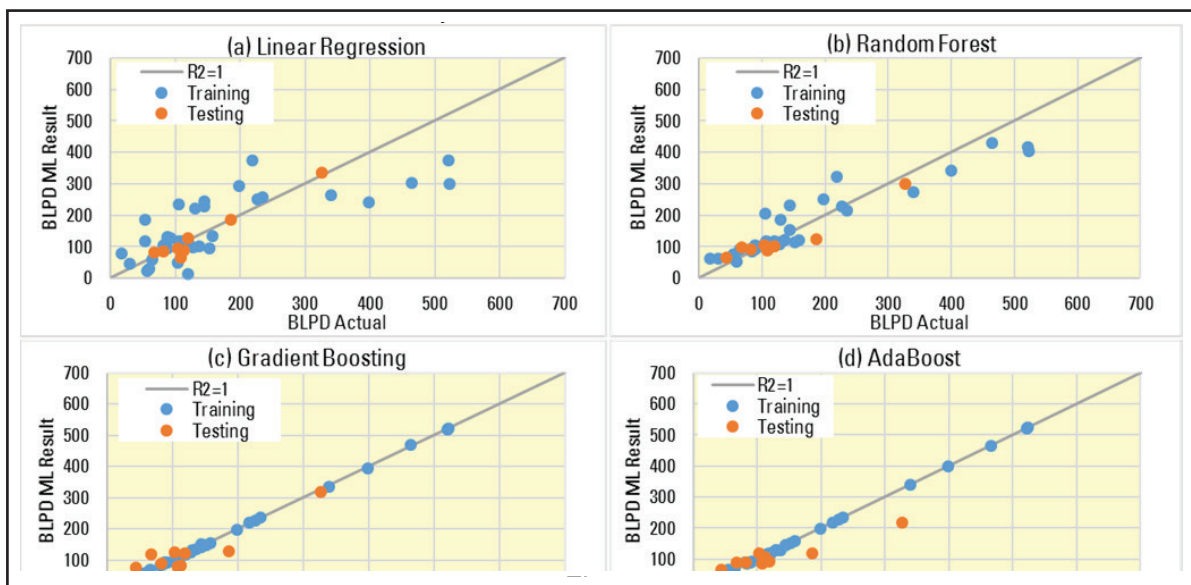| Reservoir Parameters	R	Remarks
Field	0.43	
Perforation Length	0.13	
Reservoir Pressure	0.06	Important parameter
Thickness	0.21	
GR	-0.21	
Resistivity	0.12	
Density	-0.1	
V clay	-0.31	
Perm	0.43	
kh	0.46	
Fracturing Parameters		
Proppant Type	0.26	
Proppant Volume	-0.37	Important parameter
Fluid Type	0.42	
Fluid Volume	-0.25	Important parameter
Frac Gradient	0.13	

Figure 5
Cross plot between actual production Vs production result from each ML model in phase 1.

The k-NN manipulates the training data and classifies the new test data based on distance metrics. There are some parameters that need to be tuned to improve the performance such as K value, distance metric and weights. Scaling/normalizing the data set can help to improve the k-NN performance. K value indicates the count of the nearest neighbors. Some method to define distance metric can be adjusted to have reliable model such as Euclidean, Manhattan and Chebyshev distance (Cantrell, 2000).

For the WC prediction in this case, the optimum model is obtained using k=5 and Chebyshev distance. The result of kNN on WC prediction in two fields are shown by Figure 7. Figure 7.a shows the position of well that currently producing. The WC is measured from liquid sample by laboratory testing. Figure 7.b represents the result of k-NN model in WC mapping on every coordinate on those two fields. Field 1 shows that in any well location, the wells mostly have high WC. This field has been drained since 2002 and is experiencing pressure depletion. Water injection was then applied to maintain the pressure.

On the other hand, Field 2 shows better WC at any location. This field has very low permeability thus the recovery factor is still low. The reservoir in this field has been massively developed since 2015.

E. Application on Well Candidate Selection

The most reliable of the ML models for fluid production and water cut prediction is then applied to predict the performance of well candidate after hydraulic fracturing job. There are total eigth well candidates for next hydraulic fracturing campaign. These well candidates have already had water cut from the existing zone and produce oil rate below

Table 3
ML phase 2 result evaluation

ML model	Training : 80%			Testing: 20%		
	MAE	R²	R	MAE	R²	R
Random Forest	39	0.87	0.95	47	0.77	0.91
Linear Regression	77	0.45	0.67	75	0.5	0.81
Gradient Boosting	37	0.89	0.96	52	0.78	0.9
AdaBoost	1.9	0.99	0.99	53	0.72	0.89
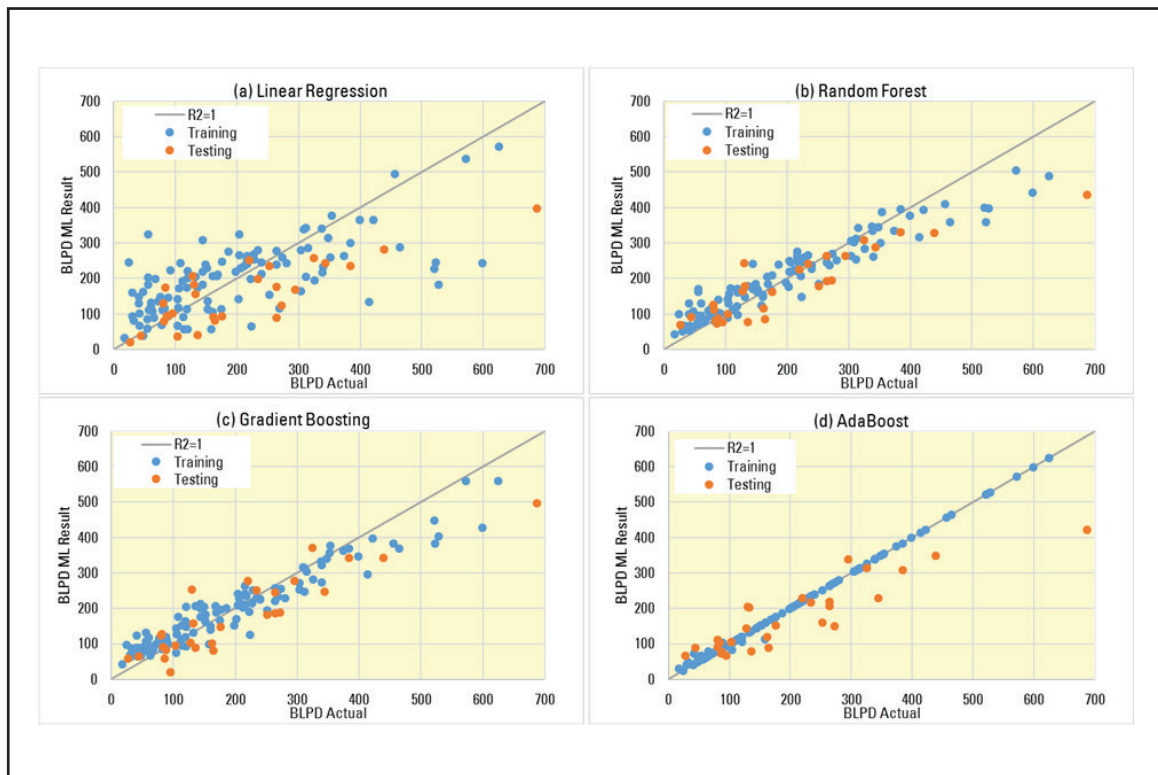
Figure 6
Cross plot between actual production Vs production result from each ML model in phase 2.

5 BOPD. Workover change layer and hydraulic fracturing as stimulation treatment will be proposed to these wells.

The prediction tool based on Gradient Boosting and k-NN is shown in Table 4. The economic cut off for hydraulic fracturing job is equivalent to the initial production 40 BOPD. Based on the prediction, there are four wells that will have initial oil production higher than 40 BOPD and three wells that lower than 40 BOPD.

Further assessment is then applied to those three wells. Preliminary optimization to the hydraulic fracturing treatment is assessed and the result is predicted. After optimization of proppant type and volume, then we can conclude that only one well can afford to get higher than 40 BOPD, while the remaining wells is still under economic cut off. Thus, the other

two wells as shown in Table 5 will be excluded from hydraculic fracturing job plan.

By this result, it can be confirmed that ML model through Gradient Boosting and k-NN model can be applied for both production rate and water cut predictions. The ML approach can be applied using primiary data that almost all wells have. Empirical correlation cannot be applied in this case because of the data limitation such as unavailability of actual transmissibility data.

The objective to develop the prediction tool that can be applied for any wells can be achieved. It enable quantitative comparison on estimated hydraulic fracturing result so that potential well candidate can be easily selected. This tool also can be utilized to ensure and guide the fracturing treatment optimization to maximize the production result.
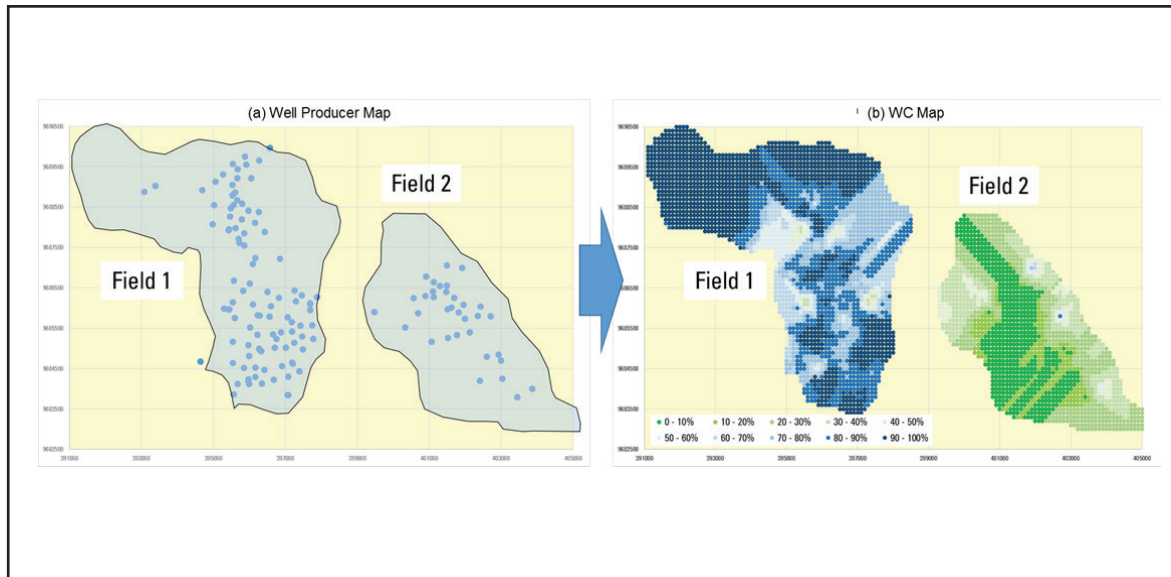

Figure 7
Water cut prediction map using k-NN model.

Table 4
Prediction result based on ML model for hydraulic fracturing well candidates

Well	Res pressure (psig)	KH (md.ft)	Proppant type	Proppant volume (klbs)	BLPD prediction	WC prediction	BOPD prediction	Remarks
W-0103	698	112	3	60	166	0.78	37	Below economic cut off
W-0313	553	266	3	60	175	0.85	26	Below economic cut off
W-0329	612	663	3	60	274	0.83	48	
W-0343	624	928	3	60	243	0.81	47	
W-0331	849	16.4	3	90	134	0.25	100	
W-0335	972	16.4	3	90	82	0.39	51	
W-0367	500	508	3	60	207	0.89	22	Below economic cut off

Table 5
Prediction result based on ML model for hydraulic fracturing well candidates after optimization

Well	Res pressure (psig)	KH (md.ft)	Proppant type	Proppant volume (klbs)	BLPD prediction	WC prediction	BOPD prediction	Remarks
W-0103	698	112	3	80	184	0.78	41	
W-0313	553	266	3	80	193	0.85	28	Below economic cut off
W-0329	612	663	3	60	274	0.83	48	
W-0343	624	928	3	60	243	0.81	47	
W-0331	849	16.4	3	90	134	0.25	100	
W-0335	972	16.4	3	90	82	0.39	51	
W-0367	500	508	3	80	225	0.89	24	Below economic cut off

CONCLUSIONS

Some conclusions can be inferred from the above discussion about the prediction of hydraulic fracturing job result using empirical correlation and machine learning model. Several points that can be inferred is below:

Empirical correlation based on Darcy equation gives maximum R^2 of 0.67 and Pearson correlation coefficient +0.82 between actual and prediction production. It can be applied as prediction tool but require input parameters which is not all wells have such as actual transmissibility and dimensionless PI.

Machine learning phase 1 (Random Forest & Gradient Boosting) using same input as empirical correlation, give better result with $R^2 > 0.75$ and Pearson correlation coefficient > 0.9 between actual and prediction production. It describes that ML approach can be utilized in prediction of hydraulic fractured well performance.

Machine learning phase 2 (Gradient Boosting) by utilizing primary data such as open-hole-log, petrophysical analysis and frac treatment data yield $R^2 > 0.8$ and Pearson correlation coefficient > 0.9 between actual and prediction production. It confirms that this method is the most reliable prediction tool with the lowest error.

The most important parameter that majorly contributed to hydraulic fracturing results is the reservoir quality that can be expressed by permeability or transmissibility data.

K-NN model can be utilized to predict the WC using coordinate and altitude well. It can give a satisfying result with R^2 value of 0.845 in the testing data set.

ML model through Gradient Boosting for production prediction and k-NN for WC prediction can be used as prediction tool for well candidate selection implementation and frac treatment optimization.

Some recommendations for further improvement in the prediction of hydraulic fracturing result using machine learning are below:

Mini-fall-off analysis should be applied and collected from all hydraulic fracturied job to create the correlation between open-hole data & petrophysycal analysis with the actual transmissibility data. It will help to create a reliable empirical correlation as prediction tools. However, it will extend the overall execution time and lead to additional extra cost.

Some parameters that also influence the fracture geometry such as shale barrier and stress contrast based on sonic log should be considered as additional feature in the ML model. This paper excludes these parameters because of the lack of sonic log data availability in the data set.

Individual ML model to determine each of reservoir properties factor and hydraulic fracturing factor may help to improve R^2 in the production prediction and enable additional optimization methods in hydraulic fracturing. Additional number of data is required for this purpose.

Additional hydraulic fracturing job data from other area (outside South-Sumatra) will improve the data diversity thus yield more reliable prediction tool. The data confidentiality and company's discrecy is the major challenge to overcome.

GLOSSARY OF TERMS

Symbol	Definition	Unit
q	Production Rate	BLPD
k	Reservoir permeability	md
Pr	Reservoir Pressure	psig
Pwf	Flowing bottom hole pressure	psig
μ	Viscosity	cp
B	Formation Volume factor	-
re	Reservoir radius	ft
rw	Wellbore radius	ft
rw'	Equivalent Wellbore radius	Ft
S	Skin	-
$\frac{kh}{\mu}$	Transmissibility, the product of permeability, reservoir thickness and fluid viscosity that represent the productivity of reservoir.	md.ft/cp
JD	Dimensionless Productivity Index	-
Np	Proppant Number	-
kf	Fracture permeability	md
xf	Fracture length	ft

Symbol	Definition	Unit
xe	Reservoir length	ft
w	Fracture width	ft
V prop	Volume proppant	ft3
V res	Volume reservoir	ft3
Hydarulic Fracturing	A type of well stimulation treatment designed to bypass near-wellbore damage and improve the fluid flow path from the formation to the well.	
Impulse Testing	A specialized well testing procedure that enables analysis of the reservoir response following a relatively short duration of fluid injection or production (Ayoub et al., 1988)	
Mini-fall-off Test	An injection-falloff diagnostic test performed before a main fracture stimulation treatment. The intent is to break down the formation to create a short fracture during the injection period, and then to observe closure of the fracture system and the reservoir response after closure	
Pearson Correlation Coeffcient (R)	The linear correlation coefficient developed by Karl Pearson that measures the strength and the direction of a linear relationship	
Machine Learning	A broad subfield of artificial intelligence aimed to enable machines to extract patterns from data based on mathematical statistics, numerical methods, optimization, probability theory, discrete analysis, geometry, etc.	

Symbol	Definition	Unit
AdaBoost	One of ensemble ML model that works by weighting the observations, putting more weight on difficult to classify instances and less on those already handled well.	
Gradient Boosting	The development of AdaBoost algorithm that identifies the shortcomings by using high weight data points. Gradient boosting performs the same by using gradients in the loss function	
Random Forest	Ensemble ML model that has algorithm to build multiple decision trees and merges them together to get a more accurate and stable prediction.	
Linear Regression	A supervised machine Learning model in which the model finds the best fit linear line between the independent and dependent variable.	

REFERENCES

Economides, M. J., Hill, A. D., Ehlig-Economides, C. & Up, D. Z., 2013. *Petroleum Production System.* 2nd ed. Masscachusetts: Prentice Hall.

Economides, M. J. & Nolte, K. G., 2010. *Reservoir Stimulation.* 3rd ed. New Jersey: Prentice Hall.

Friedman., J. H., 2001. Greedy function approximation: a gradient boosting machine. *Annals of Statistics,* 29(5), pp. 1189 - 1232.

Holditch, S. A. & Ma, Y. Z., 2016. *Unconventional Oil and Gas Resources Handbook: Evaluation and Development*:Elsevier/Gulf Professional Publishing.

Kang, S., 2021. k-Nearest Neighbor Learning with graph neural networks. *Mathematics,* 9(8), p. 830.

Makhotin, I., Koroteev,, D. & Burnaev, E., 2019. Gradient boosting to boost the efficiency of hydraulic fracturing. *Journal of Petroleum Exploration and Production Technology,* pp. 1-7.

Mutalova, R. F., Mozorov, A.D., Osiptsov, A.A., Vainshtein, A.L., Burnaev, E.V., Shel, E.V., & Paderin, G.V., 2019. Machine learning on field data for hydraulic fracturing design optimization. *Journal of Petroleum Science & Engineering. Special Issue: Petroleum Data Science,* pp. 1-21.

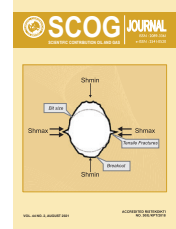**Pearson, K.**, 1920. Notes on the history of correlation. *Biometrika,* 13(1), pp. 25-45.

Ribarič, M. & Šušteršič, L., 2017. *Empirical formulas for prediction of experimental data & appendix,* Slovenia: Jožef Stefan Institute, Ljubljana.

Smola, A. & Viswanathan, S. V. N., 2008. *Introduction to machine learning.* Cambridge: Cambridge University Press.

Temizel, C., Canbaz, C.H., Palabiyik, Y., Aydin, H., Tran, M., Ozyurtkan, M.H., Yurukcu, M., & Johnson, P., 2021. *A thorough review of machine learning applications in oil and gas industry.* Virtual, SPE/IATMI.

Oil and Gas in the Dynamics of Time and Development

Ainuddin, and Muhammad Adam Suryadilaga

Universitas Islam Al-Azhar Mataram, Unizar
Jl. Unizar No. 20, Turida, Kec. Sandubaya, Kota Mataram, Nusa Tenggara Barat 83232, Indonesia
Corresponding author: veteranlast86@gmail.com

ABSTRACT - As a source of energy, industrial raw materials, and foreign exchange for exports, the oil and gas sub-sector has a strategic role in national development. In the period 2020-2024, the management and utilization of oil and gas resources will face several challenges. The purpose of this study is to determine the profile of oil and gas development. The method used and the description in the data is qualitative. The results of this study allow us to statistically understand cluster dynamics. The impact of this research is to map the dynamics of oil and gas as a whole.

Keywords: Strategic, dynamics, oil and gas.

INTRODUCTION

Due to the continuous growth of energy demand and the limitation of fossil resources, biogas as a renewable energy source is considered to be one of the alternative methods to meet energy demand. In Europe, the European Commission has proposed a comprehensive plan for energy and climate change, which includes a mandatory target of setting the proportion of renewable energy at 20% by 2020, and the European Union has adopted the 2030 Climate and Energy Framework, which sets 27% of renewable energy consumption. As a traditional agricultural country, China has produced abundant biogas resources from agriculture and related production activities. In 2010, China's annual biogas production has increased to 248 billion cubic meters. In 2012, China produced 846 million tons of crop residues and 3.21 billion tons of livestock and poultry manure. If these wastes are used for anaerobic fermentation, 4.23×10^{11} m3 of biogas can be produced. Therefore, the area of biogas exceeds 1.2×10^6 square kilometers and the grassland area is 3.9×10^6 square kilometers. Biogas has great potential in realizing China's social and economic development and environmental improvement.

China's biogas resources have huge potential, and the distributed energy system (DES) based on micro gas turbines provides an effective way for biogas utilization. In this work, numerical and experimental studies on the turbulent combustion characteristics in the combustor of a micro gas turbine used in DES were carried out, and the influence of carbon dioxide content in biogas on the turbulent flame was analyzed. Through the three-dimensional (3D) combustion diagnosis technology based on computer tomography chemiluminescence

(CTC), the turbulent flame structure of natural gas and three kinds of biogas at various equivalence ratios were measured.

The results show that the carbon dioxide content in the fuel has a great influence on the flame structure of turbulent combustion. The increase of the carbon dioxide content in the fuel not only reduces the turbulent combustion rate, but also makes the combustion stability worse. As the equivalence ratio decreases, the effect becomes greater. As the volume fraction of carbon dioxide increases, the combustion flame gradually moves away from the nozzle outlet. When the volume fraction of carbon dioxide is 50%, the distance between the combustion flame and the nozzle outlet increases by 100 mm. In addition, carbon dioxide reduces the influence of excess air on CH* distribution and turbulent flames (Liu, *et al.*, 2020).

In 2006, one of the largest oil provinces in the world, known as thepre-salt, was discovered in Brazil. The hydrocarbon reservoirs consist of carbonaceous rocks of microbial origin and underlie a thick layer of saltrock with an average thickness of 2000 m, in a water depth of 2200 m,at ~300 km from the coast. The oil in the reservoirs is of high quality with a remarkably high gas-oil ratio, above 220. The associated gas hasa high CO_2 content of mantle origin, which cannot be ventilated in theatmosphere. shows a typical geology section of the pre-salt reservoirs of the pre-salt reservoirs.The produced gas with high content of CO_2 is treated at the production platform through membrane filters. Part of the treated gas iscompressed and transported to shore through gas pipelines. The remainder gas with high content of CO_2 is reinjected into the reservoirs,working as EOR (Enhanced Oil Recovered) in the initial age of thereservoirs production.

With time the recycled gas with CO_2 increases the global CO_2 content of the associated gas. Therefore, there is a demand for CCS of large quantities of CO_2 associated with CH4 in the presalt offshore oil fields in Brazil.Salt has been identified as one of the best geological media forunderground storage of gas at high pressure (about 2000−3000 m ofrock depth and 2200 m of water depth). The main reasons include: (i)low permeability, the permeability of rock salt is about 10-21 - 10-24m², thus can provide excellent sealing of the salt cavern; (ii) good-mechanical properties, damage self-recovery capability of rock salt canensure the safety of salt cavern with frequent changes of gas pressure;(iii) solution in

water, rock salt is easily dissolved into water, which facilitates the construction and shape control of the salt cavern; (iv) abundant resources, as it is overlying the pre-salt reservoirs (Goulart, *et al.*, 2020)which performs all the offshore natural gas and CO_2 separation process with subsequent storage in off-shore underground salt caverns. Currently there is a demand for CCS of large quantities of CO_2 associated with CH4 in the pre-salt offshore oil fields in Brazil. The pre-salt reservoirs have as caprock 2000 m of continuous rock salt. This hybrid system is expected to perform, at the same time, the separation between the natural gas and CO_2, and Carbon Capture and Storage of CO_2, allowing the monetization of the separated natural gas. The Technology Readiness Levels (TRL.

Natural gas hydrates (NGHs) are white crystalline compounds formed by the interaction of light hydrocarbons, carbon dioxide,and hydrogen sulfide with water under low-temperature and high pressure coexisting conditions. Natural gas hydrate develops and exists in pores of soil sediments under deep seabed and permafrost regions, where the low-temperature and high-pressure condition guarantees the NGH generation and stability. NGH is regarded as having the most potential as alternative energy in the 21st century because of its huge potential. In recent decades, it has been a worldwide upsurge in terms of exploration, production, and development. At present, common methods of NGH exploitation include depressurization, thermal stimulation, inhibitor injection, CO_2 replacement, and solid fluidization mining methods. However, these exploitation methods have some limitations for NGH reservoirs, which are characterized by shallow burial depth, non-trap structure,low consolidation strength, non-diagenesis, and low permeability. Hydrate secondary formation and ice formation are easily caused by depressurization, which may block the permeability path of the non-diagenetic NGH reservoirs and be unfavorable for long-term exploitation.For the inhibitor injection method, injection of the chemical reagents for hydrate-bearing sediments (HBSs) is not economical, and the low permeability of the NGH reservoirs will lead to the slow action of chemical reagents on NGH formation and may induce stratigraphic disasters.6Besides, owing to the weak cementation of the hydrate reservoirs, the above three exploitation methods are based on the principle of direct decomposition of NGH, which easily causes the

instability of the formation 6 Concerning the CO_2 replacement method, the production period is long, and similarly, the low permeability of the NGH reservoirs has a great impact on mining efficiency. The exploitation of NGH reservoirs is still in the theoretical and experimental stages. Many countries, including the United States, Japan, Korean, China, and India, have launched ambitious national projects to the further exploitation of NGH reservoirs and obtained valuable experimental data and experience, but due to the problems of low production and formation sand production, noncommercial exploitation of natural gas hydrate has been achieved. In October 2019, China launched the second NGH trial production with the horizontal well in the Shenhu area of the South Chinese and obtained 860 000 m3 of natural gas, which is four times the amount of gas produced by the last trial in 2017. The reason is the horizontal section that greatly expanded the scope of influence of the production well (Zhang, *et al.*, 2020).

Fine-scale movement data has transformed our knowledge of ungulate migration ecology and now provides accurate, spatially explicit maps of migratory routes that can inform planning and management at local, state, and federal levels. Among the most challenging land use planning issues has been developing energy resources on public lands that overlap with important ungulate habitat, including themigratory routes of mule deer (Odocoileus hemionus). We generally know that less development is better forminimizing negative effects and maintaining habitat function, but we lack information on the amount ofdisturbance that animals can tolerate before reducing use of or abandoning migratory habitat. We used global positioning system data from 56 deer across 15 years to evaluate how surface disturbance from natural gas well pads and access roads in western Wyoming, USA, affected habitat selection of mule deerduring migration and whether any disturbance threshold(s) existed beyond which use of migratory habitat declined. We used resource and step selection functions to examine disturbance thresholds at 3 differentspatial scales. Overall, migratory use by mule deer declined as surface disturbance increased. Based on the weight of evidence from our 3 independent but complementary metrics, declines in migratory use related to surface disturbance were non-linear, where migratory use sharply declined when surface disturbance from energy development exceeded 3%. Disturbance thresholds may vary across regions, species, or migratory habitats

(e.g., stopover sites). Such information can help with management and land use decisions related to mineral leasing and energy development that overlap with the migratory routes of ungulates (Sawyer, *et al.*, 2020).

Adverse price trends and sharp fluctuations not only affect profit margins, but also affect the likelihood of default or even change investment incentives (eg, infrastructure and transportation) - reducing investment in favor of low risk projects. Business challenges that are directly related to, inter alia, production / purchasing costs, revenue, and availability of credit, create the need for coherent risk management practices. For oil and gas projects, where cash flows are generated almost entirely by sales of oil and gas, the volatility of prices increases the incentive to mitigate this impact. An effective natural gas hedging strategy is relevant in reducing price volatility for investors, traders, producers and commercial users in this sector. In addition, hedging policies are a key theme for policy makers and regulators to consider alternative reforms and reduce deficiencies (eg, transaction costs, poor liquidity and transparency) in the current market design. In addition, with the Paris Agreement in 2015 and its predecessor the Kyoto Protocol in 1997, there has been increasing interest in investing in low-emission energy, such as natural gas. Therefore, given the large economic and financial impact of natural gas volatility, it is important to study natural gas risk management strategies. One important parameter of future-based hedging is the hedge ratio, which is the number of forward contracts to be bought or sold for each unit of the underlying asset for which the hedge bears the risk. Previous studies (eg, Ederington, 1979) found hedge ratios that minimize spot / future portfolio variance based on the principles of portfolio theory. The Optimum Hedging Ratio (OHR) is usually found by regressing the returns for holding physical assets against the returns that hold the hedged instrument. However, the regression approach has several drawbacks (Pouliasis, *et al.*, 2020).

DATA AND METHODS

This review will be conducted using a systematic literature review. This method will help identify and make it easier for researchers to review the previous research literature. This systematic literature review was adopted from (Tranfield, Denyer, &

Smart, 2003) which makes it easier for researchers to determine inclusions that match the research theme and carry out an exclusion process that is not in accordance with the research recommendations. The use of this methodology will make it easier for researchers to obtain a comprehensive scope of literature. The methodology uses 5 stages to facilitate the literature review process, namely planning, searching, filtering, extraction, and synthesis, including reporting.

Planning Researchers try to make plans in research to be able to define research questions. The research question in this research is "What is Oil and Gas?". Answers to research questions will facilitate the content and see the theory and practice that

occurs. The next step here is to identify the research database and use key strings to find an appropriate electronic database for the research question.

Search The search process for related articles for this research question was carried out using 1 electronic database: Scopus. The selection of this article is based on articles that provide good presentations on oil and gas intentions, and related empirical research. The keywords used in this study are "oil and gas". Researchers use these keywords in order to be able to see broadly about the intentions of oil and natural gas so that they can answer generally to specific research questions (Suryadilaga, *et al.*, 2019).
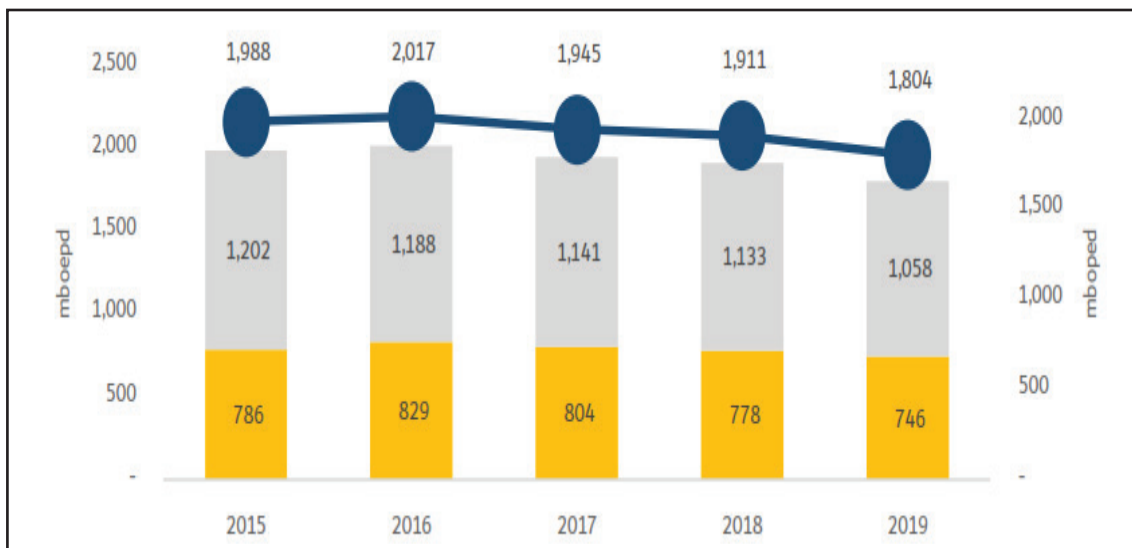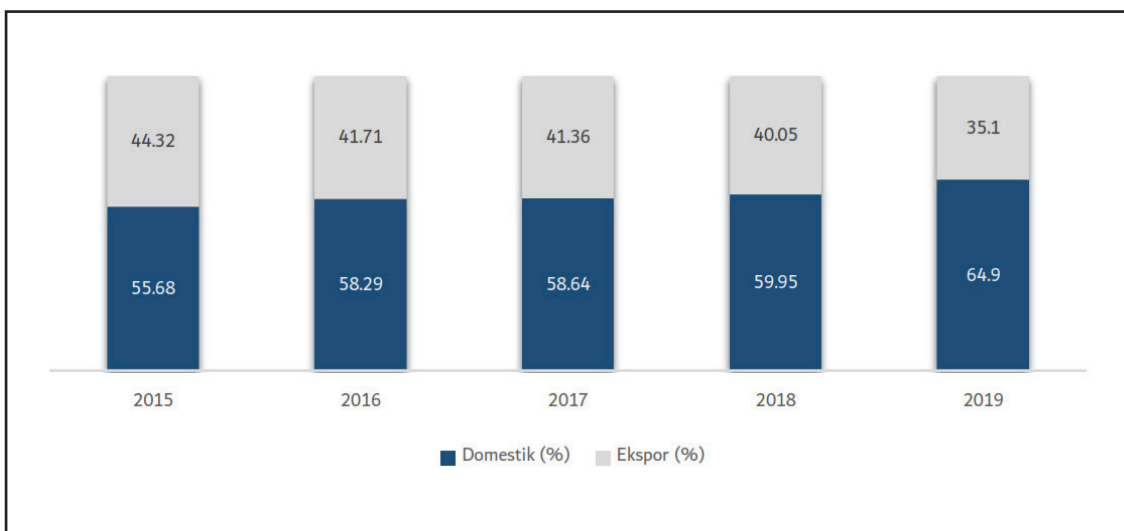

Figure 1
Realization of oil and gas lifting.

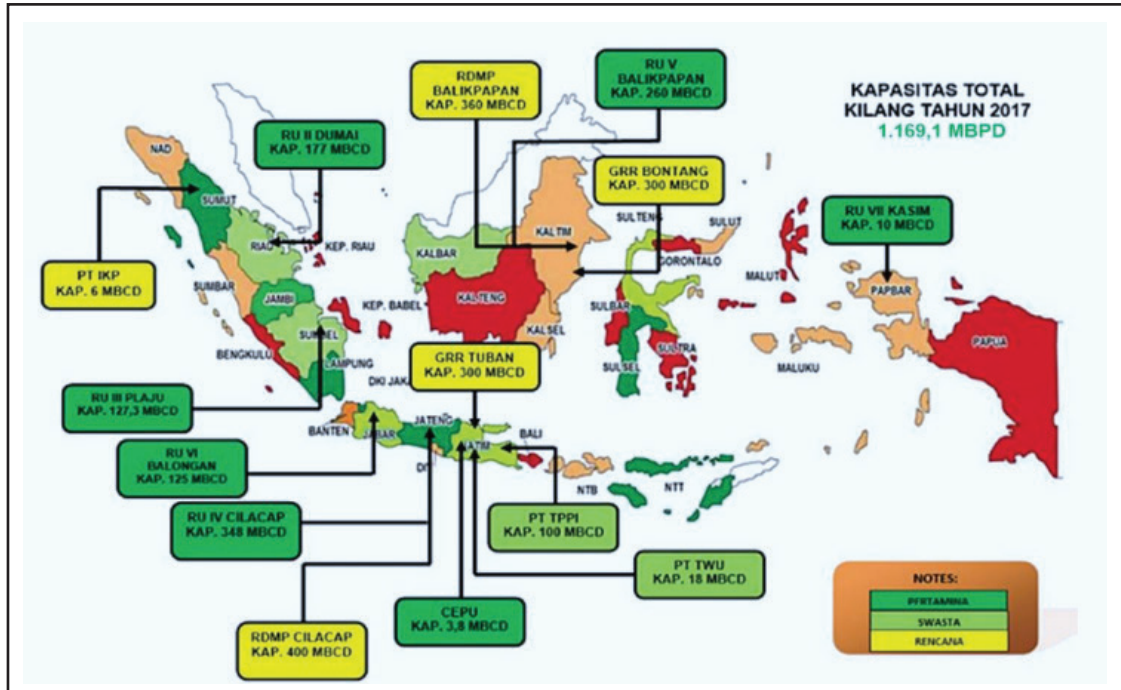Figure 2
Utilization of natural gas.
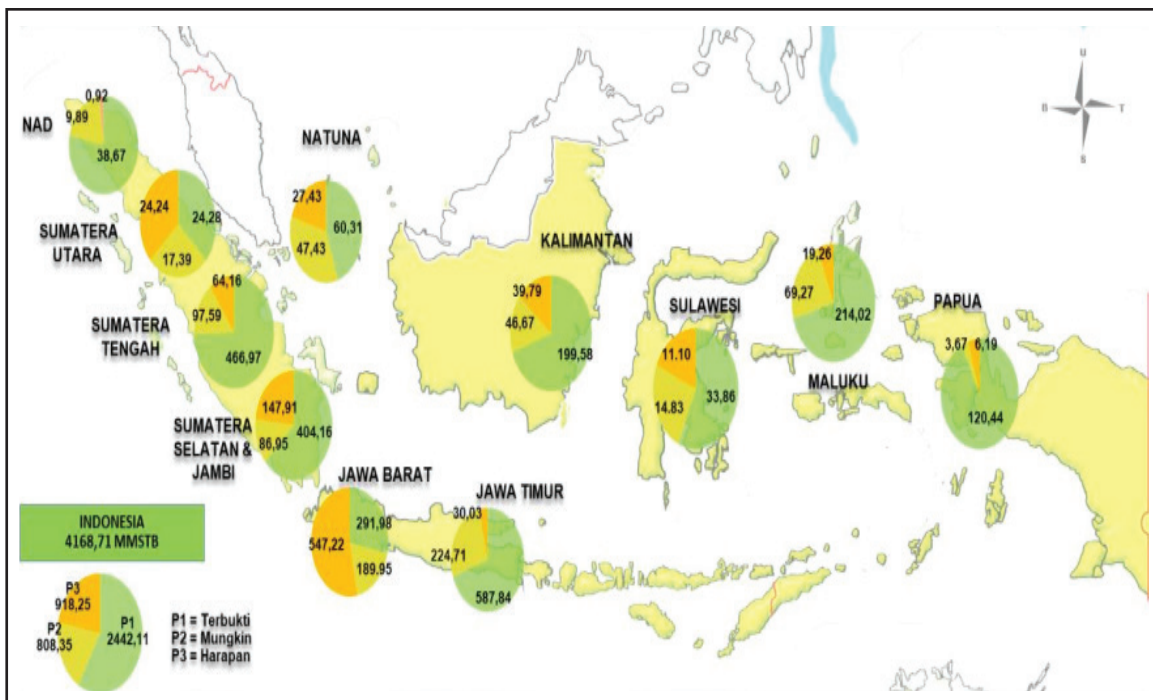
Figure 3
Oil refinery capacity.

Figure 4
Map of petroleum reserves in 2020.

RESULTS AND DISCUSSION

The early 2015-2019 period was a period full of challenges in increasing oil and gas lifting. The global recession caused oil prices to fall dramatically and exchange rates were volatile. This problem can be resolved by issuing an Economic Policy Package by the Government so as to create conducive investment conditions. With the issuance of the Economic Policy Package, Cooperation Contract Contractors (KKKS) can invest in exploitation and production. This also changes the direction of the oil and gas subsector policy, namely from increasing the lifting of oil and
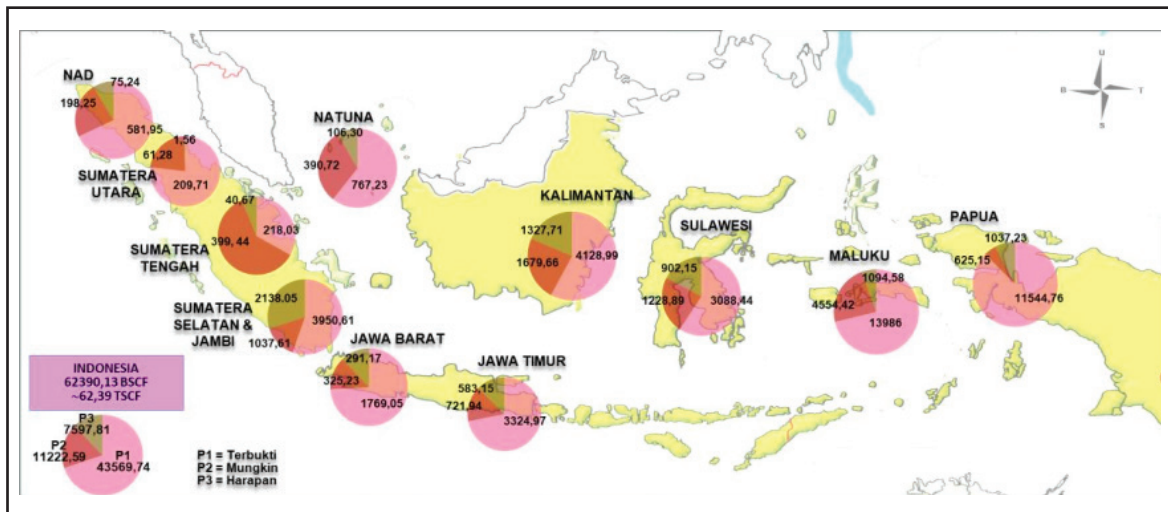
Figure 5
Map of natural gas reserves in 2020.

gas to the supply of oil and gas energy so that one of the challenges is how to maintain how production, currency exchange rates and, raise oil and gas. The performance of oil and gas lifting from 2015-2019 has decreased due to facing many errors in the field, both in operations, development activities, and other non-technical matters. The ongoing coordination among all stakeholders including oil and gas producing regions throughout Indonesia is expected to be able to maintain and increase oil and gas production in the next period.

The implementation of natural gas business activities aims to make the largest contribution to the national economy and to develop and strengthen the position of Indonesia's industry and trade. Currently, the natural gas management paradigm is implemented with energy as a driving force for the economy to provide a multiplier effect on the people's economy.

The construction of the FSRU / Regasification Unit / LNG Terminal is carried out to facilitate the distribution of natural gas between regions in Indonesia, which is an archipelagic country. In the period 2015 to 2019, Indonesia has built 3 (three) FSRU facilities that have been operating, namely the Arun-Belawan FSRU in Aceh, the Lampung FSRU, and the Tanjung Benoa FSRU in Bali. to meet domestic needs and growing LNG business opportunities.

CONCLUSIONS

Even though it has been decreasing in recent years, Indonesia's oil and gas potential is still growing. To date, out of a total of 128 basins, only about 47%

have been explored, with the status of 16% or 20 basins already in production, 21% or 27 basins have been drilled and found oil, and 10% or 13 basins have been drilled but no oil has been found. There are still 53% or 68 more sedimentary basins, mostly in Eastern Indonesia, waiting to be discovered.

In Eastern Indonesia, geological and geophysical survey (G&G) activities are primarily aimed at obtaining new data in areas where exploration activities have not been touched and with minimal data (frontier basin). Meanwhile, in the Western Region of Indonesia, which has produced more basins, a survey was conducted to look for other potentials beyond the current exploration concept.

Petroleum reserves from 8.21 billion barrels in 2008 fell to the range of 3.8 billion barrels in 2019 (in 2019 there was a change in the method of calculating oil reserves). Reserve to Production (calculated against proven reserves) is in the range of 9 years. There was an increase to 12 years in 2014 due to the significant addition of proven oil reserves, especially from the Banyu Urip Cepu Field. Furthermore, the decline in world oil prices in 2015 is seen as one of the factors in the low new reserves discoveries.

Natural gas reserves in 2008 were 170 TSCF and continued to fall to the range of 77.29TSCF in 2019. Indonesia's natural gas Reserve to Production (against proven reserves) was 18.8 years. Considering that oil and natural gas are still the dominant energy in the use of national energy, several efforts to increase oil and gas reserves are always being pursued. To increase the number of reserves, contractors need to make efforts to discover new reserves that can be

done by expanding the search area for oil and gas reserves by carrying out exploration drilling and seismic surveys as well as G&G studies.

ACKNOWLEDGEMENT

GLOSSARY OF TERMS

Symbol	Definition	Unit
DES	Distributed Energy System	
3D	Three-Dimensional	
CTC	Computer Tomography Chemiluminescence	
EOR	Enhanced Oil Recovered	

REFERENCE

Goulart, M. B. R., da Costa, P.V.M., da Costa, A.M., Miranda, A.C.O., Mendes, A.B., Ebecken, N.F.F., Meneghini, J.R., Nishimoto, K., & Assi, G.R.S., 2020. Technology readiness assessment of ultra-deep Salt caverns for carbon capture and storage in Brazil. *International Journal of Greenhouse Gas Control,* Volume 99, p. 103083.

Liu, H., Wang, Y., Yu, T., Liu, H., Cai, W., & Weng, S., 2020. Effect of carbon dioxide content in biogas on turbulent combustion in the combustor of micro gas turbine. *Renewable Energy,* Volume 147, p. 1299-1311.

Pouliasis, P. K., Visvikis, I. D., Papapostolou, N. C. & Kryukov, A. A., 2020. A novel risk management framework for natural gas markets. *Journal of Futures Markets,* 40(3), pp. 430-459.

Sawyer, H., Lambert, M. S. & Merkle, J. A., 2020. Migratory Disturbance Thresholds with Mule Deer and Energy Development. *Journal of Wildlife Management,* 84(5), p. 930–937.

Suryadilaga, M. A., Muradi, A., Sumandinata, W.S., Deliarnoor, N.A., Ruslan, B., & Nugroho, B., 2019. Systematic mapping study: Political attitudes in elections. *Opción: Revista de Ciencias Humanas y Sociales,* Volume 35, p. 198–217.

Zhang, Y., Zhao, K., Wu, X., Tian, S., Shi, H., Wang, W., & Zang, P., 2020. An innovative experimental apparatus for the analysis of natural gas hydrate erosion process using cavitating jet. *Review of Scientific Instruments,* Volume 91, p. 095107.

SUBJECT INDEX

AUTHOR GUIDELINES
THE SCIENTIFIC CONTRIBUTIONS FOR OIL AND GAS

POLICY AND GUIDELINES FOR AUTHORS

The Scientific Contribution for Oil and Gas is a national scientific journal in oil and gas, managed by the Research and Development Center for Oil and Gas Technology (LEMIGAS). Manuscript in English are accepted from scientist/researchers in any institutions throughout the country and overseas.

POLICY

Conditions of acceptance

Manuscripts are received by Scientific Contributions for Oil and Gas with the understanding that:

1) all authors have approved submission;

2) the results or ideas contained therein are original;

3) the work has not been published previously;

4) the paper is not under consideration for publication else-where and will not be submitted elsewhere unless rejected by the Scientific Contributions for Oil and Gas or withdrawn by written notification to the editor of the Scientific Contributions for Oil and Gas;

5) if accepted for publication and published, the article, or portions thereof, will not be published elsewhere unless consent is obtained in writing from the editor of the Scientific Contributions for Oil and Gas;

6) reproduction and fair use of articles in the Scientific Contributions for Oil and Gas are permitted in accordance with the Indonesia Copyright Revision Law, provided the intended use is for nonprofit educational purposes. All other use requires consent and fees where appropriate;

Return of materials

Rejected papers: When the decision is made not to publish a paper, the original typescript and illustrations are returned to the author with the author's copy of the reviews and a cover letter.

Papers returned for revision: Materials necessary for reference or to be revised are returned to the author at the time a revision is requested. If the revision is not received within 1 month or if other arrangements have not been made with the editor, the manuscript is considered to have been withdrawn.

Forms of publication

Articles: The Journal publishes articles reporting original research, primarily on oil and gas technology.

Review articles: Only scientific reviews are published. Unsolicited reviews should not be submitted, but topics may be suggested to the editor or members of the editorial board.

Critical comments: Critical comments are for correcting errors of published fact, providing alternative interpretations of published data, or presenting new theories based on published information.

Hard copy submission

All manuscripts must be prepared and submitted according to the guidelines of this section and those of the subsequent section appropriate for the category of the report.

Paper: Manuscripts are to be typed on one side only of good quality, white paper, size A4.

Typing: All parts of original manuscripts are to be typed one-and-a-half-spaced. Type should be 12 point (Times New Roman). Photo reduction, even in tables, is not acceptable. Proportional spacing and hyphenation should not be used, i.e., do not justify right-hand margin. Do not leave extra space between paragraphs in the text. Only a single font should be used.

Submission: For a new manuscript, submit the original and 3 copies prepared according to the Policy and Guidelines contained herein. When a manuscript has been accepted for publication by the editor, specific instructions for preparation of the revision will be supplied. It remains the responsibility of the author to retain a copy of the manuscript for reference and to protect against loss. Manuscripts should be addressed to: the Chief Editor of Scientific Contributions for Oil and Gas.

Articles

Manuscripts are to be organized in the following format and sequence, with all pages, beginning with that for the running head, numbered consecutively.

Running head: Provide the last names of authors (use et al. for more than 2) and a shortened title. The entire running head may not exceed 60 characters and spaces.

Title: Immediately after the running head give the title of the article, names of authors, and address of the first author. Include the email address, in italics, of the corresponding author only. The title and authors' names should be in bold type, and the same font size as the text. All other information should be in Times New Roman type. Titles should be short and descriptive, and should be written in Bilingual (English and Indonesian).

Abstract: This should follow directly after the author's address with no additional spacing between them. You should provide an abstract of the paper that does not exceed 200 words. The abstract should be factual (as opposed to indicative) and should outline the objective, methods used, conclusions, and significance of the study. The abstract is headed with the word abstract, indented, and typed in bold capital letters, ending with a colon also in bold type. Text is run in after the colon, is not subdivided, and does not contain literature citations and should be written in Bilingual (English and Indonesian).

Introduction: The introduction should follow the abstract and should be un-headed. The introduction should establish the con-text of the paper by stating the general field of interest, presenting findings of others that will be challenged or developed, and specifying the specific question to be addressed. Accounts of previous work should be limited to the minimum information necessary to give an appropriate perspective. The introduction may not be subdivided and extra spacing between paragraphs is not permitted here or throughout the text.

Methodology: This section should give sufficient information to permit repetition of the study by others. Methods and apparatus used should be indicated, but specific brand names and models need to be mentioned only if significant. The source, e.g., city and state, both spelled in full, of special equipment or chemicals should also be given. Previously published or standard techniques are to be referenced, but not detailed. Generic descriptions should be given for unusual compounds used.

The primary heading for this section should be typed in all bold capital letters and started at the left-hand margin of the page. The heading is unnumbered and ends without punctuation. Second-level headings in bold type should be on a separate line beginning at the left-hand margin. The initial letter of the first word is the only capital letter except capitals needed for proper nouns. These headings are unnumbered and end without punctuation. Third-level headings are indented for a paragraph, italicized, and end with a colon, also italicized. The initial letter of the first word is the only capital letter, except capitals needed for proper nouns. Text is run in immediately following this heading. Further subdivision should not be needed. If the materials and methods section is short, it should not be subdivided; it is unnecessary to provide headings, beyond the primary head, for a series of subsections comprising single paragraphs.

Results: This section should contain a concise account of the new information. Tables and figures are to be used as appropriate, but information presented in them should not be repeated in the text. Avoid detailing methods and interpreting results in this section. The results section may be subdivided and headed as for the materials and methods section.

Discussion: An interpretation and explanation of the relationship of the results to existing knowledge should appear in the discussion section. Emphasis should be placed on the important new findings, and new hypotheses should be identified clearly. The primary heading and subdivisions, if needed, in this section are as described for the materials and methods section.

Conclusions: They must be supported by fact or data. Conclusions are presented in brief considering the topic of the article, the purposes and objectives. They must not be presented in pointers.

Acknowledgments: These should be concise. Ethics require that colleagues be consulted before being acknowledged for their assistance in the study. The heading for this section is as for the primary head described for the materials and methods section. Subdivisions are not used in this section.

Tables: Tables are used only to present data that cannot be incorporated conveniently into the text. Ordinarily values from statistical tests are not published as tables; tests employed and probability accepted for significance can be stated in the materials and methods section with significant differences indicated in tables by footnotes or in the text by a statement.

Tables must be designed to fit in 1 or 2 columns. Only rarely may they be designed to fit the height of a printed page. Generally, if the width does not fit the height of a typed page, the table is too wide. Tables may

be continued on following pages to accommodate length, but pages may not be taped together, photo-reduced, single-spaced, oversized, or otherwise modified to contain more material.

Tables are numbered with Roman numerals in a continuous series and so referenced, in sequence, in the text. Captions are typed above the data on the same page. All columns in a table must have headings, with the first letter of the first word and proper nouns capitalized, e.g., Number sampled, % Recaptured.

Horizontal lines should be avoided in the body of the table; vertical lines are not permitted. If such symbols are necessary, the table must be prepared as a line drawing and treated as a figure. Use of letters and numbers as superscripts or subscripts is not permitted. Table designations must be used in the obligate sequence.

Figures: All figure captions are to appear consecutively, in sequence, directly after the literature cited section. Do not place figure captions on the same page as the figures. Each figure or plate of figures must have a caption. The caption is written in paragraph style, beginning with the word ''FIGURE.'' Captions are typed in roman. For plates, a summary statement should pre-cede the specific explanation of each figure. Avoid repeating information for each figure that can be placed in the summary statement. Species names are spelled out in full the first time used in each caption. The caption must contain an explanation of all abbreviations used on the figures and indicate the value of lines or bars used to show size (unless the value is shown directly on the figure). Size should not be indicated by magnification in the caption because the figure might not be printed at the size calculated.

Figures are numbered consecutively in the sequence mentioned in the text. Non parenthetical references to figures in the text are not abbreviated, i.e., Figure 1; Figures 1, 2; Figures 1–3; references to figures in parentheses in the text are abbreviated, i.e., Fig. 1, Figs. 1, 2; Figs. 1–3. All symbols used in a figure must be defined when possible by a key within the body of the figure. Style, including the form of abbreviation, must be that used in the Journal.

Figures may be used singly or grouped in a plate. In either case, the originals must be mounted on illustration board with a margin of at least 25 mm on all sides. Photographs and line drawings may not be combined in a single plate. If such a composition is necessary, the additional expense may be billed to the author. All figures are to be identified on the back by author name and figure number with the top indicated. Single figures are not numbered on the front, but each figure in a plate must include a number or letter, applied directly to the figure and, when possible, without an added background. Figures arranged to form a plate are to be abutted tightly without space or masking between.

Literature cited: All literatures used as references must be cited in text, and vice versa all literatures cited in text must be written as references. References should be at least ten sources highly related to the topic with the following conditions:

• 80% of the references must be in the category of primary sources (i.e., journal, published proceeding, thesis, dissertation).

• Multiple publications for same author

  - Same author; different years Normal conventions (author, year, title, etc).

  - Same author; same year More than one reference by an author in the same year: these are distinguished in order of publication using a lower-case alphabetical suffix after the year of publication (eg 1988a, 1988b, 1988c, etc). The same suffix is used to distinguish that reference for the in-text citations.

• The List of References is ordered alphabetically by primary authors' surnames.

  - Multiple authors. Use the sequence of authors' surnames exactly as given in the publication. The primary author, i.e., major contributor, is listed first by the publisher.

  - Same author: Different years: list the author's references chronologically, starting with the earliest date. Same year: use an alphabetical suffix (e.g. 1983a, 1983b).

Examples

1. Book

Type of Book	Citing in Text	Writing References
Single Author	**At the end of the sentence**: (Holt 2010) **At the beginning of the sentence**: Holt (2010) wrote that...	Holt, D.H., 1997, *Management Principles and Practices*, Prentice-Hall, Sydney.
Two Authors	(Laudon & Laudon 2003)	Laudon, K.C. & Laudon, J.P., 2003, *Essentials of Management Information Systems: Managing the Digital Firm*, Prentice Hall, Upper Saddle River, New Jersey.
Three Authors	**In-text: initially** (Coveney, Ganster & King 2003) **In-text: thereafter** (Coveney et al. 2003)	Coveney, M., Ganster, S. & King, D., 2003, *The Strategy Gap: Leveraging Technology to Execute Winning Strategies*, Wiley, Hoboken, New Jersey.
More than Three Authors	(Bond et al. 2011)	Bond, W.R., Smith, J.T., Brown, K.L. & George, M., 2011, *Management of Small Firms*, McGraw-Hill, Sydney.
Corporate Author	**In-text: initially** (Department of Foreign Affairs and Trade 2002) **In-text: thereafter** (DFAT 2002)	Department of Foreign Affairs and Trade, 2002, *Connecting with Asia's Tech Future: ICT Export Opportunities*, Economic Analytical Unit, Commonwealth Government, Canberra.

2. Journal, Proceeding, Thesis and Dissertation: Citing a journal, proceeding, thesis and dissertation in text should be written in the same way as citing a book

Type of Source	Citing in Text	Writing References
Journal Article: Printed Journal	**In the middle or at the end of the sentence**: (Conley & Galeson 1998) **At the beginning of the sentence**: Conley & Galeson (1998) stated that...	Conley, T.G. & Galeson, D.W., 1998, 'Nativity and Wealth in mid-nineteenth Century Cities', *Journal of Economic History*, vol. 58, no. 2, pp. 468-493.
Journal Article: Electronic Database	(Liveris 2011)	Liveris, A., 2011, 'Ethics as a Strategy', *Leadership Excellence*, vol. 28, no. 2, pp.17-18. Available from: Proquest [23 June 2011].
Conference Proceeding: Print	(Eidenberger, Breiteneder & Hitz 2002)	Eidenberger, H., Breiteneder, C. & Hitz, M., 2002, 'A Framework for Visual Information Retrieval', in S-K. Chang, Z. Chen & S-Y.Lee (eds.), *Recent Advances in Visual Information Systems: 5th International Conference, VISUAL 2002 Proceedings,* Hsin Chu, Taiwan, March 11-13, 2002, pp. 105-116.
Conference Proceeding: Electronic	(Fan, Gordon & Pathak 2000)	Fan, W, Gordon, MD & Pathak, R 2000, 'Personalization of Search Engine Services for Effective Retrieval and Knowledge Management', *Proceedings of the Twenty-first International Conference on Information Systems*, pp. 20-34. Available from: ACM Portal: ACM Digital Library. [24 June 2004].

Conference Proceeding: Unpublished	(Brown & Caste 2009)	Brown, S & Caste, V 2009, 'Integrated Obstacle Detection Framework'. Paper presented at the *IEEE Intelligent Vehicles Symposium*, IEEE, Detroit MI.
Thesis or Dissertation: Unpublished	(Hos 2005)	Hos, J.P., 2005, *Mechanochemically Synthesized Nanomaterials for Intermediate Temperature Solid Oxide Fuel Cell Membranes*. Ph.D. dissertation, University of Western Australia.
Thesis or Dissertation: Published	(May 2007)	May, B., 2007, *A Survey of Radial Velocities in the Zodiacal Dust Cloud*. Bristol UK, Canopus Publishing.
Thesis or Dissertation: Retrieved from a Database	(Baril 2006)	Baril, M., 2006, *A Distributed Conceptual Model for Stream Salinity Generation Processes: A Systematic Data-based Approach*. WU2006.0058. Available from: Australasian Digital Theses Program. [12 August 2008].

3. World Wide Web

Type of Source	Citing in Text	Writing References
Document on the WWW (author/sponsor given but not dated)	According to Greenpeace (n.d.), genetically modified foods are … or Greenpeace (n.d.:1 of 2) recommends that 'fewer genetically …'.	Greenpeace n.d., *The Future Is GE Free*, viewed 28 September 2005, from http://www.greenpeace.org.au/ge/farming/canola.html. **Note:** The title of a webpage is treated like the title of a book. It is written in *italics* in the reference list.
Identifiable, personal author	(Arch & Letourneau 2002)	Arch, A. & Letourneau, C., 2002, 'Auxiliary Benefits of Accessible Web Design', in *W3C Web Accessibility Initiative*, viewed 26 February 2004, from http://www.w3.org/WAI/bcase/benefits.html.
E-book	(Eck 2002)	Eck, D.J., 2002, *Introduction To Programming Using Java*, 3rd edition., OOPWeb.com, viewed 26 February 2004, from http://www.oopweb.com/Java/Documents/IntroToProgrammingUsingJava/VolumeFr ames.html.
E-journal	(Mueller , Heckathorn & Fernando 2003)	Mueller, J.K., Heckathorn, S.A. & Fernando, D., 2003, 'Identification of a chloroplast dehydrin in leaves of mature plants', *International Journal of Plant Sciences* vol. 164, no. 4, pp. 535-542, viewed on 10 September 2003, from http://www.journals.uchicago.edu/IJPS/journal/no.s/v164n4/164053/164053.html.
Maps: Online	(maps.com 1999)	maps.com, 1999, *Bhutan*, viewed 11 September 2003, from http://www.maps.com/cgi-bin/search/hyperseek.cgi?search=CAT&Category=Asia%3ABhutanP&Qualifier=

4. Other Sources

Type of Source	Citing in Text	Writing References
Maps: Print	(Viking O'Neil 1991:32-33)	Viking O'Neil, 1991, *Australian Road Atlas*, 10th edition., Penguin Books Australia, Melbourne, pp. 32-33.
Government Publication	(Department of Education, Science & Training 2000)	Department of Education, Science & Training, 2000, *Annual Report 1999-2000*, AGPS, Canberra.
		Department of Immigration and Multicultural Affairs 2001, *Immigration: Federation to Century's End 1901-2000*, Statistics Section, Business Branch, Department of Immigration and Multicultural Affairs, Canberra.
Government Regulation and Legislation	(Presidential Decree of the Republic of Indonesia No 55 Year 2012)	Presidential Decree No 55 Year 2012 on *Annex National Strategy on Corruption Prevention and Eradication 2012-2014 and 2012-2025*
		Presidential Regulation of the Republic of Indonesia No 36 Year 2010 on *List of Business Fields Closed to Investment and Business Fields Open, with Conditions, to Investment*
Standards	According to the Standards Association of Australia (1997), …	Standards Association of Australia, 1997, *Australian Standard: Pressure Equipment—Manufacture*, (AS4458-1997), Standards Australia, North Sydney.
Patents	Tan and Arnold (1993) formalized and protected their ideas … Or Tan and Arnold (1993, n.p.) protected their ideas by '…'	Tan, I.S. & Arnold, F.F., (US Air Force) 1993, *In-situ Molecular Composites Based on Rigid-rod Polyamides*, US patent 5 247 057.

SCIENTIFIC CONTRIBUTION
OIL AND GAS